ISTANBUL TECHNICAL UNIVERSITY ★ GRADUATE SCHOOL OF SCIENCE
ENGINEERING AND TECHNOLOGY

RF ENERGY HARVESTING
IN WIRELESS COMMUNICATION SYSTEMS:
STATISTICAL MODELS FOR BATTERY RECHARGING TIME

M.Sc. THESIS

Doğay ALTINEL

Department of Electronics and Communication Engineering

Telecommunication Engineering Programme

JUNE 2014

RF ENERGY HARVESTING
IN WIRELESS COMMUNICATION SYSTEMS:
STATISTICAL MODELS FOR BATTERY RECHARGING TIME

M.Sc. THESIS

Doğay ALTINEL
(504121313)

Department of Electronics and Communication Engineering

Telecommunication Engineering Programme

Thesis Advisor: Assoc. Prof. Dr. Güneş KARABULUT KURT

JUNE 2014

İSTANBUL TEKNİK ÜNİVERSİTESİ ★ FEN BİLİMLERİ ENSTİTÜSÜ

**KABLOSUZ HABERLEŞME SİSTEMLERİNDE
RF ENERJİ HASATLAMA:
PİL ŞARJ ZAMANI İÇİN İSTATİSTİK MODELLER**

YÜKSEK LİSANS TEZİ

**Doğay ALTINEL
(504121313)**

Elektronik ve Haberleşme Mühendisliği Anabilim Dalı

Telekomünikasyon Mühendisliği Programı

Tez Danışmanı: Doç. Dr. Güneş KARABULUT KURT

HAZİRAN 2014

Doğay ALTINEL, a M.Sc. student of ITU Graduate School of Science Engineering and Technology 504121313 successfully defended the thesis entitled **"RF ENERGY HARVESTING IN WIRELESS COMMUNICATION SYSTEMS: STATISTICAL MODELS FOR BATTERY RECHARGING TIME"**, which he prepared after fulfilling the requirements specified in the associated legislations, before the jury whose signatures are below.

Thesis Advisor :   **Assoc. Prof. Dr. Güneş KARABULUT KURT**   ....
Istanbul Technical University

Jury Members :   **Assist. Prof. Dr. Özgür ÖZDEMİR**   ....
Istanbul Technical University

Assist. Prof. Dr. Ali Emre PUSANE   ....
Boğaziçi University

Date of Submission :   **05 May 2014**
Date of Defense :   **02 June 2014**

To my parents, my wife, and my son,

FOREWORD

After a long time, I made a fresh start to my educational life by being a graduate student. This was a very interesting and exciting experience for me.

Specially, I would like to express my gratitude to my supervisor Assoc. Prof. Dr. Güneş Karabulut Kurt for her guidance and invaluable contributions throughout my masters programme and thesis. It was a great opportunity to study at Wireless Communication Research Laboratory that has a good ambiance for research thanks to my supervisor.

I am grateful to the academic members of telecommunication engineering programme who trusted me and accepted my application. I would like to thank all my lecturers in Istanbul Technical University for their teaching efforts.

I would also like to thank my friends, both in Istanbul Technical University and Istanbul Medeniyet University that kept encouraging and helping me through my masters education.

In the end, I would like to give my greatest thanks to my family who supported me always. Life is meaningful with you.

June 2014   Doğay ALTINEL

x

TABLE OF CONTENTS

ABBREVIATIONS

3GPP   : 3rd Generation Partnership Project
AF   : Amount of Fading
AM   : Amplitude Modulation
AWGN   : Additive White Gaussian Noise
CDF   : Cumulative Distribution Function
CMOS   : Complementary Metal Oxide Semiconductor
D-AMPS   : Digital Advanced Mobile Phone System
DC   : Direct Current
DTV   : Digital Television
EIRP   : Effective Isotropic Radiated Power
FM   : Frequency Modulation
GSM   : Global System for Mobile Communications
ISM   : Industry Science Medical
ITU   : International Telecommunication Union
LAN   : Local Area Network
LED   : Light Emitting Diode
Li-ion   : Lithium Ion
LOS   : Line of Sight
LTE   : Long Term Evolution
M2M   : Machine to Machine
MGF   : Moment Generation Function
MIMO   : Multiple Input Multiple Output
MOSFET   : Metal Oxide Semiconductor Field Effect Transistor
MPPT   : Maximum Power Point Tracking
NiCd   : Nickel Cadmium
NiMH   : Nickel Metal Hydride
NMT   : Nordic Mobile Telephony
PCS   : Personal Communications Service
PDC   : Personal Digital Cellular
PDF   : Probability Density Function
RF   : Radio Frequency
RFID   : Radio Frequency Identification
SLA   : Sealed Lead Acid
WAN   : Wide Area Network
W-CDMA   : Wideband Code Division Multiple Access

LIST OF TABLES

LIST OF FIGURES

RF ENERGY HARVESTING
IN WIRELESS COMMUNICATION SYSTEMS:
STATISTICAL MODELS FOR BATTERY RECHARGING TIME

SUMMARY

For electrical equipment, energy is the most important need to run. Moreover, the importance of energy is much greater for wireless electrical devices. Is it possible to provide sufficient energy to all devices in time? How can we reduce the energy dependence of electrical devices? In the literature, the scope of research on energy is quite large. Green energy is an emerging research area all over the world. Our thesis can be evaluated as a research on energy of wireless communication systems. The energy harvesting systems contribute to energy requirements of low-power devices as renewable energy sources. In this thesis, RF energy harvesting is emphasized for providing energy to wireless communication devices.

Before giving the details of study, the basic informations about the energy harvesting for wireless communications need to be explained. Energy harvesting is used to ensure self-powered devices by gathering energy from ambient sources. It converts the received energy into direct current (DC) signal energy. The RF signal as a source of energy is one of the alternatives available for energy harvesting. The RF signal can be a good choice with the increasing use of wireless communication technologies. The research activities on the energy harvesting tend to increase continuously. The significant distinction of research is the type of energy source used in the energy harvesting systems. We specifically focus on the RF energy harvesting and the related basic issues in the literature review. In the literature, the papers on the energy allocation are of great importance. On the other hand, the papers on RF energy harvesting usually try to increase the efficiency of energy harvesting components. Currently, there are no contributions about the impact of wireless channels on the RF energy harvesting systems.

In communication systems, the statistical models describe the behaviour of wireless channels to the incident electromagnetic signal. The impacts of wireless channels are caused by path loss, reflection, diffraction, and scattering of signals. An overview for wireless channel models are given as background information, which include small scale and large scale effects. Among them, the lognormal shadowing distribution, the Nakagami-m distribution, and the generalized-K distribution are well-known models and used in this study.

The parameters of wireless channel directly affect the received power at the front end of antenna. The equations for the received power are known for various channel types. In addition to this information, it is shown in our thesis that the battery recharging time is inversely proportional to the received power. Depending on the relationship between the battery recharging time and the received power, it is possible to derive the distribution equations of the battery recharging times for the given channels.

Initially, the closed form expressions for the battery recharging times are derived in the presence of a single RF source. We derive the probability density function (PDF), the mean, and the variance expressions of battery recharging time for the lognormal shadowing distribution, the Nakagami-m distribution, and the generalized-K distribution. Moreover, the cumulative distribution function (CDF) and the moment generation function (MGF) are also derived for the generalized-K distribution. Next, we investigate the battery recharging time in the presence of multiple RF sources. In this context, the transformation of multiple random variables is reminded to find the expressions of the battery recharging time. We express a cascaded convolution equation to calculate the PDF of the battery recharging time for the generalized-K distribution.

In order to simplify the statistical expressions analytically, the Gamma distribution is used for channel approximation by means of the moment matching method with an adjustment factor. The Gamma distribution provides a close approximation for the generalized-K distribution. We derive the closed form expressions of the PDF, the CDF, the MGF, the mean, and the variance of the battery charging time for this Gamma distribution. These expressions are available for both single RF source and multiple RF sources.

In addition to theoretical modeling studies, the numerical and simulation analyses are performed for various channel conditions. The effects of channel parameters and the number of RF sources are presented via the numerical results. The derived expressions of the battery recharging time are verified by simulation results. Moreover, testbeds are implemented to show real applications of the RF energy harvesting. The tests on the energy harvesting of an wireless sensor node from RF sources are performed, and results are presented.

As a conclusion, the effects of channel conditions should be taken into account while designing an RF energy harvesting system. The derived parametric expressions can be used for RF energy harvesting systems. We propose the battery recharging time as a critical parameter for RF energy harvesting devices, especially for the wireless sensor networks to ensure the sustainability of the system.

KABLOSUZ HABERLEŞME SİSTEMLERİNDE
RF ENERJİ HASATLAMA:
PİL ŞARJ ZAMANI İÇİN İSTATİSTİK MODELLER

ÖZET

Teknolojinin büyük bir hızla geliştiği günümüzde, cihazların çalışabilmesi için gerekli olan enerji bir numaralı kaynak olarak ortaya çıkmaktadır. Haberleşme sistemlerinde de frekans bandı ile beraber en önemli iki kaynaktan birisi enerjidir. Enerjinin sınırlı bir kaynak olduğu ve verimli olarak kullanılması gerektiği açık bir şekilde ortadadır. Bu sebeple, günümüzde kullanılan klasik enerji kaynakları yanında, yeni ve yenilenebilir enerji kaynakları araştırılmaktadır. Yeni bir enerji kaynağı olarak nitelenebilecek olan enerji hasatlama sistemleri, enerji kullanan her cihazın çevrede bulunan güneş, rüzgar, basınç, ısı ve elektromanyetik işaretler gibi mevcut enerji kaynaklarını kullanarak, enerji bakımından kendi kendine yetmesi olarak açıklanabilir. Özellikle düşük güç harcayan cihazlarla kullanıldığında enerji hasatlama bütünleyici bir çözüm olarak ortaya çıkmaktadır.

Endüstriyel alanda kablosuz sensör şebekeler, radyo frekansı ile tanımlama sistemleri, tıbbi ve askeri cihazlar enerji hasatlamanın sayılabilecek bazı uygulama alanlarıdır. Tüketici elektroniği alanında ise mobil cihazlar ve dizüstü bilgisayarlar, gelecekteki teknolojik gelişmelere bağlı olarak, enerji hasatlamanın kullanıldığı önemli cihazlar olabilir. Enerji hasatlama teknolojisinin bu gün geldiği noktada hareket enerjisini, güneş enerjisini, elektromanyetik işaret enerjisini elektrik enerjisine çevirerek enerji hasatlayan mikro üreteçler yapılmaktadır. Bu ürünlerin, özellikle düşük güç harcayan sensörlerden oluşan kablosuz sensör şebekelerde kullanımı mümkündür. Bu sayede çok sayıda olan sensörlerin kablolama ve pil değiştirme maliyetlerinden kurtularak ekonomik ve operasyonel kazanç sağlanmaktadır.

Elektromanyetik frekans spektrumunun bir bölümü olarak tanımlanabilecek olan RF işaretleri de, haberleşme sistemleri için enerji hasatlama yapılabilecek enerji kaynaklarından biridir. Çevremizde heryerde bulunan RF işaret kaynakları gelişen kablosuz haberleşme teknolojilerinin yaygınlaşması ile beraber devamlı olarak artmaktadır.

Enerji hasatlayan cihazlar, elde ettikleri enerjiyi doğrudan kullanabildikleri gibi enerji depolama birimlerinde de depolayabilirler. Genellikle, hasatlanan enerji doğrudan kullanım için yeterli olmadığından bir pil veya süper kapasitörün şarj edilerek kullanılması uygun görülmektedir. Bu tezde, RF işaretinden enerji hasatlama konusu ele alınmakta ve RF işaretinden enerji hasatlama sistemlerinde pil şarj zamanının istatistiki olarak nitelenmesi üzerine bir çalışma yapılmaktadır. Pil şarj zamanı, bir pilin veya bir kapasitörün belli bir yük doluluk oranına ulaşması için gereken süre olarak tanımlanabilir. Pil şarj zamanı, RF işaret kaynağı ve enerji hasatlama düğümü arasındaki kablosuz kanalın istatistiki modeline dayanılarak modellenmektedir. Teorik çalışmalar sonucu elde edilen ifadeler, bilgisayar ortamında

yapılan benzetim çalışmaları ve enerji hasatlama geliştirme kitleri ile yapılan test çalışmalarıyla desteklenmektedir. Pil şarj zamanı, RF enerji hasatlama devresi bulunan kablosuz cihazlar için önemli bir parametre olarak önerilmektedir.

Enerji hasatlama son yıllarda oldukça ilgi çeken bir araştırma alanı haline gelmiştir ve bu alanda bir çok araştırma yapılmaktadır. Literatürde, enerji kaynağının türüne ve enerji hasatlama sisteminin üzerinde çalışılan birimine göre farklı makaleler ile karşılaşılmaktadır. RF işareti dışındaki enerji kaynaklarıyla ilgili çalışmalar konumuzun dışındadır. Bu sebeple, genel olarak enerji hasatlama ve özellikle RF işaretinden enerji hasatlama üzerine kapsamlı bir literatür taraması yapılmıştır. Literatürde, ilgi alanımıza giren enerji hasatlama konusu esas olarak iki eksen üzerinde ele alınmaktadır. Bunlardan ilki elde edilen enerjinin yönetilerek optimum şekilde kullanılması, diğeri de RF işaretinden DC işaret elde etmeye yarayan devrelerin tasarımıdır. Enerji yönetimi ile ilgili makalelerde, enerjinin hangi kaynaktan alındığı üzerinde durulmamıştır. Bu makalelerde, enerjinin ve verinin paketler halinde geldiği düşünülerek sistem modeli oluşturulmuştur. Bu sistem modeline göre hasatlanan enerjinin kablosuz şebekelerde veri gönderimi için optimum olarak kullanımı üzerine çalışılmıştır. RF işaret kaynağı kullanılan çalışmalarda ise ağırlıklı olarak anten ve devre tasarımı üzerine yoğunlaşıldığı görülmüştür. Bunların yanında enerji ve verinin birlikte iletimi üzerine ve bilişsel radyo şebekelerde enerji hasatlama üzerine de çalışmalar mevcuttur. Açık bir alan olarak gördüğümüz ve tezimizde ilgilendiğimiz konu; kablosuz kanalın RF enerji hasatlamaya etkisinin gösterilmesi ve pil şarj zamanının modellenmesidir. Bu bağlamda tezimizde, çalışmamıza temel oluşturan RF enerji hasatlama sisteminin yapısı ve kanal modelleri ayrı birer bölüm olarak ele alınmış ve açıklayıcı bilgiler verilmiştir.

Bir RF enerji hasatlama sistemi anten, gerilim şartlandırma ve enerji depolama ana birimlerinden oluşturmaktadır. Anten tarafından alınan RF enerjisi, DC enerjiye dönüştürülerek depolanmakta ve kullanılmaktadır. Anten, havadaki RF işaretini elektrik işaretine dönüştüren bir birimdir. Antenin çıkışında elde edilen elektrik işareti cihazları çalıştırmakta doğrudan kullanılamaz. Bu sebeple antenden gelen işaret, gerilim şartlandırma devresinde DC işarete çevrilir ve genellikle bu işaretin gerilimi düşük olduğu için yükseltilerek istenilen seviyeye getirilir. Burada elde edilen enerji, enerji depolama birimi olan bir pilin veya bir süper kapasitörün şarj edilmesinde kullanılabilir. Yeterli doluluk oranına ulaşan pil veya süper kapasitördeki enerji cihaz tarafından kullanılır.

Kablosuz haberleşme sistemlerinde, alıcı ile verici arasında elektromanyetik işareti etkileyen bir kanal vardır. Vericiden gönderilen işaret, iletim ortamında bulunan coğrafi yapılara, binalara ve nesnelere çarparak yansıma, kırılma ve saçılma etkilerine maruz kalır. Bunun sonucunda, gönderilen işaret değişerek ve uzaklık sebebiyle yol kaybına uğrayarak alıcıya ulaşır. Kablosuz haberleşme sistemlerinde, alıcı ile verici arasındaki kanalın elektromanyetik işarete etkisini tanımlamak için kanal modelleri kullanılır. Yol kaybı, gölgeleme ve sönümleme diye genel olarak tanımlanan kanal etkileri kapalı formda eşitliklerle ifade edilebilmektedir. Tezimizde, bu modeller anlatılmış ve iyi bilinen Lognormal, Nakagami-m ve Genelleştirilmiş-K dağılımları pil şarj zamanı için kullanılmıştır.

Kablosuz kanalı modelleyen dağılımlarda kullanılan parametreler, anten tarafından alınan işaretin gücünü doğrudan etkiler. Kanalın etkisine bağlı olarak alınan gücü ifade eden eşitlikler, çeşitli kanal tipleri için önceden belirlenmiştir. Bunun dışında, pil şarj zamanının alınan güç ile ters orantılı olduğu tezimizde gösterilmektedir. Pil şarj zamanı ve alınan güç arasındaki bu ilişkiye dayanarak, verilen kanal modelleri için pil şarj zamanının dağılımını gösteren eşitlikler türetmek mümkündür.

Çalışmamızda öncelikle tek RF kaynağı olması durumunda pil şarj zamanı için kapalı formda ifadeler elde etmek için çalışılmıştır. Lognormal gölgeleme, Nakagami-m sönümleme ve Genelleştirilmiş-K bileşik dağılımları için pil şarj zamanının olasılık yoğunluk fonksiyonu, ortalama ve varyans ifadeleri türetilmiştir. Ayrıca, Genelleştirilmiş-K bileşik dağılımı için birikimli dağılım fonksiyonu ve moment üretim fonksiyonu da türetilmiştir. Daha sonra, birden fazla RF kaynağı olması durumunda pil şarj zamanının nasıl ifade edileceği araştırılmıştır. Pil şarj zamanının bulunabilmesi için bir ön bilgi olarak, çoklu rastgele değişkenlerin dönüşümü ayrı bir konu olarak anlatılmıştır. Buna göre Genelleştirilmiş-K dağılımı için, ard arda konvolüsyonlar alarak pil şarj zamanının olasılık yoğunluk fonksiyonu elde edilebilmektedir.

Kapalı formda ifadeler bulup analitik olarak ilerleyebilmek için, Genelleştirilmiş-K yerine Gama dağılımı yaklaşımının kullanılması önerilmiştir. Gama dağılımı, moment uyumu metodu ile Genelleştirilmiş-K dağılımına yaklaştırılmaktadır. Moment uyumu metodu yanında bir düzeltme parametresi kullanılması durumunda, Gama dağılımı Genelleştirilmiş-K dağılımına daha iyi bir yaklaşım sağlamaktadır. Gama dağılımı kullanılarak pil şarj zamanı için kapalı formda olasılık yoğunluk fonksiyonu, birikimli dağılım fonksiyonu, moment üretim fonksiyonu, ortalama ve varyans ifadeleri türetilmiştir. Bu ifadeler, ortamda hem tek RF kaynağı hem de birden fazla RF kaynağı bulunması durumunda kullanılabilir.

Tezimizde teorik modelleme çalışmalarımıza ek olarak, çeşitli kanal koşulları için bilgisayar ortamında sayısal ve benzetim analizleri yapılmıştır. Sayısal sonuçlar vasıtasıyla, kanal parametrelerinin ve RF kaynak sayısının pil şarj zamanı üzerine etkisi gösterilmiştir. Pil şarj zamanı için elde ettiğimiz ifadeler, benzetim sonuçları ile doğrulanmıştır. Bunun yanında, RF enerji hasatlama için üretilen geliştirme kitleri kullanılarak test ortamı oluşturulmuştur. Bu test ortamlarında gerçek RF enerji hasatlama uygulamalarının gösterilmesi amaçlanmıştır. Kablosuz sensör düğümün enerjisinin RF enerji hasatlama ile elde edilmesi ve kullanılması için testler gerçekleştirilmiş ve test çıktıları sunulmuştur.

Sonuç olarak, bir RF enerji hasatlama sistemi tasarlanırken kablosuz kanal koşullarının dikkate alınması gerektiği görülmektedir. Pil şarj zamanını, RF enerji hasatlama cihazları ve özellikle kablosuz sensör ağlarında sürdürülebilirliğin sağlanması için önemli bir parametre olarak önerilmektedir. Çalışmamızda elde edilen parametrik ifadeler RF enerji hasatlama sistemlerinde kullanılmak üzere sunulmuştur.

1. INTRODUCTION

In human life, the role of wireless communication devices increases day by day. The development and deployment of supporting systems continue on all areas of mobile and wireless communication networks. As one of the most common communication systems, cellular mobile communication systems are experiencing major changes in a short time. It is reported in February 2014 that 268 Long Term Evolution (LTE) networks were commercially launched in 100 countries, although the launch of the first LTE network in Sweden is performed in December 2009 [1]. In addition to that, according to the forecasts, the number of machine-to-machine (M2M) connections will grow to 12 billion in 2020 [2]. Moreover, the number of wireless sensors deployed per year will grow significantly with the increase of deployment of wireless sensor networks. The communication industry is responding to these growing demands by producing new user-friendly, fast, and smart wireless devices and systems. However, researchers have some challenges to develop the technology of wireless communication systems. The main constraint is the energy, which is one of two primary resources for the communication systems. The absence or scarcity of energy obstructs the realization of proposed new technologies and makes mobility difficult in the wireless communication systems.

Currently, main mechanisms to provide energy are the energy storage devices and the power cables. In the wireless communication systems, it is not meaningful and possible to use power cable for all applications. Mainly, it causes the loss of mobility for mobile devices, and high investment cost for stationary devices. On the other hand, the energy storage devices are in wide use to power wireless communication equipments. The most common energy storage devices are disposable or rechargeable batteries. The disposable batteries have problems like more cost and replacement difficulties due to the working environment. The rechargeable batteries need a corresponding recharging point and enough time for recharging. And both

of disposable and rechargeable batteries increase the size and the weight of devices, and cause environmental problems. Moreover, the expiring of batteries inhibits sustainability of the communication systems that are sensitive to the outage of energy.

Hence, researchers investigate green, renewable, robust, and reliable energy sources that are the requirements of communication devices. As a prominent and practical idea, the energy harvesting systems are considered to power wireless devices like energy sources. Energy harvesting implies to obtain energy from ambient energy sources. A device with an energy harvesting circuit exploits the energy of the medium to provide its own energy. In this regard, energy harvesting is very intriguing for researchers. However, the first question that comes to mind is whether energy harvesting achieves the required energy for powering electrical devices or not. The amount of harvested power should be at least as much as the power required for device. In order to ensure this condition, the energy harvesting technology and the power consumption of electrical device are selected according to each other. The use of rechargeable micro-batteries and supercapacitors in energy harvesting circuits facilitates the implementation of energy harvesting technologies. Furthermore, energy harvesting seems more suitable for low-power devices. Today, the micro-generators that convert mechanical energy, solar energy, and RF signal energy into electrical energy by energy harvesting technologies are produced and used in the market. As an example, Arveni [3], which is a piezo energy harvesting company, develops a harvesting technology used to produce a batteryless remote control device.

The RF signal energy can be used as an energy source for energy harvesting systems. Although the power of RF signal decreases severely with increasing of distance, RF signal is ubiquitous, which is the main advantage of RF signal. As a realized product, Powercast Corporation [4] produces microchips that convert RF signal into DC signal. The RF signal energy available in the medium is received by the antenna of RF energy harvesting system, and converted to DC signal energy to power the electrical device.

The RF energy harvesting systems can be deployed in many wireless communication systems, which have already been using RF signals. Today, the most common use area of RF energy harvesting systems can be considered as the wireless sensor network. The wireless sensor networks, whose nodes consume low power, are good candidates

2

to use RF energy harvesting technology. A wireless sensor node of the wireless sensor network transmits message when the amount of stored energy is sufficient. Thus, a wireless sensor node with energy harvesting becomes self-sufficient as an autonomous device. As a result, the RF energy harvesting systems ensure sustainability of wireless sensor networks by increasing the lifetime of sensor nodes.

In the literature, energy harvesting is a relatively new research field with increasing popularity. There have been many papers on the different aspects of energy harvesting. The details of literature will be explained in the next chapter. In this thesis, we deal with RF energy harvesting. The open issue in the literature is the effect of channel conditions in the energy harvesting systems. Especially, we emphasize the battery recharging time as an important parameter in the wireless sensor networks. Since the aim of a wireless sensor network is to maximize data transmission rates or to increase transmission time, the energy harvesting wireless sensor nodes with finite energy capacity need to estimate the amount of harvested power and the battery recharging time. Thus, each node can perform tasks to ensure performance criteria of the wireless network by prediction of the harvested power and the battery recharging time. The equations of probability distributions for the received power are available in the presence of various channel conditions, whereas there is no study to obtain closed form expressions of statistical models for the battery recharging time. However, the prediction of the received power is not enough by itself. The knowledge of battery recharging time is a requirement. The sensor nodes can set their sleep and active periods according to the battery recharging time. Based on these facts, it can be concluded that the battery recharging time is an important performance parameter for energy harvesting systems, and the associated statistical characterizations in the presence of wireless channel impairments will be investigated in this thesis.

1.1 Scope of Thesis

In this thesis, we focus on energy harvesting from RF signal source. The research consists of six main chapters, as given below.

In the second chapter of this thesis, we present an overview and basics of energy harvesting, which includes the motivation and necessity of harvesting energy from

ambient sources. Further, the details of RF energy harvesting are presented. RF energy harvesting system that consists of antenna, energy conditioning unit, and energy storage unit are explained in separate sections.

In the third chapter, the literature review part investigates the related articles on energy harvesting. The papers on energy allocation and transmission policy hold an important place in the review. These research results presented for single-user, multi-user, and cooperative communication are independent from the source of energy. On the other hand, the papers on RF energy harvesting, which is our main research area, depend on the design of RF energy harvesting circuit. They contain generally the design of the device components of energy harvesting systems. In review sections, we highlight issues in the articles related to the subjects such as antenna, conditioning circuit, or storage unit. Additionally, our review mentions cognitive radio, and simultaneous information and power transfer in the context of energy harvesting. These papers are interested in both transmission policy and RF energy harvesting.

In the fourth chapter, we present the channel models for the wireless communication systems, on which we study the statistical distributions of battery recharging times. The signals transmitted from RF sources change in the wireless medium due to the small scale and the large scale effects. Path loss and lognormal shadowing are explained as the principal channel models for the large scale effect. The Nakagami-m distribution for the small scale effect is also explained. Moreover, we present the generalized-K distribution as a composite channel model. It is proposed to combine the small scale and the large scale effects in a channel model. The appropriate channel model is chosen according to transmission environment.

In the fifth and sixth chapters, we investigate a statistical model for the battery recharging time in the energy harvesting systems [5]. Our analyses are based on the channel models, as mentioned before. We define the relationship between the received power and the battery recharging time. In the next step, we also define the relationship between the distribution of received power and the distribution of battery recharging time. Hence, it is possible to obtain the distributions of battery recharging times for all considered channel models. Initially, we derive statistical equations for only a

single RF signal source, and then for multiple RF sources. The numerical results and simulations are also presented to show the accuracy of equations.

Finally, we work to establish the test environment for RF energy harvesting with the develoment kits of Powercast company. RF energy harvesting tests are performed for a single RF source for different distances. And then, a testbed is implemeted for two RF sources. We measure the received power and the recharging time of supercapacitor as a storage unit. We compare the test results with numerical results.

The conclusions are given in the last chapter.

1.2 Contributions

The purpose of this thesis is to present the effect of wireless channels on RF energy harvesting. We have introduced the battery recharging time in energy harvesting systems as a parameter for the wireless systems. As contributions of this thesis we present and discuss the following points:

- Statistical models in RF energy harvesting systems in the presence of single RF source and also multiple RF sources,

- Deriving the statistical equations of battery recharging time for corresponding models,

- Showing the effects of wireless channels on the distribution of battery recharging time by performing simulations,

- Supporting the numerical and simulation results with test results.

In the single RF source case, we study the statistical characterization of battery recharging time as a function of the received power using well known channel models: lognormal shadowing and the Nakagami-m fading. We also extend the results to the generalized-K channel that jointly models the large scale and the small scale effects. We derive the closed form expressions for the associated PDFs. We calculate the mean and the variance of battery charging time for a wide range of channel conditions. Additionally, we obtain the CDF and the MGF for the generalized-K channel. We

provide numerical results for a rechargeable micro-battery and verify our theoretical analysis via simulations. We demonstrate that the effects of small scale and large scale fading factors should be taken into account while designing an RF energy harvesting system.

After the single RF source case, we study the statistical characterization of battery recharging time for multiple RF sources case. We investigate closed form expressions in the presence of the generalized-K channel conditions. However, it is not straightforward with the generalized-K distribution for multiple RF sources case. We decided to use an approximation with the Gamma distribution instead of the generalized-K distribution. We derive the closed form expressions for the PDFs, the mean, and the variance of battery charging time for the Gamma distribution. Moreover, we obtain the CDF and the MGF of battery recharging time. We simulate our expressions and channel conditions for battery recharging time.

We also set up two testbed implementation for RF energy harvesting. We make test with a single RF source and two RF sources. We calculate small scale and shadowing coefficients. We investigate whether test results and equations fit together.

2. ENERGY HARVESTING

Energy harvesting is a system that targets gathering energy from external ambient sources for the purpose of providing energy to the electrical equipments. The magnitude of harvested energy can be in macro scale or micro scale according to the aim of the harvesting system. As examples of macro scale, solar panels or wind tribunes can produce sufficient energy to provide energy to high power lines in regional areas. These are very important operations in industrial area to produce energy from renewable sources. However, in micro scale, the harvested energy can be on the order of milliwatts or microwatts for low-power devices. Each device obtains its energy with an additional energy harvesting circuit. Considering our study, it will be more appropriate to use the energy harvesting term in the meaning of micro scale energy harvesting from now on.

The block diagram of energy harvesting system is presented in Figure 2.1. The harvested energy from ambient source is converted to DC signal energy and then directly used or stored into a storage device. After storing energy, the energy is managed for optimum usage.
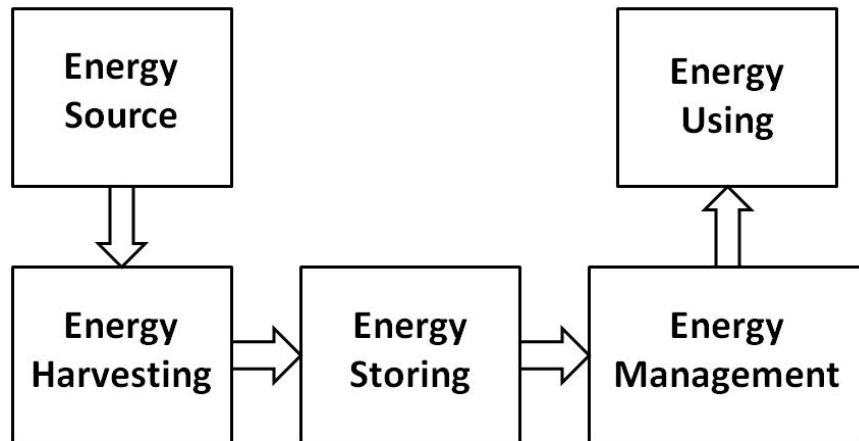
Figure 2.1: Block diagram of an energy harvesting system. Energy harvesting, energy storing, and energy management blocks are designed according to the type of energy source.

The energy sources for harvesting could be classified as radiant energy, thermal energy, and mechanical energy. The examples of these classes and their power densities are indicated as given below [6].

- Radiant Energy

    - RF signal: $40\mu W/cm^2$ at $10m$.

    - Solar wave: $100mW/cm^3$ at outside.

- Thermal Energy

    - Body heat: $60\mu W/cm^2$ at $5\,^\circ$C.

    - External heat: $135\mu W/cm^2$ at $10\,^\circ$C.

- Mechanical Energy

    - Body motion: $800\mu W/cm^3$.

    - Air flow: $177\mu W/cm^3$.

    - Vibration: $4\mu W/cm^3$.

Each energy source has advantages and disadvantages for energy harvesting. The maximum energy is obtained from solar waves, but its efficiency is low inside a building. Similarly, RF signals attenuate with distance and obstacles, which decrease signal level in building. In order to obtain thermal energy from body heat and external heat, high temperature difference is required. Mechanical energy depends on motion at the deployed area or surrounding. Besides, energy is harvested by using piezoelectric materials that convert the mechanical stress into electrical energy. The behaviour of piezoelectric material in the presence of mechanical stress affects the efficiency of system.

The design of an energy harvesting circuit depends on the exploitation of one or a combination of these sources, if it is convenient for application conditions. The design criteria depend on the availability of source, the amount of harvested power, and sustainability of the target system. The application areas of energy harvesting extend

from industry to personel devices, will increase with the development of harvesting technologies.

Considering the use of energy, the ideal case is to use the harvested energy to power device directly. However, usage of rechargeable storage devices are preferred as the harvested energy can be sporadic, random or small. Furthermore, it may not be available when required. Hence, the storage devices are critical for the energy harvesting systems, and the most frequently used storage devices are rechargeable micro batteries. Herein, the benefit of using energy harvesting system is to use smaller batteries, which decrease the size and weight of device, and environmental waste.

Energy management unit allocates energy to ensure efficient use of energy that is used to power devices. According to the profile of incoming energy and the tasks of device, the energy allocation is performed.

In this thesis, the research area is the RF energy harvesting systems as they will have an important role to ensure the ease of mobility. RF signals are everywhere every time and their intensity is increased by installation of TV towers, cellular base stations, and Wi-Fi access points continuously.

2.1 RF Energy Harvesting

RF refers to a frequency band of electromagnetic wave spectrum in the range of around 3 kHz to 300 GHz. It is possible to use electromagnetic waves for producing energy in the wireless communication systems. It is possible to use the intentional RF signal sources for providing energy to the electrical devices. When an intentional RF signal source is introduced in the system, it can be referred to RF energy transport [7]. The history of wireless energy transport goes back to famous Wardenclyffe Tower that Tesla built (1901–1917) in Shoreham, New York [8]. His aim was to send wireless energy from this tower to the whole devices over the world.

On the contrary of energy transport, electromagnetic signals can be obtained from environment. RF signal energy can be acquired from all wireless communication units such as stationary networking equipments and mobile user devices. When RF signals are harvested from ambient, such an operation is called as RF energy harvesting. If
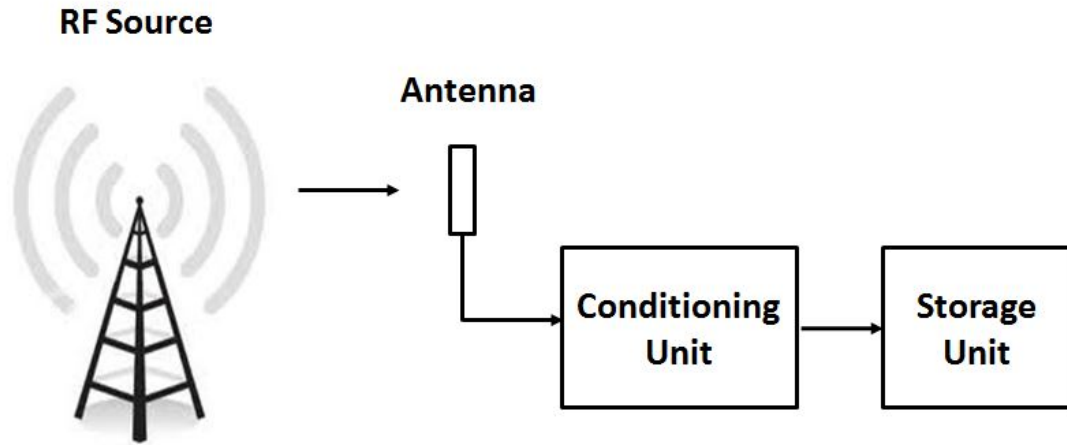
Figure 2.2: Operation of an RF energy harvesting system. RF signals are captured, conditioned and stored to power the target device.

the power density of ambient is not sufficient to harvest energy, we have to apply RF energy transport. However, the difference between the energy transport systems and the energy harvesting systems can be ignored in the sense of their targets, because both of them aim to ensure the operation of devices by obtaining wireless energy. So, the structure of both systems has same characteristics. In this context, it is convenient to name them as active and passive RF energy harvesting [9] or simply as RF energy harvesting.

Note that in short-range, the radio frequency identification (RFID) technology is a current application of energy transmission. RFID devices use the license-free industry–science–medical (ISM) frequency bands around 0.9, 2.4, and 5.8 GHz. We mention about the structure of RF energy harvesting system in far-field.

Mainly, the RF energy harvesting system is composed of successive antenna, energy conditioning, and energy storage units [10]. The operation of RF energy harvesting system is presented in Figure 2.2. RF signals propogated from communication devices are captured by the antenna that converts RF energy into electrical energy. In the conditioning circuit, the signal coming from antenna is rectified to obtain DC signal, and then multiplied by voltage multiplier to obtain desired voltage level. The harvested energy is used for providing energy to the target device. The parts of an energy harvesting system are explained in detail below.
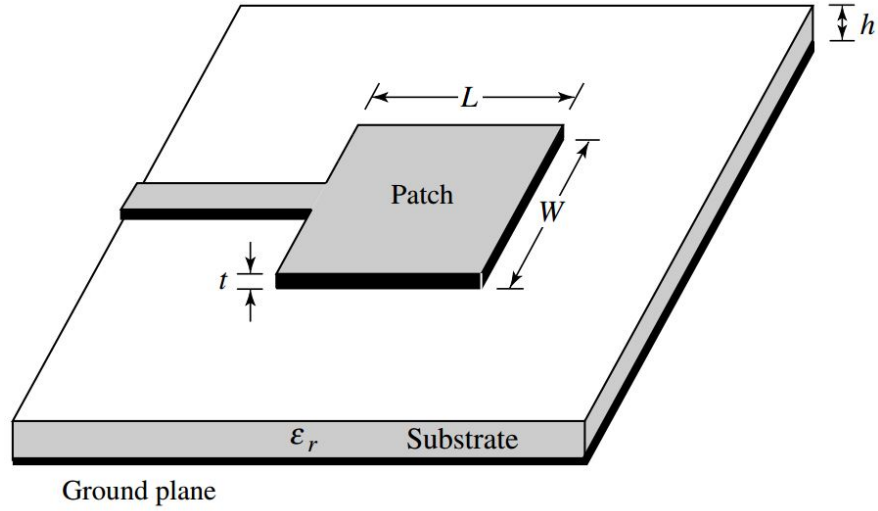
Figure 2.3: Rectangular microstrip (patch) antenna [11].

2.1.1 Antenna

The antenna is a transducer that converts a signal in one form of energy to another form of energy. Similarly, the antenna is defined as the transitional structure between free-space and a guiding device for radiating or receiving radio waves [11]. The transmitting antenna converts electrical signal into RF signal while the receiving antenna converts RF signal into electrical signal. The basic antenna characteristics are pattern, gain, directivity, radiation efficiency, impedance, current, and polarization of antenna. There are many types of antennas such as wire, aperture, microstrip, array, reflector, and lens antennas. In Figure 2.3, the rectangular microstrip (patch) antenna is shown as an example.

$$Z_A = (R_L + R_r) + jX_A$$
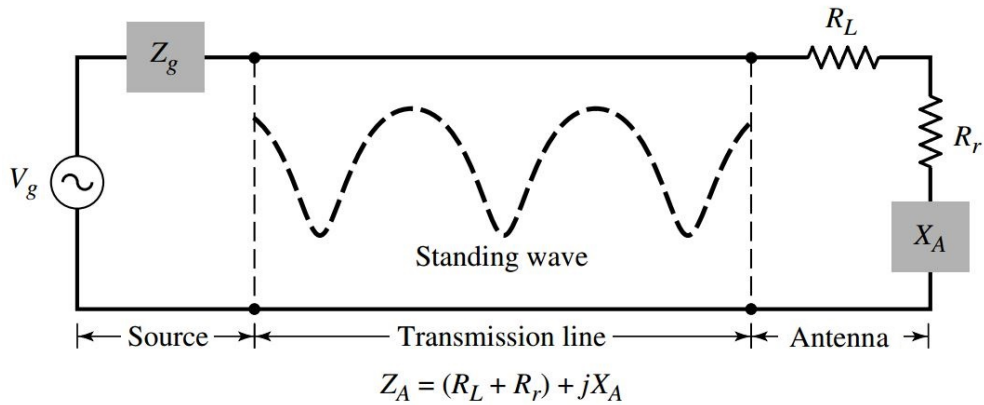
Figure 2.4: Transmission-line Thevenin equivalent of transmitting antenna. Antenna is considered as a load with complex impedance [11].

An antenna in transmitting mode can be considered as a load Z_A shown in Figure 2.4. The resistance of R_L and R_r represent conduction-dielectric losses and radiation part of antenna, respectively. X_A represents the imaginary part of impedance in Thevenin equivalent of antenna. The maximum power transfer from source to the antenna is delivered under conjugate matching case. The standing waves are caused by the reflected waves from interface between the transmission line and the antenna. For antenna system design, the internal impedance of source, line loss, and reflection loss should be considered to ensure signal transmission properly.

The antenna is the front end of RF energy harvesting systems. It captures RF signal, and converts to electrical signal as an input to the conditioning circuit. There are many studies to design antennas such as microstrip patch, helical, loop or Yagi-Uda antennas for the RF energy harvesting systems [12–18]. Most of the studies on RF energy harvesting systems are using microstrip single antennas. The microstrip antennas have small size and high efficiency, convenient for energy harvesting. As an example of microstrip antennas, prototype and radiation pattern of a microstrip antennas is shown in Figure 2.5. In addition to single antennas, the array form of antennas are used to harvest more energy, which increases the size of antenna as an undesired situation.
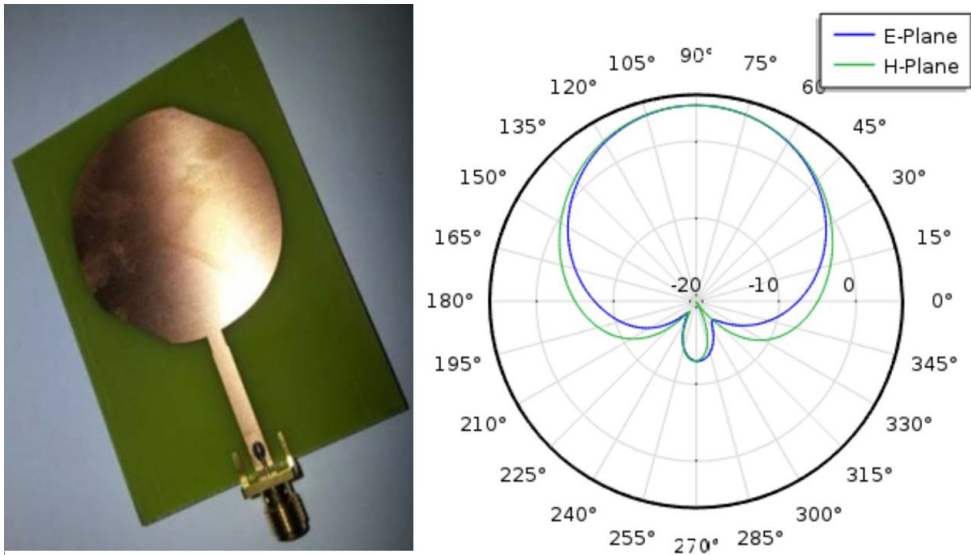
Figure 2.5: Prototype and radiation pattern of the microstrip single patch antenna [13].

In the antenna system design, the informations about the location of transmitter, the operation frequency, and the bandwidth of antenna are primary design factors [14]. If the location of the transmitter is unknown, the antenna need to be omnidirectional

that has low gain. Otherwise, the directional antennas are used with higher gain capacity. If the antenna capture RF signals of all frequencies, it is necessary to design an antenna for broadband. If not, a narrowband antenna with matching circuit should be used to capture the maximum power. Besides, other basic antenna characteristics are determined according to the requirements of application. Consequently, the antenna design affects the harvested power and also the whole performance of RF energy harvesting system.

2.1.2 Conditioning unit

The energy conditioning unit consists of one matching circuit, one rectifier circuit, and one voltage multiplier circuit. A simple conditioning circuit is indicated in Figure 2.6. The matching circuit is used to address the impedance mismatch at the interface between the rectifier circuit and the antenna. A simple impedance matching circuit is formed by a series combination of lumped elements such as inductors and capacitors. It provides efficient RF to DC conversion by serving good impedance matching.
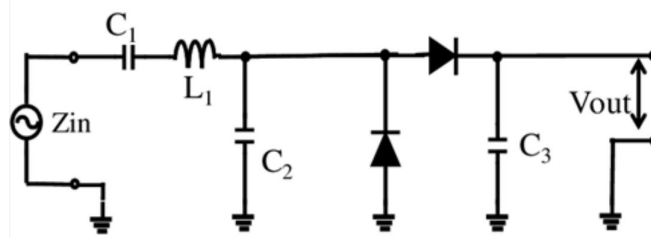
Figure 2.6: A simple conditioning circuit [15]. It performs the functions of matching, rectifying, and multiplying.

In energy harvesting from RF signals, the received power density is low due to severely decreasing of energy with the distance from the source. Because of low power density at the receiver, the obtained voltage level becomes in low mV and μV levels, although the low-power electrical devices are usually powered by more than 1V DC voltage. Therefore, it is necessary to use the rectifier and the voltage multiplier. The rectifier is an electrical circuit that converts the received power from antenna into DC power. The basic rectifier circuit is designed a combination of a diode as a rectifying device, a shunt capacitor, and the load resistor.

Since, the output voltage of the rectifier circuit is too low for directly powering of electrical devices, the voltage multiplier circuit is added to the output of the rectifier

circuit. The voltage multiplier circuit boosts a lower voltage to a higher DC voltage using a combination of capacitors and diodes [15]. The characteristic of diode is very important to ensure the conversion from RF signal energy into DC signal energy efficiency [16]. Schottky diode has low forward voltage and high switching speed, which provides both high power conversion efficiency and high voltage gain. Hence, Schottky diode is usually used in the rectifier and the voltage multiplier circuits [17]. In order to increase the voltage sensitivity value, it is possible to use cascaded Schottky diodes. The voltage multiplier circuit can be one-stage or multi-stage to increase DC voltage from low level to the required high level. Figure 2.7 presents the schematics of a 5-stage modified Dickson charge pump as an example of multi stage voltage multiplier. Additionally, the output voltage of rectifier circuit changes with the changing value of input power. The voltage multiplier circuit regulates the rectified voltage to the voltage of device to be used.
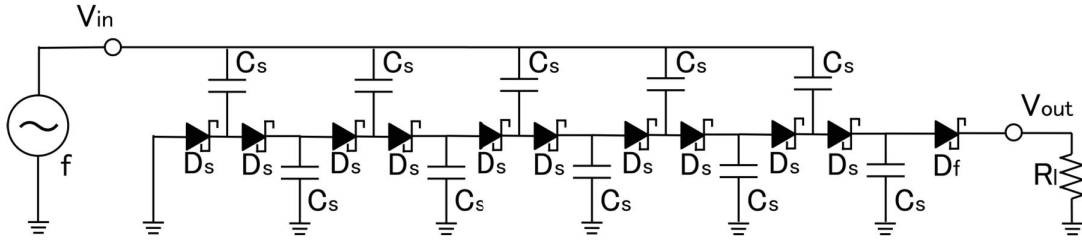
Figure 2.7: Schematics of a 5-stage modified Dickson charge pump [18]. Voltage is boosted up at each stage.

2.1.3 Storage unit

The RF energy harvesting systems need an energy storage unit, because the amount of harvested energy is usually not sufficient to power electrical devices directly. The most common energy storage units are rechargeable batteries for energy harvesting systems. There are mainly 3 types of rechargeable battery technologies, which are lead-based, nickel-based, and lithium-based such as Sealed Lead Acid (SLA), Nickel Cadmium (NiCd), Nickel Metal Hydride (NiMH), and Lithium Ion (Li-ion). The performance of battery technologies are evaluated according to output voltage, capacity, energy density, power density, efficiency, self-discharge rate, memory effect, charging method, and recharge cycles. Depending on these parameters, lithium-based

and NiMH battery technologies have been proposed for energy harvesting systems [19].

Recently, a technological trend in rechargeable battery is of thin film solid-state batteries [20]. Infinite Power Solutions [21] and Cymbet Corporation [22] are two main manufacturers of rechargeable thin film solid-state batteries with a charging capacity of 0.1 to 2.5 mAh. Cymbet Corporation produces EnerChip^{TM}, and states that EnerChip is more than 10x smaller than nonrechargeable coin cell batteries. Moreover, it lasts 3x longer than conventional coin cell batteries. These batteries have very light weight which are less than 1g, and very thin thickness which is less than 200μm, and also very long lifetime which is up to 100,000 recharging cycles. The rechargeable thin film solid-state batteries can be recharged by trickle charging that is appropriate to the nature of energy harvesting systems. Figure 2.8 shows the rechargeable thin film solid-state battery of Infinite Power Solutions, Thinergy^{TM}.

Figure 2.8: A rechargeable thin film solid-state battery of Infinite Power Solutions, a charging capacity of 0.7 mAh [21].

Supercapacitors are other alternatives to use in the energy harvesting systems for storing energy with higher energy density than normal capacitors. The order of millions recharging cycles is possible in the operation of supercapacitors. They also have higher power density than batteries, which provide a large amount of energy in a short duration. However, the self-discharge rate of supercapacitors is higher than batteries. Hence, there is a tradeoff between supercapacitors and batteries.

In the energy harvesting systems, the use of both rechargable micro-batteries and supercapacitors provides low size, low weight, and don't require to access the device

for replacement. According to differences between their characteristics, the suitable storage unit is chosen for a given energy harvesting application.

2.2 Conclusions

In this chapter, we explain the scope of energy harvesting term. Energy sources for energy harvesting and their energy capacities are investigated. RF signal is ubiquitous due to common wireless networking applications. It can be seen that RF signal is a possible energy source for energy harvesting systems. The main parts of RF energy harvesting system are antenna, conditioning unit, and storage unit, which are explained in detail. Antennas, matching circuits, rectifiers, voltage multipliers, batteries, and supercapacitors are important parts for wireless systems. They can be designed according to the requirements of RF energy harvesting systems. The related literature is reviewed in the following chapter.

3. LITERATURE REVIEW

Recently, the number of energy harvesting related publications increase in parallel to the usage of energy harvesting systems in wireless networking applications. A comprehensive literature review is given on common research areas of energy harvesting. The encountered papers during review vary according to the type of energy source and the part of interest of energy harvesting system. The reviewed papers can be classified into two groups, which are the papers about energy allocation in energy harvesting systems and the papers about RF energy harvesting systems. The details of reviewed papers are given in the following sections.

3.1 The Literature on Energy Allocation in Energy Harvesting Systems

The most popular area is about optimal transmission policy and energy allocation of devices that are equipped by the energy harvesting systems. The goals of transmission policies are transmission completion time minimization and short-term throughput maximization. Transmission completion time minimization implies to minimize the time at which all bits have been sent by transmitter for given a number of bits. Short-term throughput maximization implies to maximize the number of bits sent before the end of transmission for given a deadline. The most relevant papers are explained according to main characteristics.

3.1.1 Single-user communication systems

The following two papers are about single-user communication with an energy harvesting transmitter. The optimal scheduling policies are developed for different scenarios.

Yang and Ulukus [23] investigate the optimal packet scheduling in a single-user energy harvesting wireless communication system. The system model is shown in Figure 3.1. The incoming data and the harvested energy reach to transmitter, and are queued in
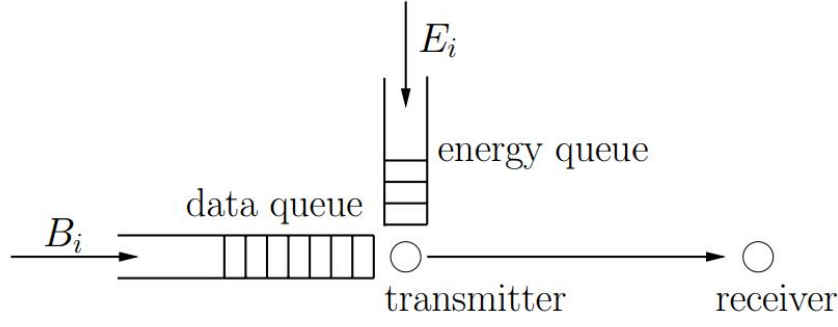
Figure 3.1: An energy harvesting communication system model for single-user. B_i denotes the number of bits and E_i denotes the amount of harvested energy in the ith arrival [23].

the data queue and in the energy queue, respectively. In this model, it is assumed that both the energy harvesting times and amounts, and the data packets arrival times and sizes are known before the transmission starts. The transmitter sends data with a fixed amount of harvested power to ensure a transmission rate, which is a function of harvested power. The goal of research is to sent all data packets in the minimum time by adaptively setting the transmission rate under constraints such as the data traffic and available harvested energy. The optimal offline transmission policies are developed for different cases to minimize transmission completion time.

In a system that contains an energy harvesting transmitter with finite energy storing capacity, Tutuncuoglu and Yener [24] consider the optimal transmission policy for single link. An optimal power allocation policy is proposed, which solves short-term throughput maximization problem for a given deadline. The feasible energy tunnel defines the area between energy arrivals upper staircase and finite battery constraint lower staircase as graphical description. The energy consumption curve must be in the feasible energy tunnel. It is shown that maximum amount of data transfer for a given deadline has same meaning with the minimum completion time for a given of amount of data. It is proved that the proposed algorithm of transmision policy provide optimal solution for energy harvesting system.

3.1.2 Multi-user communication systems

After single-user systems, the optimal scheduling policies for multi-user communication systems are investigated as stated below.

Ozel et al. [25] research the optimal transmission policy for transmission completion time minimization problem in a multi-user system. There is a system that consists of M receivers with an energy harvesting rechargable transmitter sending data in an additive white Gaussian noise (AWGN) broadcast channel. The system model is illustrated in Figure 3.2. Energy is harvested during transmission between transmitter and receiver. It is proved that M-user channel has same power structure as single user channel. A cut-off power is found for stronger user in two-user case. If the optimal total transmit power is lower than cut-off power, the total power is allocated to the stronger user. Otherwise, the total power is allocated to the weaker user. The result is extended to multi-user channel. The iterative algorithm is developed based on the structure of optimal policy.
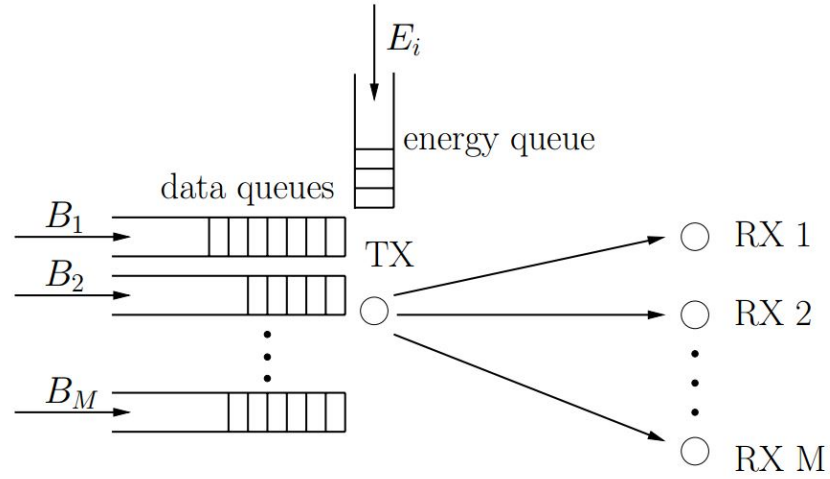
Figure 3.2: An energy harvesting communication system model for multi-user. TX represents transmitter. RX 1, ... , RX M represent receivers [25].

In [26], for the multi-user broadcast system, an energy harvesting transmitter is used with a finite capacity rechargeable battery storing energy. Ozel et al. study for developing the optimal transmission policy to minimize the transmission completion time under finite battery constraint. An algorithm is proposed for optimal offline policy that uses directional water-filling iteratively. It is proved that there are M-1 cut-off power levels to determine power allocation of M users.

3.1.3 Cooperative communication systems

It is possible to use energy harvesting nodes in different areas of cooperative communication. The following three papers are the most relevant works.

In [27], the cooperative transmission is performed to maximize throughput for a given deadline by a battery operated sensor node and an energy harvesting sensor node. In order to find the jointly optimal transmission policy for transmitting a common message to a distant base station, Berbalov et al. propose the jointly optimal transmission policy. The simulation results show that joint optimization of transmit policies in combination with beamforming provides a significant amount of throughput gains. When the energy of harvesting sensor and battery operated sensor are same, the obtained throughput gain becomes the highest gain.

Moreover, energy harvesting systems can be used in cooperative wireless networks. The usage of energy harvesting nodes as cooperative relay in wireless sensor networks is investigated by Bhargav et al. [28]. The energy harvesting sensor nodes amplify signals received from source node, and then forward to destination node. Herein, energy constrained and energy unconstrained concepts are introduced. The amount of harvested energy, the transmit power of relay and the total number of relays in the system affects the decision of energy constrained or energy unconstrained of a relay. As a result, energy harvesting relay systems give good results for enhancing performance when compared with conventional relay systems.

Also, the energy harvesting nodes can share their energy in an energy harvesting network, which is named as energy cooperation. Two-hop relay channel with energy harvesting source and relay nodes, and one-way energy transfer from the source node to the relay node are indicated in Figure 3.3. When a node needs a fixed amount of energy, an other node sends a portion of its available energy wirelessly. The main goal is to improve the performance of system by means of energy cooperation. Gurakan et al. [29] investigate the optimal power allocation in such a system with energy cooperation. A two-dimensional directional water-filling algorithm is proposed to control the flow of harvested energy between users in time. The proposed algorithm
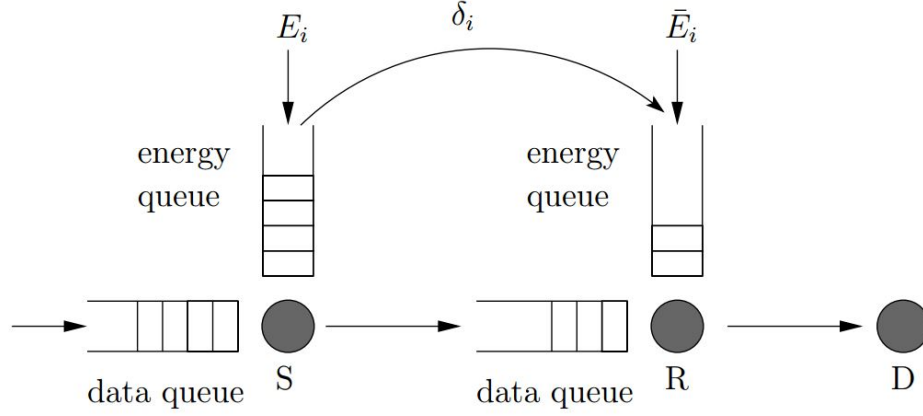
Figure 3.3: An energy harvesting communication system model with energy cooperation. *S*, *R*, and *D* indicate source, relay, and destination nodes, respectively [29].

ensures to transfer energy from one user to another while maintaining optimal allocation in time.

It is possible to increase the number of samples of energy allocation and optimal transmission policy [30–32]. Generally, these papers are independent from the type of source. Since the main research area is RF energy harvesing in this thesis, the papers on RF energy harvesting are reviewed in the next section.

3.2 The Literature on RF Energy Harvesting Systems

There are several research works according to various aspects of RF energy harvesting systems. Mostly, the improvement of energy conditioning circuits and antennas are handled to maximize the harvested power by maximizing conversion efficiency of energy harvesting circuit. The conversion efficiency is the ratio of the harvested power to the received power.

The reviewed papers perform designs by changing one or a few of equipment specifications such as type of antenna, type of storage device, value of capacitor, type of Shottky diode, number of stage used in voltage conditioning circuit etc. The related papers presented in the following sections are grouped to draw attention to the different aspects of RF energy harvesting systems, although they have some common issues with other groups.
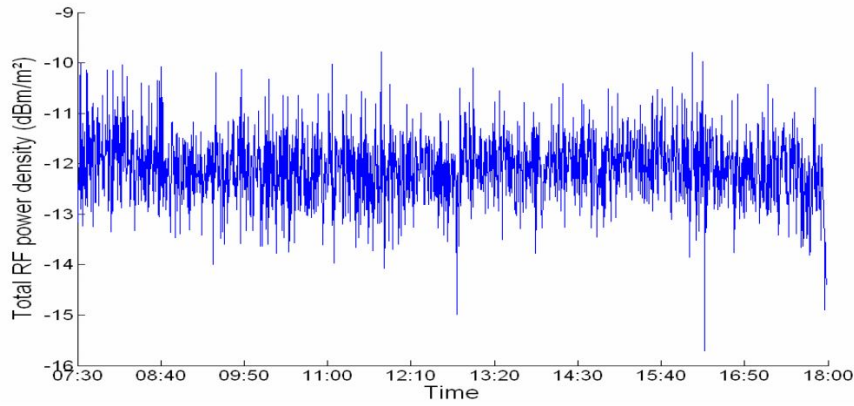
Figure 3.4: Total RF power density in the urban area, which is measured around -12dBm/m^2, versus time [33].

3.2.1 RF surveys

Before harvest energy, RF survey should be performed to know the potential capacity of ambient using a spectrum analyser. The structure of energy harvesting is based on RF survey to design broadband or narrowband circuit.

Bouchouicha et al. [33] present a study on RF energy harvesting techniques. RF power density in the different points in the urban environments is measured between -60dBm/m^2 and -14.5dBm/m^2 for the 680MHz-3.5GHz band. In addition, the total power density of all signals is measured around-12dBm/m^2, which is presented in Figure 3.4. An RF/DC converter circuit at broadband is designed with spiral antenna. And then, a matching circuit is added to the energy harvesting system to maksimize harvested power for narrowband. A prototype of antenna and rectifier, also called as rectenna, is fabricated. The harvested DC power with matching circuit rises from 12.5pW to 400pW. According to results, the harvested power is not sufficient to power a device directly, it needs a battery or super capacitor for storage and antenna array for maximizing input power.

The feasibility of energy harvesting is investigated with Powercast energy harvester. Baroudi et al. [34] perform an RF survey by scanning the available power spectrum at six different locations inside the King Fahd University campus. The following values of power is measured using Powercast omnidirectional (dipole) antenna.

- Whole spectrum (1MHz-2.7GHz) = -14.4dBm

22

- Band (900MHz-950MHz) = -31.0dBm

- Band (902MHz-928MHz) = -33.8dBm

- Band (500MHz-1500MHz) = -20.0dBm

The measured results show that the energy of ambient is not sufficient to harvest energy with a Powercast device. It needs more power than -10dBm via a dedicated transmitter. Also, the outdoor and indoor experiments are performed for different azimuths and elevations along radial line between transmitter and receiver. It is observed that the variations of azimuth and elevation values affect both of the received signal strength indicator and recharging time.

3.2.2 Antenna design

The characteristics of antenna are crucial for energy harvesting systems. The number, type, pattern, and structure of antennas can be changed to obtain the maximum power.

Gunathilaka et al. [10] design an RF energy harvesting circuit, which includes transducer, energy conditioning unit, and energy storage unit. The design of antenna includes the determination of antenna specifications such as gain, radiation pattern, bandwidth, efficiency, center frequency, and size. Tree types of antennas are examined with conditioning circuit and super capacitor that is used for energy storage. The harvested power from internet dongle and mobile phone is used to drive both of an light emitting diode (LED) and calculator. Figure 3.5 shows energy harvesting using micro strip antenna near mobile phone as 2.385V. The experiments show that dipole and micro strip antennas give better results than monopole antennas.

Mi et al. [35] propose the usage of multiple energy harvestig antennas to increase the amount of harvested energy. As an example, a design of four cooperating antenna is performed, which gives 300% more power by an increase of 83% in the area is presented. The utility factor is calculated by dividing 4 by 1.83 to get 2.18. The result shows that the use of multiple antennas is very useful method for energy harvesting. Also, it is possible to obtain better results with different antenna structures and dimensions.

Figure 3.5: Energy harvesting from mobile phone by using micro strip antenna. The measured voltage is 2.385V [10].

In [36], Visser et al. express that the rechargeable batteries charged by dedicated RF signals can be used for indoor wireless sensors. The received RF energy and therefore energy efficiency becomes low because of path loss. In order to increase efficiency, a transmit antenna with beam-shaping capabilities is performed by using six Yagi-Uda array antennas. Transmit antenna radiation pattern is adapted to the propagation channel characteristics, so the input power of the antenna and rectifier is maximized without increasing the effective isotropic radiated power (EIRP) of transmitter.

Keyrouz et al. [37] target to design an energy harvesting circuit from Digital TV stations. A broadband Yagi-Uda antenna is presented with a voltage conditioning circuit and antenna matching circuit, which works at 470-810MHz frequency band. The antenna have a reflector and a single director. The length of the director, the distance between the feed and the director, and the distance between the feed and the reflector are designed to obtain the widest bandwidth for receiving the digital television (DTV) broadcasting signals. The results show that the gain of proposed Yagi-Uda antenna is higher than 4.27dBi in the DTV frequency band. This value is suitable for energy harvesting from DTV stations.

3.2.3 Conditioning unit design

In the following papers, the design of energy harvesting systems are performed with different stages of multiplier circuit.

Arrawatia et al. [38] presents an energy harvesting system to harvest energy near a cellular base station. Firstly, a square micro strip antenna is designed, which gives 9.1dB antenna gain at 877-998MHz frequency band. Secondly, silicon based Schottky diode having threshold voltage of 230mV and diode capacitance of 0.26pF is used to design Dickson voltage conditioning circuits. The fabrication of single stage and 6-stage voltage conditioning circuit are achieved. 6-stage voltage conditioning circuit is used for lower power levels, whereas single stage circuit is used higher power levels. It is shown that a voltage of 2.78V is measured at a distance of 10m from the cellular tower.
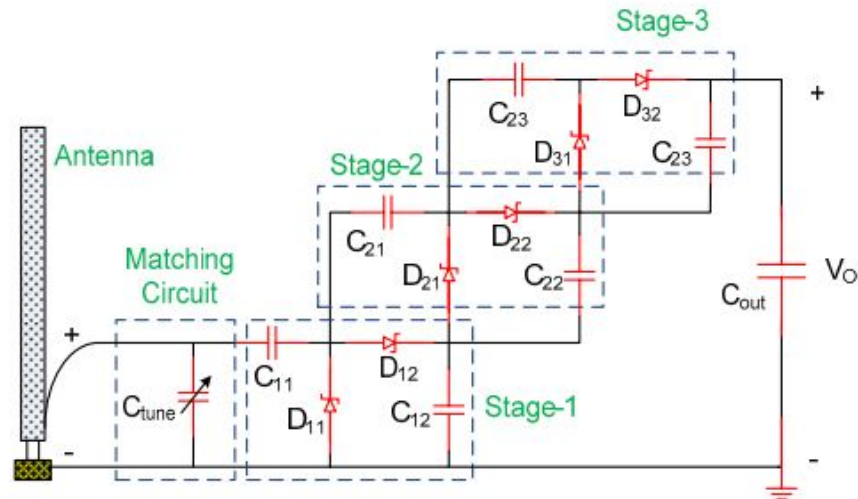
Figure 3.6: Schematics of a 3-stage Villard voltage conditioning circuit. It is a combination of capacitors and Schottky diodes [39].

Schottky diodes are suitable for voltage doubler circuits in RF energy harvesting systems with low forward voltage and high switching speed. Practical and simulation results are presented for Schottky based circuits at different frequencies from 400MHz to 2.4GHz in [39]. The schematic of a 3-stage Villard voltage conditioning circuit is shown in Figure 3.6. It is possible to use complementary metal oxide semiconductor (CMOS) transistor based voltage conditioning circuit instead of Shottky based circuit. Jabbar et al. also propose a new CMOS transistor based Villard voltage conditioning

circuit, which gives 160% more power than a traditional Villard voltage multiplier circuit at 0dBm input power.

In [40], Nintanavongsa et al. propose a dual-stage energy harvesting circuit composed of a 7-stage and 10-stage conditioning circuit design for low input power and high input power ranges. An optimization framework is developed to decide the switchover point between 7-stage and 10-stage conditioning circuit to obtain the highest efficiency. According to measurements, the fabricated prototype of proposed energy harvesting circuit gives 100% more performance between -20dB - 7dB than Powercast 1100 energy harvesting device.

ElAnzeery and Guindi [41] perform a simulation survey to show the effect of frequency in energy harvesting systems. Different frequencies ranging from 50MHz to 9GHz are chosen to accomplish simulations for 3, 9, and 13-stage conditioning circuits. The output voltages of conditioning cicuits change for different frequency values. The results show that 500MHz is the most suitable for a 3-stage conditioning circuit, and 915MHz is the most suitable for a 9-stage conditioning circuit. As a result, there is a relation between used frequency and the stage of circuit which affect the size of energy harvesting circuit.

ElAnzeery et al. [42] also present an energy harvesting model for RFID system that works at 2.1-2.45MHz frequency band. Various frequencies starting from 50MHz up to 9GHz, capacitor values from 560pF to 1μF, number of stages from 1 to 11, and six different Shottky diode types are experimented to obtain output voltages in simulations. The output voltage values vary from 0V up to 4.222V, which show the effect of operation frequency and chosen equipments. According to results, wireless sensor nodes and RFIDs can be powered with the proposed energy harvesting system.

Because of variation in the power density during RF transmission, it is useful to use power management circuit to obtain maximum power independent of the load behavior.

It is expressed that an efficient application below mW levels has not been realized due to constraints in current control circuits [43]. In order to perform online optimization and efficient operation over a wide range of operating conditions, Dolgov et al. propose a smart microcontroller based maximum power point tracking (MPPT) power
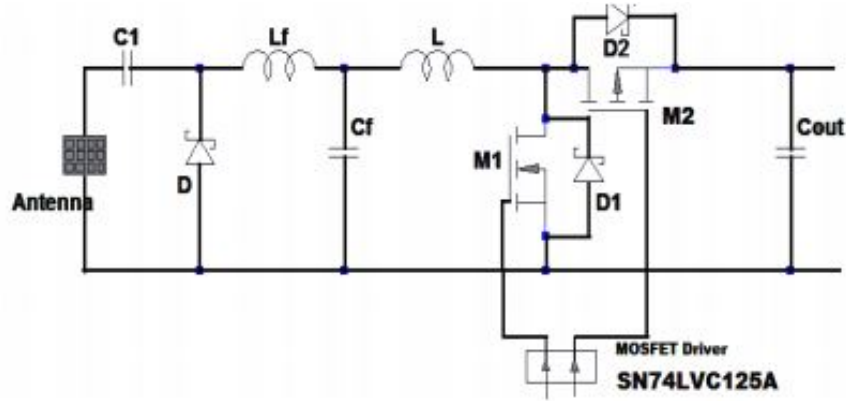
Figure 3.7: Schematics of conditioning circuit with power management circuit [44].

management system. The results are presented for the input powers of converter, which have values between 10μW - 1mW. Near a cellular base station, the proposed power management system provides 7 times more energy storage than direct connection to battery.

Mishra et al. [44] design a 2.4GHz square slot antenna and power management circuit for RF energy harvesting. Four square slots are used to improve the gain of antenna that has 5.7dBi simulated gain. The power management is accomplished by combining conditioning circuit with the N-channel and P-channel Metal oxide semiconductor field effect transistors (MOSFETs) to improve efficiency of the overall system. The schematic of conditioning circuit with power management circuit is illustrated in Figure 3.7. The proposed circuit with power management gives 412mV output for the input power of -20dBm. Moreover, it is possible to obtain power for -50dBm rectifier input.

3.2.4 Storage unit design

RF energy harvesting is an alternative energy source with some challenges because the obtained energy is generally low. If the incoming RF signal is not sufficient to power a device directly, a storage unit should be used in energy harvesting systems. In most applications, the use of rechargable micro battery, super capacitor or thin-film battery is preferred in energy harvesting systems.

Ghao et al. [45] design an energy harvesting system which is composed of a broadband antenna, 3- stage voltage conditioning circuit, and new thin-film battery. New

lightweight flexible thin-film battery is developed that offers the highest specific charge storage capacity. The picture of flexible thin-film battery is shown in Figure 3.8. Lithium batteries need more than 3V to recharge. The developed thin-film battery can be recharged with a voltage of less than 1.2 V. The system is experimented by recharging battery with RF signals from a walkie-talkie. It is measured that the energy harvesting efficiency of system is achieved as 11.6%.

Figure 3.8: A flexible thin-film battery prepared in the laboratory [45].

3.2.5 Cognitive radio networks

At the same time, there have been researches for the usage of energy harvesting systems in cognitive radio networks.

Lee et al. [46] propose a novel communication and energy harvesting method for cognitive radio networks. Secondary transmitters harvest energy from the communication process established by primary transmitters when primary transmitters are close. Otherwise, secondary transmitters transmit message when primary transmitters are far away. A harvesting zone and a guard zone are defined for primary transmitters. The radius of harvesting zone is smaller than the radius of guard zone. The details can be seen in Figure 3.9. Energy is harvested in harvesting region, and information is transmitted at the outside of guard zone by secondary transmitters. It is observed from the numerical results that the densities of primary and secondary

transmitters affect the transmission probability and the maximum throughput for secondary transmitters.
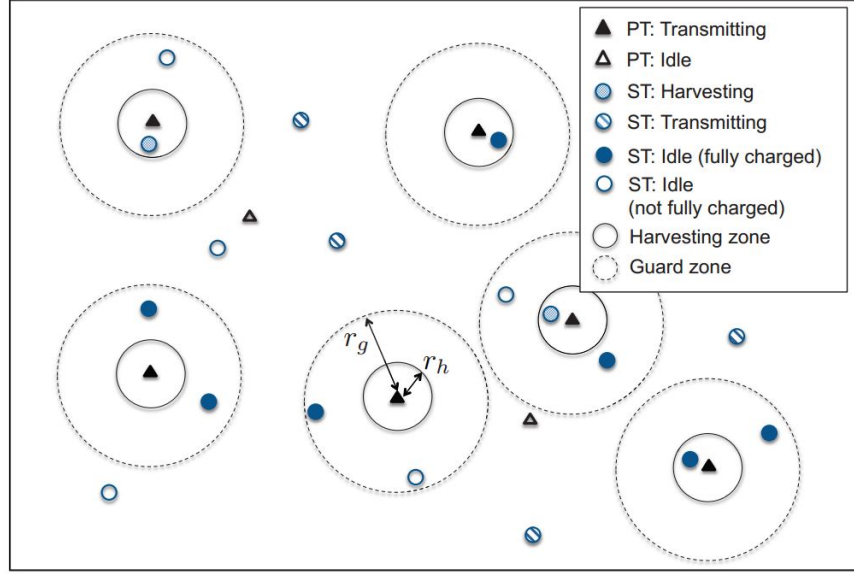
Figure 3.9: A wireless energy harvesting cognitive radio network in which primary transmitter (PT) and secondary transmitter (ST) are distributed [46].

Park et al. [47] study on the mode selection of sensor node in cognitive radio network whether it harvest RF energy from primary network or use the frequency spectrum. An optimal mode selection policy is proposed to maximize an expected total throughput. The proposed policy depends on the spectrum occupancy state of the primary network and available energy of sensor node in secondary network. It finds a balance between throughput and energy.

3.2.6 Simultaneous information and power transfer

RF signals that are used for wireless information transfer are considered as a viable new source for wireless power transfer. There are a few papers on wireless power and information transfer simultaneously.

In [48], it is expressed that Nikola Tesla designed a wireless power transfer circuit with coupled inducttors to deliver power to the load. However, Claude Shannon used it to send information as a communication device. Grover and Sahai investigate simultaneous information and power transfer, which is possible for most applications. At the same time, there is a tradeoff between information and power transfer on the same link. Because, power efficiency is maximized at low frequencies, but information

requires to use large bandwidth and high frequencies to maximize throughput. An optimal tradeoff between the rate of information transfer and the received power on a coupled-inductor circuit is developed, which can be used for any system with a slow frequency selective channel.

Zhou et al. [49] state that there is no practical circuit to harvest energy from RF signals and to decode information simultaneously. A theoretical receiver operation is proposed, which splits the received RF signal to energy harvesting part and information decoding part. The power ratio of each part can be static or adjusted by time switching and power splitting shown in Figure 3.10. The separated and integrated information and energy receiver architectures are proposed. For these two receivers, the optimal transmission strategies are developed and compared according to obtained rate-energy tradeoff results.
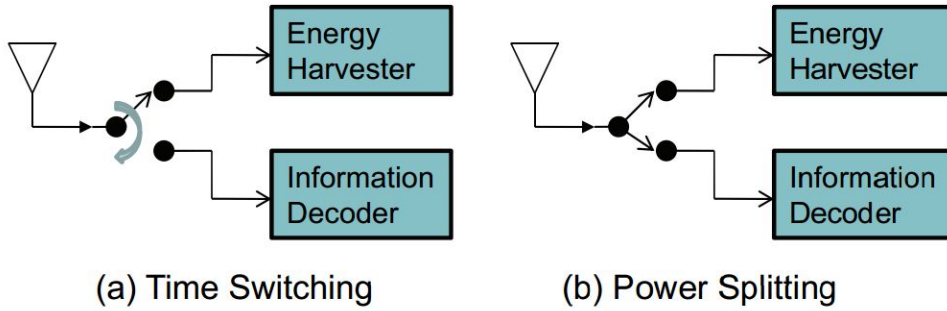
Figure 3.10: Two designs for the co-located energy and information receivers, time switching and power splitting [50].

In [50], it is indicated that wireless power transfer can be perfomed by using inductive coupling , magnetic resonate coupling, and electromagnetic radiation. Simultaneous wireless information and power transfer is possible by RF signals. Zhang and Ho study on a multiple-input multiple-output (MIMO) wireless broadcast system, which consists of an energy harvesting receiver, an information decoding receiver, and a common transmitter nodes with multiple antennas. A MIMO broadcast system for simultaneous wireless information and power transfer is indicated in Figure 3.11.The optimal transmission strategy in the presence of seperated and co-located receiver scenarios is developed to obtain different tradeoffs for maximum information rate versus energy transfer.
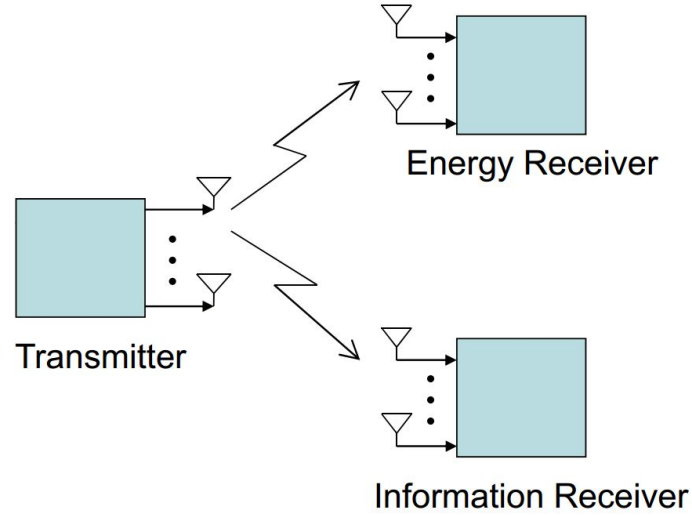
Figure 3.11: A MIMO broadcast system for simultaneous wireless information and power transfer [50].

3.2.7 Other researches

Apart from grouped papers above, we can mention about other some researches. The design of energy harvesting systems should be performed according to application properties.

In [51], two wireless power transfer system is introduced by Intel Research Seattle. Sample and Smith study on RF energy harvesting techniques from RFID reader and TV station. Firstly, an energy harvesting system for small sensor devices that spend power between 2μW - 2mW is designed and powered from a few meters by the RFID reader. Secondly, an energy harvesting circuit is placed at a distance of 4.1km from a TV station that broadcast at UHF and VHF band. The broadcast power is 960kW at 674-680MHz, and 60μW power is harvested from 4.1km distance by energy harvesting circuit. The thermometer/hygrometer that consumes 25μA at 1.5V is powered and functioned properly by harvested power. The operation of system can be seen in Figure 3.12.

Also, there are researches about medical applications of RF energy harvesting. Cheng et al. [52] intend to run wireless sensors on human body by means of RF energy harvesting. A base station that transmits at 434.16MHz was used to send signals to four sensor nodes. These nodes are placed on a human standing 1.4m away from base station. The placement of system is shown in Figure 3.13. The voltage

Figure 3.12: Operating a temperature and humidity meter (including LCD display) using only ambient RF power [51].

measurements of 1.1V and 0.56V are taken as harvested supply voltages by using two $100\mu F$ surface-mount capacitors. Hence, the proposed techniques will help to use disposable wearable sensors by decreasing of size and cost of sensors for various applications in the future.

Additionally, a laboratory established at the University of Alcalá (Spain), which is used for RF energy harvesting researches is introduced in [53]. Boquete et al. state that students have used this laboratory to understand the concept of RF energy harvesting and to design energy harvesting systems for three academic years. The lectures are about antennas, Friss equation, transmitter-receiver block diagram, and ZigBee, Bluetooth, and Wi-Fi protocols. The laboratory practises depend on harvesting energy from an operating mobile phone by using designed antenna and conditioning circuit for different applications.
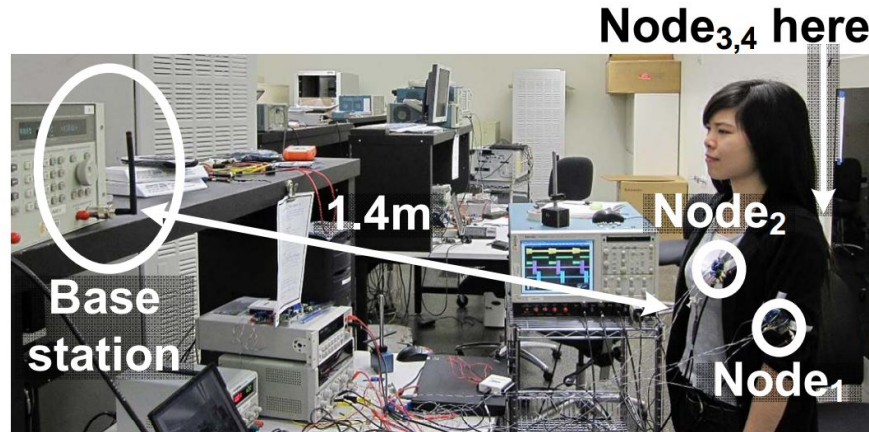
Figure 3.13: The placement of a base station and four sensor nodes from the front/back of person [52].

3.3 Conclusions

A comprehensive literature search is performed in accordance with the scope of thesis. Energy allocation and transmission policy studies in energy harvesting systems are very popular recently. Various optimum policies are developed for different system scenarios such as single-user, multi-user, and cooperative communication systems. On the other hand, RF energy harvesting research areas can be classified as antenna-circuit design area, cognitive radio network applications area, and simultaneous information and energy transmission area. The antenna-circuit design targets to improve the efficiency of harvested energy for given RF input signal. In the cognitive radio network applications, secondary users aim to exploit primary network for both transmitting information and harvesting energy. The research about simultaneous wireless information and power transfer investigate rate-energy tradeoff during transmission on the same link.

All of mentioned research papers are mainly related to maximization of harvested energy after receiving of RF signal , but not interested in the effect of wireless channel conditions on harvested energy. Moreover, the battery recharging time has a crucial role to increase and sustain the life of wireless networks. There is no any study about the effect of wireless channels on battery recharging time in energy harvesting systems. The channel models for wireless communications are explained in the next chapter.

4. CHANNEL MODELS

In this thesis, we propose statistical models for battery recharging time in RF energy harvesting systems. In this context, we start with an overview of wireless fading channels that will be used to model channels between RF signal source and energy harvesting node.

4.1 Overview of Wireless Communications

Wireless communication allows people the possibility of mobility during communication, which is the main reason of rapid development and spread of wireless systems. If it is done a brief summary, the history of wireless radio communication goes to the last decade of 19th century. In 1895, Guglielmo Marconi realized to establish the first radio transmission link between the Isle of Wight and a boat sailing 18 miles away. In 1930s, amplitude modulation (AM) and frequency modulation (FM) radio techniques were invented for wireless communication systems. After the development of cellular concept in Bell Laboratories, the first 1G analog cellular system named as Nordic Mobile Telephony (NMT) started to operation commercially in 1981. However, analog network was not sufficient to carry all mobile voice traffic. Therefore, it was an unavoidable change from 1G analog systems to 2G digital systems for cellular mobile communication.

The most prominent 2G digital cellular technology names as Global System for Mobile Communication (GSM) can be considered as a breakpoint for the widespread use of mobile communication. The first GSM network was launched in 1991 and has seen great demand by the people. GSM addressed the requirements for voice traffic greatly although it was slow for data traffic. After GSM and similar 2G systems such as Digital Advanced Mobile Phone System (D-AMPS), Personal Digital Cellular (PDC), and Personal Communications Service (PCS), 3G systems offered wide band for multi media communication. 3G systems depend on International Mobile

Telecommunications-2000 (IMT-2000) standards determined by The 3rd Generation Partnership Project (3GPP) group in International Telecommunication Union (ITU). In 2001, the first commercial 3G network based on wideband code division multiple access (W-CDMA) technology was began operations in Italy. Due to the rapid growth of large amounts of data need, the use of larger frequency bands, higher degree modulation techniques, and multiple input multiple output (MIMO) antenna systems was considered and applied to the cellular systems. While the data rates of 3G systems have been developed continuously, 4G systems such as Long Term Evolution (LTE) standards was determined. The first LTE network started operations in Norway in 2009. Up to date, 4G systems has operated in 100 countries of the world. Moreover, LTE Advanced standards aimed to reach 1Gbps downlink data rate by using multiple carrier bands, adaptive modulation techniques, and MIMO systems.

These major changes in data rate from kbps to Gbps took only about 20 years. Now we are talking 5G cellular mobile systems and new technologies that will take us into the future. The history of cellular mobile systems explains many things about the development of wireless communication systems. Beside, broadcast TV, satellite, local area network (LAN), and wide area network (WAN) systems are other applications of wireless communication like cellular systems. The developed communication tecniques have been applied all related wireless systems. Each application of wireless communication need different requirements. Hence, the disadvantages of wireless communication become advantages as the wireless tecnologies grow up in time. Finally, wireless communications play more important role than wired communication in humanlife today.

4.2 Radio Frequency Propagation

In the wireless communication systems, the used part of electromagnetic frequency is named as RF spectrum between 3kHz and 300GHz. The radio spectrum is a scarce source for wireless communication. Therefore, the radio spectrum is allocated for the use of different wireless communication systems by authorized government agencies of countries. Frequency allocation of the radio spectrum can be licensed or unlicensed

according to the purpose of use. In Table 4.1, a part of the radio spectrum allocated to licensed and unlicensed wireless communication systems is shown for Turkey [54].

Table 4.1: Frequency allocation of the radio spectrum.

Wireless System	Frequency Band
AM Radio	$148.5 - 283.5$ KHz
	$526.5 - 1606.5$ KHz
FM Radio	$88 - 108$ MHz
Broadcast TV (UHF)	$470 - 790$ MHz
2G - GSM 900	$890 - 960$ MHz
2G - GSM 1800	$1.71 - 1.725$ GHz
	$1.805 - 1.82$ GHz
3G - IMT-2000	$1.92 - 1.97$ GHz
	$2.01 - 2.015$ GHz
	$2.11 - 2.16$ GHz
ISM Band	$2.446 - 2.454$ GHz

RF signals provide communication between transmitter and receiver in the wireless systems. The information sended by transmitter should be detected and estimated truely by receiver for reliable communication. However, the detection and estimation of sended information on RF signals are not straightforward in wireless communication unlike wired communication because of transmission medium.

RF signals, namely electromagnetic waves, propagate in different ways through the medium between transmitter and receiver. During propagation, electromagnetic waves are affected from reflection, diffraction, and scattering due to buildings, geographical shapes and other objects. The incident electromagnetic wave is reflected from the smooth surface of buildings or mountains, and diffracted from the knife-edges of buildings, which changes the direction of wave. While electromagnetic wave impinges upon an object with rough surface, the wave split into the number of signals due to scattering effect. Reflection, diffraction, and scattering of radio frequency wave is presented in Figure 4.1. At the end of the travel, electromagnetic waves with impediments that change over time arrive at the front end of receiver. Moreover, the power of electromagnetic wave attenuates dramatically with distance. Because
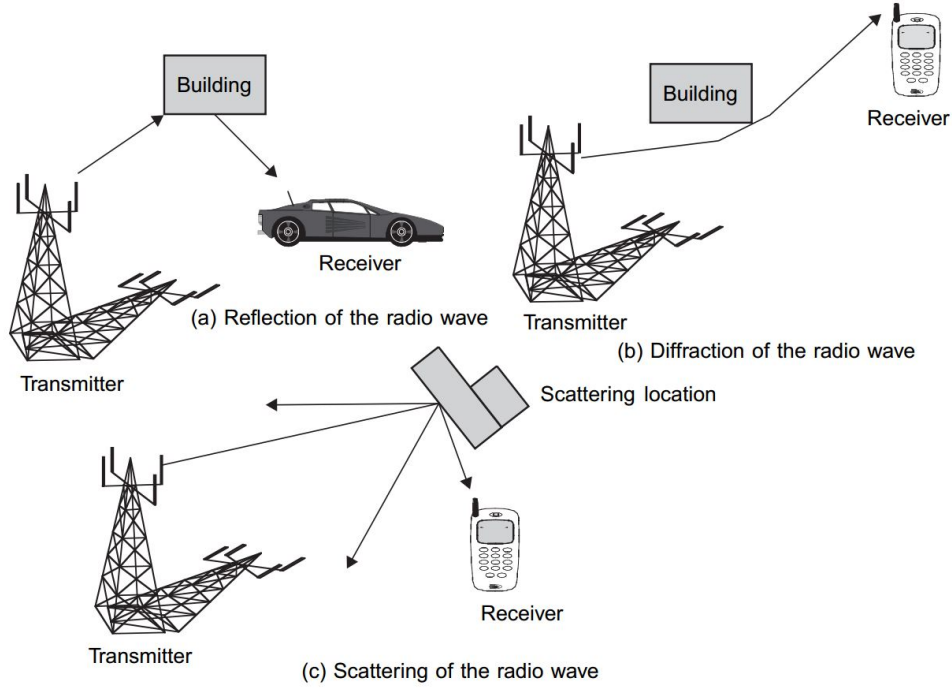
Figure 4.1: Reflection, diffraction, and scattering of radio frequency wave [55].

of power attenuation, mobility, and impediments such as noise and interference, it is difficult to estimate sended RF signal.

In order to address the mentioned challenges, a valid approach is to model the communication channel between transmitter and receiver. The simplest channel model is AWGN, which is an undesired noise added to all frequencies in the transmission channel. But AWGN is not a sufficient model for many wireless communication systems , hence it is necessary to consider more complex multiplicative channel models.

Mainly, the variations of signal in the transmission channel should be considered to form the right channel model. The prediction of average signal strength for a given distance gives us coverage area of transmitter, which is important for planning of wireless network. The channel effects for average value of signal strength are called as large scale fading effect [56]. At the same time, the received signal strength changes quickly in the wide range for the same distance. The channel effects for the rapid fluctuations of received signal strength are named as small scale fading effect. The reasons of rapid fluctuations are multipath components of same signal that have the greatest impact on small scale effect. Path loss, shadowing, and multipath effects
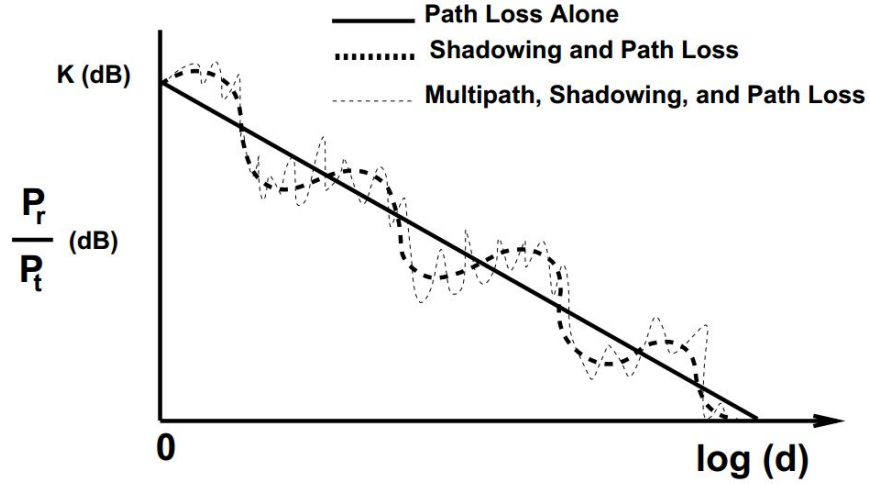
Figure 4.2: Path loss, shadowing, and multipath effects versus distance [57].

versus distance is shown in Figure 4.2. The wireless radio channel models are designed to include one of large scale effects such as path loss and shadowing or small scale effects. There are also composite channel models that includes both of them. The details of channel models are explained in the following sections. Our aim is not to explain all channel models. The explained models are selected for the understanding of the subject.

4.3 Large Scale Channel Models

Free-space path loss, the simplified path loss, the Hata model, and the lognormal shadowing channel models are described for the large scale effects.

4.3.1 Path loss

Path loss implies the attenuation of transmitted signal power during propagation. The linear path loss is defined as the ratio of transmitted power to received signal power, the path loss in dB is also defined as the difference in dB between the transmitted and received power. According to definitions, the lineer path loss is [57]

$$P_L = \frac{P_t}{P_r},$$
(4.1)

where P_t and P_r represent transmitted and received power, respectively. And the path loss in dB is

$$P_L[dB] = 10\log_{10}\frac{P_t}{P_r}.$$
(4.2)

39

In the line-of-sight (LOS) case, there are no obstruction between the transmitter and receiver. The transmitted wave propagates in free space directly. The received power is a function of the transmitted power, the wavelength (λ), the antenna seperation distance (d) between the transmitter and receiver, the gain of transmitting antenna (G_t), and the gain of receiving antenna (G_r). In free space, the Friis transmission equation states that [57]

$$P_r(d) = P_t G_t G_r \left(\frac{\lambda}{4\pi d}\right)^2. \tag{4.3}$$

The effect of channel conditions will be more understandable with our simulations in Matlab. The system parameters for simulations are listed in Table 4.2.

Table 4.2: Simulation parameters for channel models.

Parameters	Values
Frequency (f)	915 MHz
Transmit Power (P_t)	1 W
Gain of Transmitting Antenna (G_t)	8 dBi
Gain of Receiving Antenna (G_r)	3 dBi
Dimensions $(x \times y)$	100×100 m

We define a coverage area whose dimensions are 100×100 meters. A transmitter with omni directional antenna is placed at a point with coordinates $(20, 20)$. The receivers at each point have directional antennas. In Figure 4.3, the coverage of received power for defined area is shown. The different colors represent the different power levels of received power (dBm) at each point in the defined area.

In another simulation, we would like to show the variation of received power according to distance between transmitter and receiver. It is seen in Figure 4.4 that the received power is decreasing with increasing distance, which shows of the path loss effect.

Free-space propagation is usually considered for satellite-to-satellite links. Because of obstacles and other distorting efects, the transmission environment is not simple like free-space propagation. In order to model the attentuation between the transmitter and receiver in complex environments, the commonly used simplified path loss model is

$$P_r(d, \beta) = P_r(d_0) \left(\frac{d_0}{d}\right)^\beta, \tag{4.4}$$

40
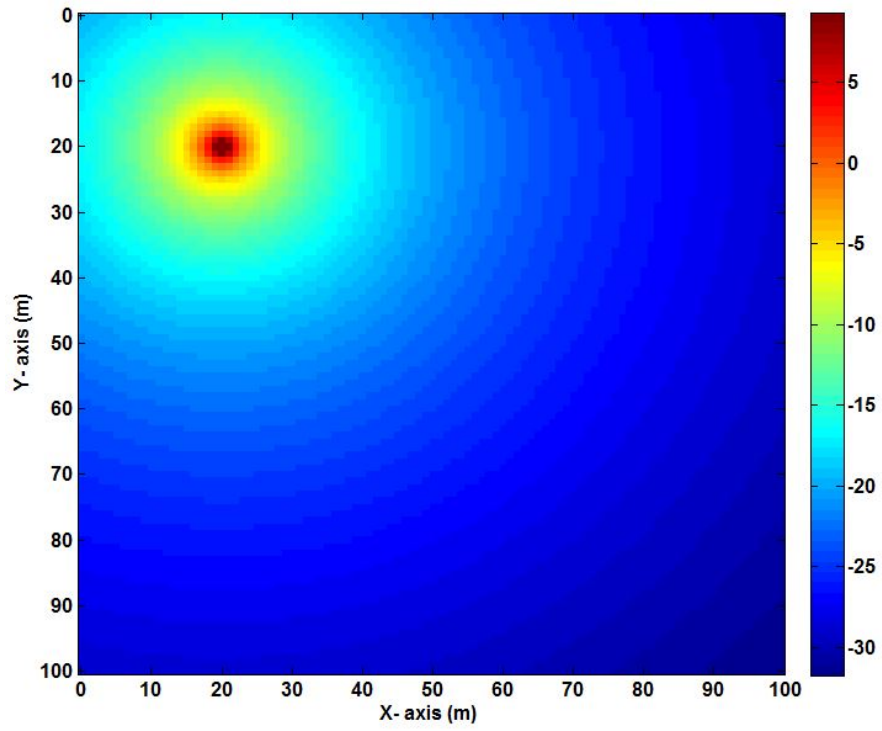
Figure 4.3: The coverage of signal strength (dBm) for 100×100 m area. The transmitter is placed at $(20, 20)$ coordinates.
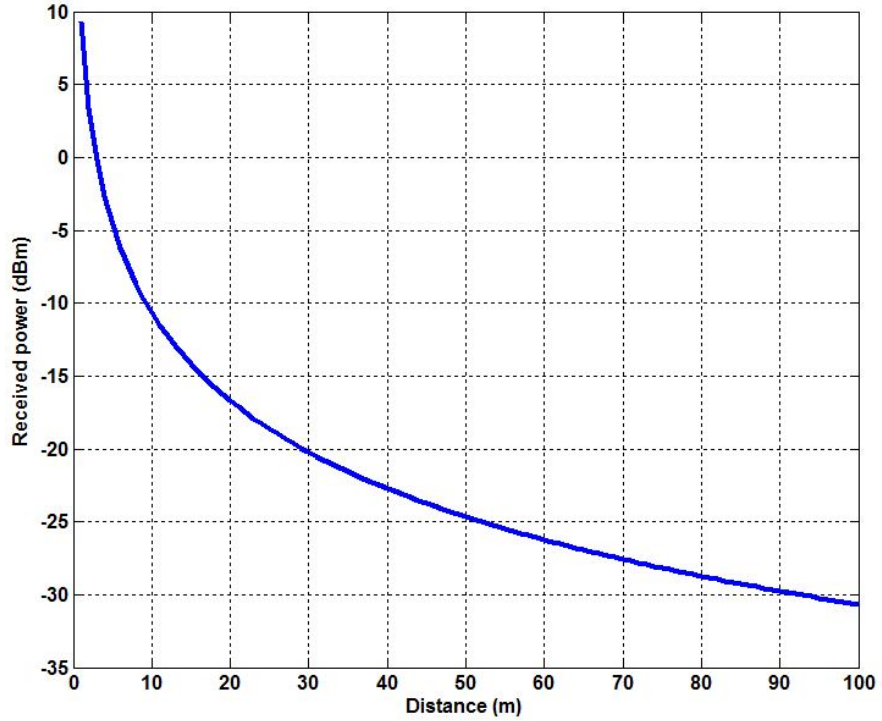
Figure 4.4: The variation of signal strength (dBm) versus distance (m).

where d_0 is a reference distance for the antenna seperation and β is the path loss exponent. The value of β depends on the propagation environment. Generally, it takes a value between 1.6 and 6.5, for example β can be equal to 1.6 in office buildings [57].

Furthermore, the other ways to model more complex propagation environments are the empirical path loss models. The residential areas are classified as urban, suburban, rural, etc. areas, which depend on the characteristics of wireless environment. One of the familiar emprical path loss models is the Hata model, which simplifies prediction of path loss at frequencies between 150-1500 MHz. The parametric closed-form path loss in dB formula of the Hata model for urban areas is [57]

$$P_L(d) = 69.55 + 26.16\log_{10}(f_c) - 13.82\log_{10}(h_t) - a(h_r) \tag{4.5}$$
$$+ (44.9 - 6.55\log_{10}(h_t))\log_{10}(d),$$

where the carrier frequency is denoted by f_c. The parameters of h_t and h_r represent the base station antenna height and the mobile receiver antenna height, respectively. $a(h_r)$ is a correction factor for the mobile receiver antenna height based on the size of the coverage area. The correction factor in dB for small to medium sized cities is expressed as

$$a(h_r) = (1.1\log_{10}(f_c) - 0.7)h_r - (1.56\log_{10}(f_c) - 0.8) \tag{4.6}$$

and for larger cities at frequencies $f_c > 300MHz$, it becomes

$$a(h_r) = 3.2(\log_{10}(11.75h_r))^2 - 4.97. \tag{4.7}$$

The Hata model for urban area can be expanded to suburban and rural areas by corrections. The models like the Hata model is valid for general coverage prediction, whereas it is not convinient for any specific transmission link.

The Okumura model, COST 231 model, and ray tracing models such as two-ray and ten-ray models are other examples of path loss models [57]. After path loss models, in order to quantify the fluctuations of the received signal powers with respect to (**4.3** and **4.4**) here we consider, shadowing, small scale, and also composite fading models.

4.3.2 Shadowing

As a large scale fading effect, shadowing occurs when large objects such as a hill or large buildings block paths of propagation between the transmitter and receiver. It causes random slow fluctuations of the received power over small distances. The other reasons of shadowing are the reflection and scattering of signals due to objects in the middle range. Shadowing is frequently modeled as a multiplicative lognormal random variable. Let μ_s and σ_s represent the mean and the standard deviation of P_r in dB ($P_{r,dB} = 10log_{10}P_r$), respectively. The variable of x represents a random variable for lognormal shadowing. The PDF of the instantaneous received power in the presence of shadowing, $f_{P_S}(x)$, is lognormal distribution [57]

$$f_{P_S}(x) = \frac{\xi}{\sqrt{2\pi}\sigma_s x}\exp\left(-\frac{(10\log_{10}x - \mu_s)^2}{2\sigma_s^2}\right), \qquad x > 0, \tag{4.8}$$

where $\xi = \frac{10}{\ln 10}$. The mean of shadowing distribution is calculated as

$$E[P_S] = \exp\left[\frac{\mu_s}{\xi} + \frac{\sigma_s^2}{2\xi}\right]. \tag{4.9}$$

From above equations, it is possible to derive lognormal shadowing distribution for the value of x in units of dB, x_{dB}, as below

$$f_{P_S}(x_{dB}) = \frac{1}{\sqrt{2\pi}\sigma_s}\exp\left(-\frac{(x_{dB} - \mu_s)^2}{2\sigma_s^2}\right), \qquad x_{dB} > 0, \tag{4.10}$$

The equation in (4.10) shows that x_{dB} has Gaussian distribution with the mean value of μ_s and the variation value of σ_s^2 in dB. When the mean value of μ is calculated according to the simplified path loss model with path loss exponent β, the lognormal shadowing effect can be considered as the summation of path loss and shadowing effect, which represents the large scale effect.

We would like to show the effects of shadowing with different variance on the received power. Figure 4.5 shows our simulations for lognormal shadowing with the variance values of $\sigma_s^2 = -10$dB and $\sigma_s^2 = 4$dB. It is obvious that the higher values of variance increase the variation of received power around the path loss efffect.

The lognormal shadowing channel model is useful for practise, but does not allow further mathematical analysis. Therefore, other channel models are proposed such as
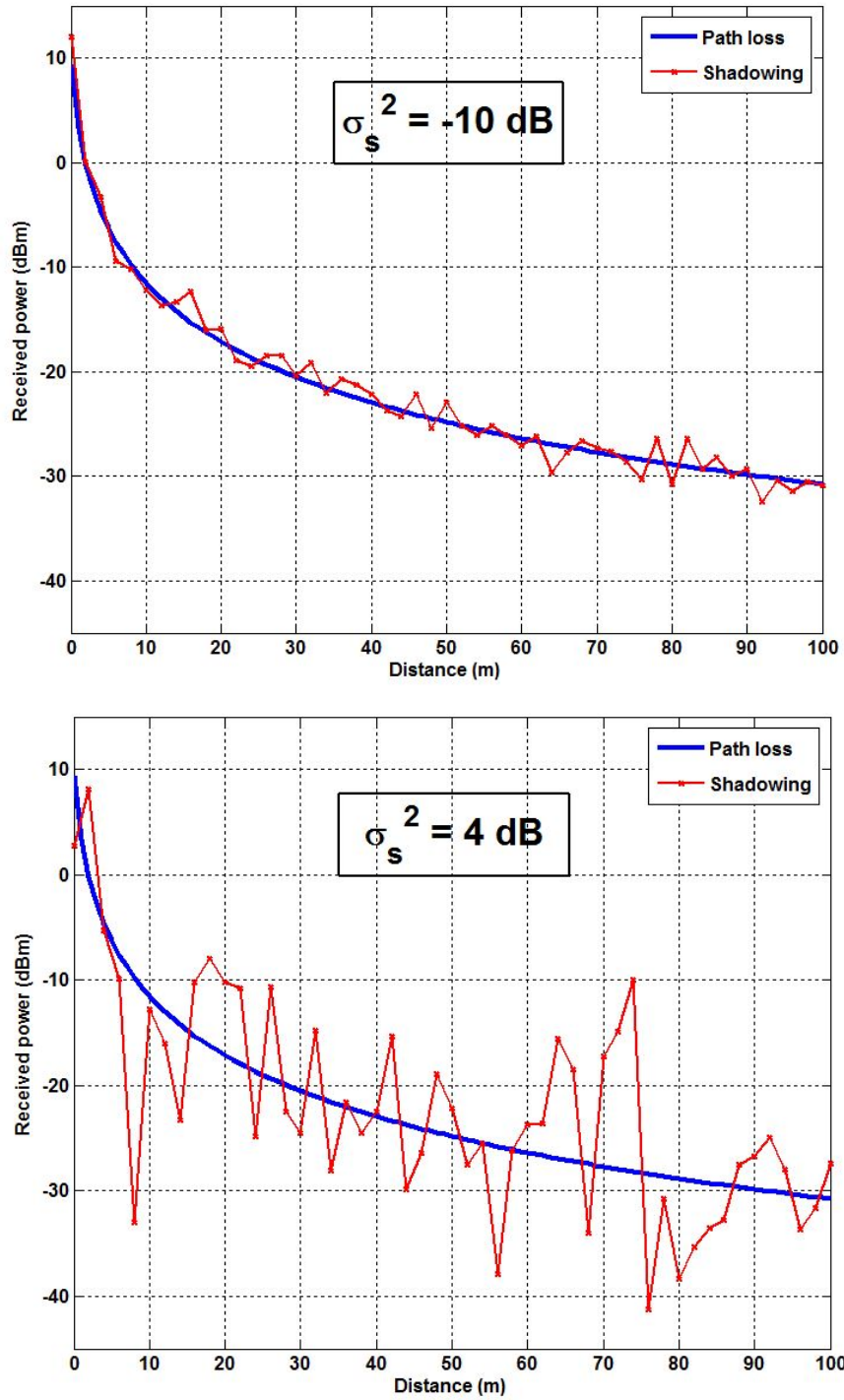
Figure 4.5: The variation of received power due to shadowing effect with the values of $\sigma_s{}^2 = -10$dB and $\sigma_s{}^2 = 4$dB.

the Rayleigh-lognormal and the Nakagami-lognormal. These models have a structure that is composite of shadowing and small scale fading. In later sections, we mention about the composite models. The small scale channel models are explained in the following section.

4.4 Small Scale Channel Models

The small scale effect is also called as small scale fading or only fading. The transmitted signal is splitted into more than one signal during travel through the wireless medium. The copies of transmitted signal propagate and arrive at the receiver in different ways, which is called multipath. The multipath components of signal are combined at the receiver antenna. Because of multipath signals, the amplitude of received signal changes rapidly over a short time interval and small travel distance. At the same time, mulipath effect causes changes in the phase of received signal. The presence of reflecting and scattering objects, the speed of transmitter, the speed of receiver, the speed of surrounding objects and the transmission bandwidth of the signal are important factors effecting the small scale fading.

In order to model small scale fading effects, the Rayleigh and Nakagami-m distributions are commonly used. Now, the Rayleigh and Nakagami-m channel models are explained in the following sections.

4.4.1 Rayleigh fading

The Rayleigh distribution is used to model channel, if the radio channel has no LOS or dominant component of multipath signal. The Rayleigh distribution describes the envelope of received signal that varies in time. At the same time, the Rayleigh distribution equals to the envelope of a complex variable whose real and imaginary parts are zero-mean Gaussian distributed with no correlation. The Rayleigh distribution is given as [56]

$$f_{P_R}(x) = \frac{x}{\sigma^2} \exp\left(-\frac{x^2}{2\sigma^2}\right), \qquad x \geq 0, \tag{4.11}$$

where σ^2 is not variance of the Rayleigh distribution, it is the time-average power of the received signal before envelope detection. The variance is calculated as $0.4292\sigma^2$

45

by using expectation formulas. Moreover, the average of Rayleigh distribution is also calculated as 1.2533σ.

When the envelope of the signal is Rayleigh distributed, the PDF of received power has an exponential distribution shown as [58]

$$f_{P_R}(x) = \frac{1}{\mu_r}\exp\left(-\frac{x}{\mu_r}\right), \qquad x \geq 0, \tag{4.12}$$

where μ_r is the average power of received signal.

The Rayleigh distribution represents bad channel condition that means there are many objects in the environment to fade signal. Hence, it can be used to model channel in dense urban areas where there is no LOS between the transmitter and receiver.

4.4.2 Nakagami-m fading

The Nakagami-m distribution is a common small scale fading model, which is parameterized by the Nakagami parameter (m). The Nakagami parameter is also called as *shape parameter* representing the effect of fading. The Nakagami-m channel model is an approximation of the Rician channel and the generalized form of the Rayleigh channel (for $m = 1$). It is possible to obtain different channel conditions by changing m parameter. For $m = \frac{1}{2}$ the distribution goes to one-sided Gaussian distribution, which has worse channel condition than the Rayleigh distribution. For $m = \infty$ the distribution goes to impulse that means there is no small scale fading. The Nakagami-m distrbution is expressed as [57]

$$f_{P_N}(x) = \frac{2m^m x^{2m-1}}{\Gamma(m)\mu_n^m}\exp\left(\frac{-mx^2}{\mu_n}\right), \qquad m \geq \frac{1}{2}, \tag{4.13}$$

where $\Gamma(\cdot)$ is the Gamma function and μ_n is the average received power.

The PDF of instantaneous received power in the presence of Nakagami-m fading becomes Gamma distributed given as [57]

$$f_{P_N}(x) = \frac{m^m x^{m-1}}{\Gamma(m)\mu_n^m}\exp\left(\frac{-mx}{\mu_n}\right), \qquad x > 0, m \geq \frac{1}{2}, \tag{4.14}$$

The Nakagami-m distribution provides flexibility to model wireless channels. Hence, it can be preferred to use for small scale fading instead of the Rayleigh and Rician fading models.

46

In Figure 4.6, the amount of variations on the received power due to the small scale effect is shown by our simulation. The small scale channel is modeled by using the Nakagami-m distribution with $m = 2$ and $m = 8$. The reason of fluctuations is multipath signals. It is seen that the amount of variations changes simultaneously. The scale of fluctuations decreases with increasing value of m. $m = 8$ has a range between 1.5dBm and -2.5dBm in this realization.

4.5 Composite Channel Models

The large and small scale fading models are commonly used for modeling wireless radio channels, but using only one of them may not provide sufficient accuracy for real-life scenarios. In most cases, it is necessary to take into account the simultaneous effect of fading and shadowing on the received signal. The composite channel models are used for jointly considering the shadowing and multipath fading. The Rayleigh-lognormal, the Nakagami-lognormal, the generalized-K, the generalized Gamma are distributions to model the received power in shadowed fading channels. Here, the generalized-K channel model is described as a proposed composite channel model.

4.5.1 Generalized-K fading

The generalized-K distribution has been proposed to model the instantaneous received power as a composite channel model. It is also called as the Nakagami-Gamma distribution. In the generalized-K distribution, the Nakagami-m and the Gamma distributions are used jointly for small scale fading and shadowing, respectively. The Nakagami-lognormal distribution has no closed-form expression. Therefore, the Gamma distribution is preferred to represent shadowing instead of the lognormal distribution. The generalized-K distribution is given in the closed-form expression as [59]

$$f_{P_G}(x) = \frac{2b^{m+c}x^{\frac{m+c}{2}-1}}{\Gamma(m)\Gamma(c)}K_{c-m}(2b\sqrt{x}), \qquad x > 0, \qquad \textbf{(4.15)}$$

where $K_{c-m}(\cdot)$ is the modified Bessel function of the second kind with order $(c-m)$. The parameter of b is defined as $b = \sqrt{\frac{mc}{\mu_g}}$ and μ_g denotes the average received
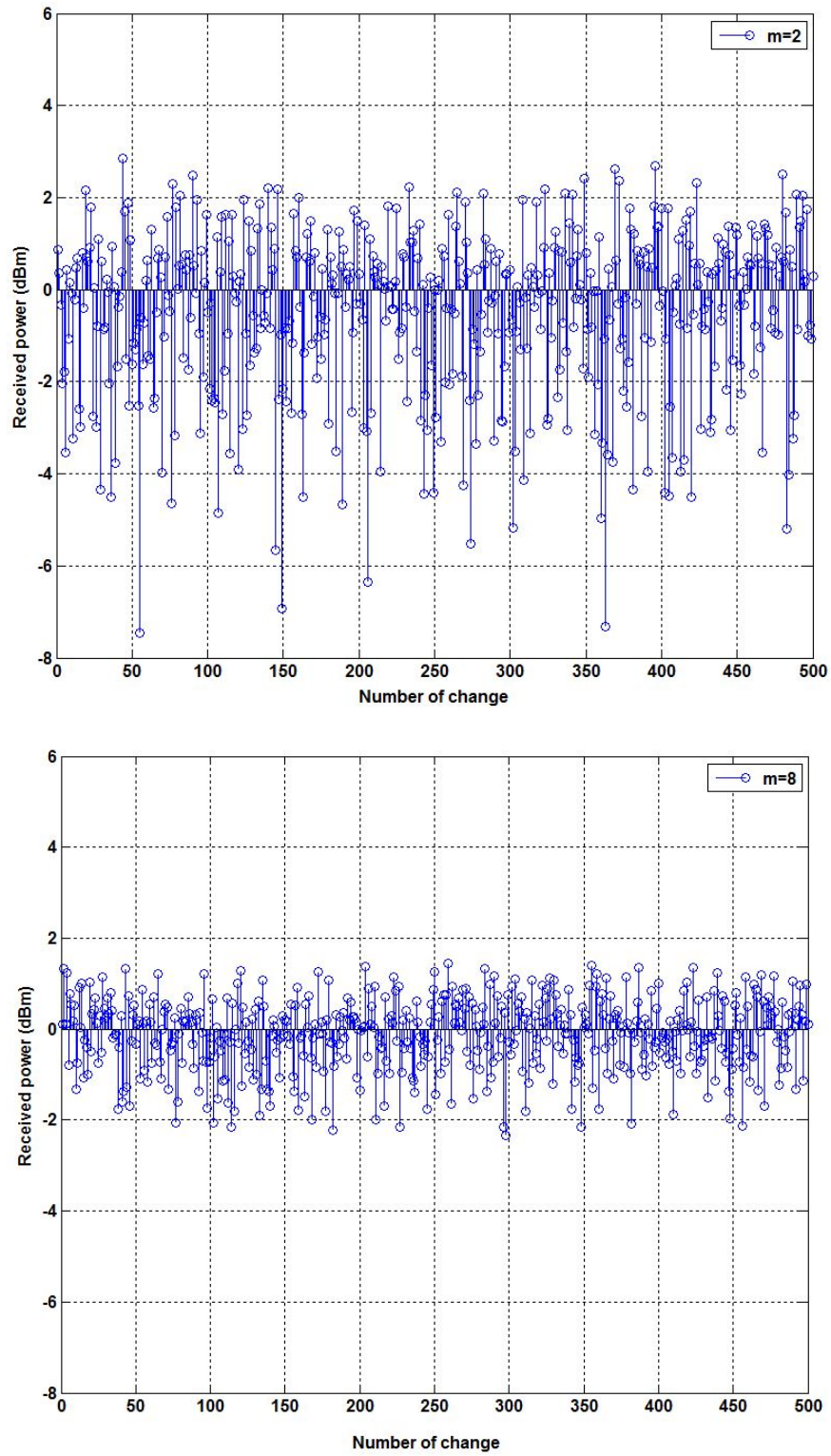
Figure 4.6: The amount of variations on the received power due to the Nakagami-m channel with $m = 2$ and $m = 8$.

power. The parameters of *m* and *c* are small scale fading and shadowing parameters, respectively. The increasing of *m* and *c* values leads to the decreasing of destructive effects. As $c \to \infty$ the generalized-K distribution is reduced to the Nakagami-m distribution. For $m = 1$ the generalized-K distribution goes to the K distribution. The K distribution is shown to be as [58]

$$f_{P_G}(x) = \frac{2b^{c+1}x^{\frac{c-1}{2}}}{\Gamma(c)}K_{c-1}(2b\sqrt{x}), \qquad x > 0, \tag{4.16}$$

The generalized-K channel model is analytically simpler than lognormal shadowed fading models. Therefore, it seems to be appropriate for jointly modeling of shadowing and fading in wireless communication channels.

Our simulations for the received power in case of the generalized-K distributed channel are shown in Figure 4.7. The red line represents the condition of $m = 2$ and $c = 2$ while the black line shows $m = 10$ and $c = 10$ case. It can be seen that the fading of channel decrease with the increasing values of *m* and *c*, namely, for $m = c = 10$ the distribution approaches to Gaussian distribution. The blue line is simulated for $m = 2$ and $c = 50$ that means nearly no-shadowing case. Hence, both of shadowing and small scale fading effects can be demonstrated by means of the generalized-K distribution.

4.6 Conclusions

In this chapter, we give an overwiew of wireless communication and summary of primary models to understand the concept of wireless channels. Wireless channel models characterize the behaviour of wireless channels between transmitter and receiver during signal transmission. All of given models from the simplest to more complex models are used according to the requirement of communication system. Friis equation for free-space path loss, the Hata model as an emprical path loss model, lognormal distribution for shadowing, the Rayleigh and the Nakagami-m distribution for small scale fading are frequently used wireless channel models.

The statistical model that describes wireless channel model should be appropriate for analytical studies. Therefore, it is useful to use the statistical models that have closed-form expressions. Moreover, the selection of channel model is very important to ensure high reliability in the wireless system design. In our thesis, we use lognormal
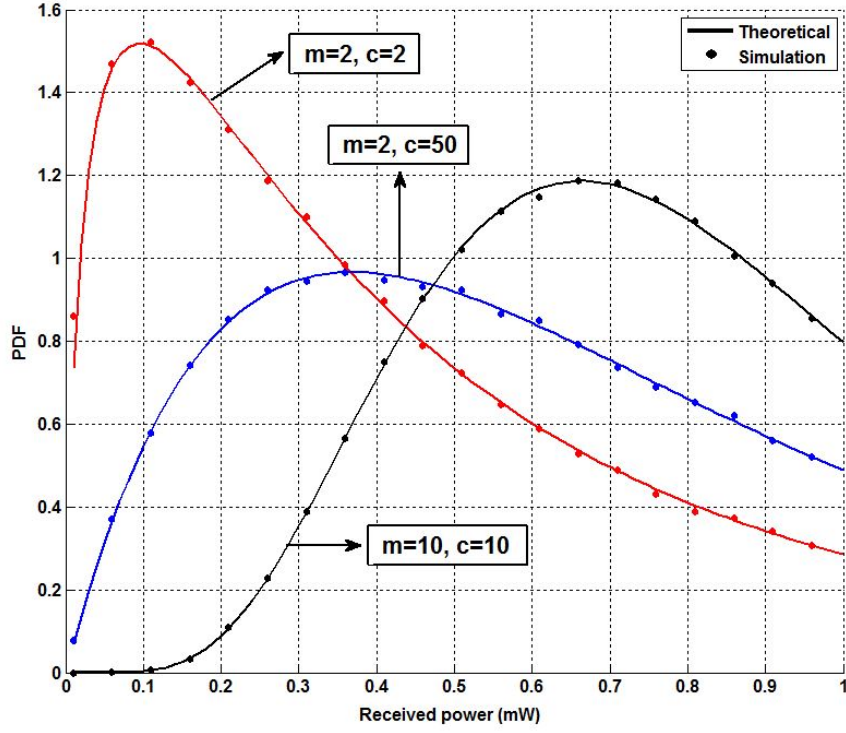
Figure 4.7: The distribution of received power due to the generalized-K composite channel. The simulation plots for the values of parameters $m = c = 2$, $m = c = 10$, and $m = 2, c = 50$.

shadowing, the Nakagami-m fading, and the generalized-K composite fading models. We derive distributions over these channels for battery recharging time in the following section.

5. BATTERY RECHARGING TIME FOR SINGLE SOURCE

5.1 Purpose

The open issue in the related literature is the characterization of battery recharging time of an energy harvesting receiver node. RF energy harvesting has challenges due to the wireless propagation environment and conversion efficiency. On the propagation side, the different channel models between source and harvesting node should be taken into account in order to obtain realistic results. Our aim is to propose statistical models for battery recharging time for the Nakagami-m and the generalized-K fading channels. We also include the effects of lognormal shadowing. We derive the associated closed form probability density function, cumulative distribution function, moment generation function, mean, and variance expressions for battery recharging time. The simulations are used to verify the theoretical results. The results show that analytical and simulation results fit to each other. Also, simulations shows that the channel model and conversion efficiency affect battery recharging time directly. This chapter was published as a conference paper [5].

5.2 System Description and Channel Models

5.2.1 System model

The main goal of energy harvesting is obtaining energy from ambient sources. In our system model, the source node (S) acts as the ambient source by continuously transmitting RF signal. The energy is harvested by our harvesting node (H), while S is transmitting a message signal to the intended destination (D), as shown in Figure 5.1. The harvesting node has a micro-battery with finite capacity for storage. It is well known that the channel between the source node and the destination node (h_{SD}) characterizes the behavior of the system, affecting several performance metrics such
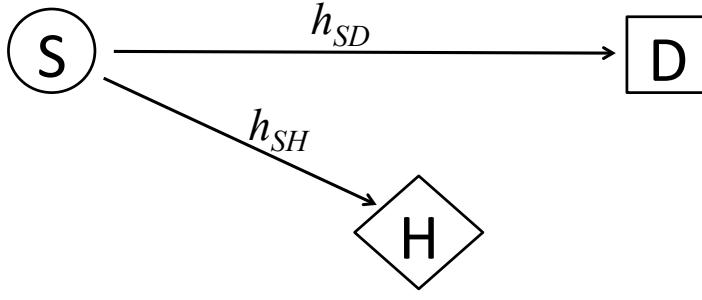
Figure 5.1: RF energy harvesting system model. S is the RF transmitter, and D is the intended receiver. H is the harvesting receiver node. H and D are physically separated.

as the outage probability and error rates. Based on this fact, it can be inferred that the channel between the source node and the harvesting node (h_{SH}) will have a significant impact on the battery charging time. To quantify this impact, it is necessary to know the impact of channels on the distrbutions of instantaneous received power (P_r), where $P_r \propto |h_{SH}|^2$.

5.2.2 Channel models

We have already explained an overview of wireless fading channels in Chapter 4. However, we would like to highlight the channel models that will be used in our study to characterize h_{SH}. We will use the lognormal shadowing, the Nakagami-m fading, and the generalized-K composite fading channels as tree important models for deriving the statistical expressions of battery recharging time. Moreover, the Friis transmission equation for path loss will be used in simulations. The instantaneous received powers, P_r, in the presence of wireless channels used in our study are given as

- *Path Loss*

$$P_r(d) = P_t G_t G_r \left(\frac{\lambda}{4\pi d} \right)^2, \tag{5.1}$$

where P_t is the transmit power, λ is the wavelength, d is the distance between the source and the receiver, G_t is the gain of transmitting antenna and (G_r) is the gain of receiving antenna.

- *Lognormal Shadowing*

$$f_{P_S}(x) = \frac{\xi}{\sqrt{2\pi}\sigma_s x}\exp\left(-\frac{(10log_{10}x - \mu_s)^2}{2\sigma_s^2}\right), \qquad x > 0, \tag{5.2}$$

where $\xi = \frac{10}{ln10}$. μ_s and σ_s represent the mean and the standard deviation of P_r in dB $(P_{r,dB} = 10log_{10}P_r)$, respectively.

- *Nakagami-m Fading*

$$f_{P_N}(x) = \frac{m^m x^{m-1}}{\Gamma(m)\mu_n^m}\exp\left(\frac{-mx}{\mu_n}\right), \qquad x > 0, m \geq \frac{1}{2}, \tag{5.3}$$

where $\Gamma(\cdot)$ is the Gamma function and μ_n is the average received power. m represents the effect of fading as fading parameter.

- *Generalized-K Fading*

$$f_{P_G}(x) = \frac{2b^{m+c}x^{\frac{m+c}{2}-1}}{\Gamma(m)\Gamma(c)}K_{c-m}(2b\sqrt{x}), \qquad x > 0, \tag{5.4}$$

where $K_{c-m}(\cdot)$ is the modified Bessel function of the second kind with order $c-m$ and $b = \sqrt{\frac{mc}{\mu_n}}$. The parameters of m and c are small scale fading and shadowing parameters, respectively.

5.3 Statistical Models for Battery Recharging Time

The models for the instantaneous received power, P_r, given in (**5.2**), (**5.3**), and (**5.4**) represent large scale, small scale, and composite fading effects, respectively. The power harvested by the harvesting receiver node (P_h) can be calculated as

$$P_h = P_r\eta, \tag{5.5}$$

where η is the conversion efficiency of RF signal to DC signal. The recharging current (I_b) of a battery can be calculated from P_h according to

$$I_b = \frac{P_h}{V_b} \tag{5.6}$$

for a battery with a constant operating voltage (V_b). Assuming that the capacity of battery (C_b) and the discharge depth (D_d) are known, the battery recharging time (T_r) can be obtained as

$$T_r = \frac{C_b D_d}{I_b}. \tag{5.7}$$

Defining the conversion coefficient, $\alpha > 0$, as

$$\alpha = \frac{C_b D_d V_b}{\eta}, \tag{5.8}$$

it can be seen that the battery recharging time becomes inversely proportional to the received power

$$T_r = \frac{\alpha}{P_r}. \tag{5.9}$$

The distribution of battery recharging time can be obtained by using the distribution of received power through the Jacobian approach using (**5.9**). It can be shown that the PDF of the battery recharging time, $f_{T_r}(\tau)$, is

$$f_{T_r}(\tau) = \frac{\alpha}{\tau^2} f_{P_r}\left(\frac{\alpha}{\tau}\right). \tag{5.10}$$

Here, $f_{P_r}(p)$ is the PDF of received power with possible distributions as given in (**5.2**), (**5.3**), and (**5.4**). Thus, the closed form expression of the PDF of the battery recharging time can be derived for the above-mentioned channel models.

5.3.1 Lognormal shadowing

Considering only shadowing effects, the PDF of battery recharging time, $f_{T_S}(\tau)$, derived by using (**5.10**) is

$$f_{T_S}(\tau) = \frac{\xi}{\sqrt{2\pi}\sigma_s \tau} \exp\left(-\frac{(10 log_{10}(\frac{\alpha}{\tau}) - \mu_s)^2}{2\sigma_s^2}\right), \qquad \tau > 0. \tag{5.11}$$

The mean can be obtained via statistical expectation as

$$\mu_{T_S} = \int_0^\infty \tau f_{T_S}(\tau) d\tau = \alpha 10^{-\frac{\mu_s}{10}} \exp\left(\frac{\sigma_s^2}{2\xi^2}\right), \tag{5.12}$$

and the variance is shown to be

$$\sigma_{T_S}^2 = \alpha^2 10^{-\frac{\mu_s}{5}} \exp\left(\frac{\sigma_s^2}{\xi^2}\right)\left[\exp\left(\frac{\sigma_s^2}{\xi^2}\right) - 1\right]. \tag{5.13}$$

5.3.2 Nakagami-m fading

The PDF of the battery recharging time in presence of the Nakagami-m channel, $f_{T_N}(\tau)$, can be derived as

$$f_{T_N}(\tau) = \frac{\alpha^m m^m}{\Gamma(m)\mu_n^m \tau^{m+1}} \exp\left(-\frac{\alpha m}{\mu_n \tau}\right), \qquad \tau > 0, m \geq \frac{1}{2} \qquad (5.14)$$

with the mean that can be shown to be

$$\mu_{T_N} = \frac{\alpha m \Gamma(m-1)}{\mu_n \Gamma(m)}, \qquad \varepsilon > 0, m > 1, \qquad (5.15)$$

where $\varepsilon = \frac{\alpha m}{\mu_n}$. The variance can be obtained as

$$\sigma_{T_N}^2 = \left(\frac{\alpha m}{\mu_n}\right)^2 \left[\frac{\Gamma(m-2)}{\Gamma(m)} - \left(\frac{\Gamma(m-1)}{\Gamma(m)}\right)^2\right], \qquad \varepsilon > 0, m > 2. \qquad (5.16)$$

5.3.3 Generalized-K fading

Considering the generalized-K distribution as a channel model, the PDF of the battery recharging time, $f_{T_G}(\tau)$, becomes

$$f_{T_G}(\tau) = \frac{2b^{m+c}\alpha^{\frac{m+c}{2}}}{\Gamma(m)\Gamma(c)\tau^{\frac{m+c}{2}+1}} K_{c-m}\left(2b\sqrt{\frac{\alpha}{\tau}}\right), \qquad \tau > 0, m \geq \frac{1}{2}, c > 0. \qquad (5.17)$$

The mean value is derived as

$$\mu_{T_G} = \alpha b^2 \frac{\Gamma(m-1)\Gamma(c-1)}{\Gamma(m)\Gamma(c)}, \qquad \delta > 0, m > 1, c > 1, \qquad (5.18)$$

where $\delta = 2b\sqrt{\alpha}$, and the variance is obtained to be

$$\sigma_{T_G}^2 = \alpha^2 b^4 \left[\frac{\Gamma(m-2)\Gamma(c-2)}{\Gamma(m)\Gamma(c)} - \left(\frac{\Gamma(m-1)\Gamma(c-1)}{\Gamma(m)\Gamma(c)}\right)^2\right], \qquad (5.19)$$

$$\delta > 0, m > 2, c > 2.$$

In addition to the PDF, mean, and variance expressions, the CDF and the MGF expressions can be derived. The CDF of the instantaneous received power for the generalized-K channel, $F_{P_G}(x)$, is expressed in [59] as (5.20) where $_pF_q(\cdot)$ is the generalized hypergeometric function, p and q are integers.

$$F_{P_G}(x) = \pi\csc(\pi(c-m))\left[\frac{(b^2 x)^m {}_1F_2(m; 1-c+m, 1+m; b^2 x)}{\Gamma(m)\Gamma(1-c+m)\Gamma(1+m)}\right.$$

$$\left. - \frac{(b^2 x)^c {}_1F_2(c; 1+c-m, 1+c; b^2 x)}{\Gamma(c)\Gamma(1+c-m)\Gamma(1+c)}\right], \qquad x > 0 \qquad (5.20)$$

55

It is used for deriving the CDF of battery recharging time. Since (**5.9**) expresses the relation between power and time, the relation between their CDF expressions for the generalized-K channel model becomes

$$F_{T_G}(\tau) = 1 - F_{P_G}\left(\frac{\alpha}{\tau}\right), \tag{5.21}$$

by substituting $F_{P_G}(x)$ in (**6.37**), the CDF of battery recharging time, $F_{T_G}(\tau)$, can be shown to be as given in (**5.22**).

$$F_{T_G}(\tau) = 1 - \pi csc(\pi(c-m)) \left[\frac{(b^2\frac{\alpha}{\tau})^m {}_1F_2(m; 1-c+m, 1+m; b^2\frac{\alpha}{\tau})}{\Gamma(m)\Gamma(1-c+m)\Gamma(1+m)} \right.$$
$$\left. - \frac{(b^2\frac{\alpha}{\tau})^c {}_1F_2(c; 1+c-m, 1+c; b^2\frac{\alpha}{\tau})}{\Gamma(c)\Gamma(1+c-m)\Gamma(1+c)} \right], \quad \tau > 0 \tag{5.22}$$

The MGF of the generalized-K distribution, $\Phi_{P_G}(s)$, has been derived as in (**5.23**), [60].

$$\Phi_{P_G}(s) = \left(\frac{b^2}{4s}\right)^{\frac{m+c-1}{2}} \exp\left(-\frac{b^2}{8s}\right) W_{\frac{1-m-c}{2},\frac{c-m}{2}}\left(\frac{b^2}{4s}\right) \tag{5.23}$$

From the following definition of MGF

$$\Phi_{T_G}(s) = \int_0^\infty \exp(-s\tau) f_{T_G}(\tau) d\tau, \tag{5.24}$$

by substituting $f_{T_G}(\tau)$ in (**5.24**), the MGF of battery recharging time, $\Phi_{T_G}(s)$, is derived as in (**5.25**).

$$\Phi_{T_G}(s)) = 4 \left[{}_0F_2(; 1-c, 1-m; b^2\alpha s) + \frac{2^{c+m}}{\Gamma(m)\Gamma(c)} \right.$$
$$\left(b^{m+3c}\alpha^{\frac{m+3c}{2}} s^c \Gamma(-c)\Gamma(-c+m) {}_0F_2(; 1+c, 1+c-m; b^2\alpha s) + \right. \tag{5.25}$$
$$\left. b^{3m+c}\alpha^{\frac{3m+c}{2}} s^m \Gamma(-c)\Gamma(-c+m) {}_0F_2(; 1+m, 1+m-c; b^2\alpha s) \right) \right]$$

5.4 Numerical and Simulation Results

The numerical analyses and simulations are conducted to show the effects of channel conditions and the correctness of the derived expressions. The system parameters for simulations are listed in Table 5.1.

Table 5.1: Simulation parameters for single source.

Parameters	Values
Frequency (f)	915 MHz
Transmit Power (P_t)	20 W
Gain of Transmitting Antenna (G_t)	0 dBi
Gain of Receiving Antenna (G_r)	6 dBi
Battery Charging Voltage (V_b)	1.2 V
Battery Capacity (C_b)	10 mAh
Conversion Efficiency (η)	0.5
Discharge Depth (D_d)	0.4
Dimensions ($x \times y$)	10×10 m

Firstly, we want to show the varying of battery recharging time according to distance between the source node and the harvesting receiver node. We define a coverage area whose dimensions are 10×10 meters. The source node is placed at the center of this area with coordinates $(5,5)$. Each point in this area is considered as a potential harvesting receiver node with an omnidirectional antenna. And the source node transmits in an omnidirectional fashion. Figure 5.2 illustrates solely the deterministic path loss effect, which is the variation of battery recharging time in defined area. It can be seen that battery recharging time is changing dramatically due to distance but has very low values within close proximity of the source node, as expected.

Secondly, we demonstrate both the small scale and large scale effects on the PDF of battery recharging time. We placed the harvesting receiver node at $(3,3)$ coordinates and the source node at $(5,5)$. The closed form calculations and simulations are done for the generalized-K channel. The values of m and c are changed to different values, and theoretical PDFs and matching simulation histograms are plotted in Figure 5.3. The plots show that at low values of m and c, i.e. when more intensive fading conditions are encountered, the average of battery recharging time increases. At high values of m and c, i.e. at more favorable fading conditions with partial line of sight and less intense shadowing, the battery average recharging time decreases, and the variance of distribution is also reduced, improving the reliability of the RF energy harvesting system. This is an expected result, battery recharging time increases when the channel
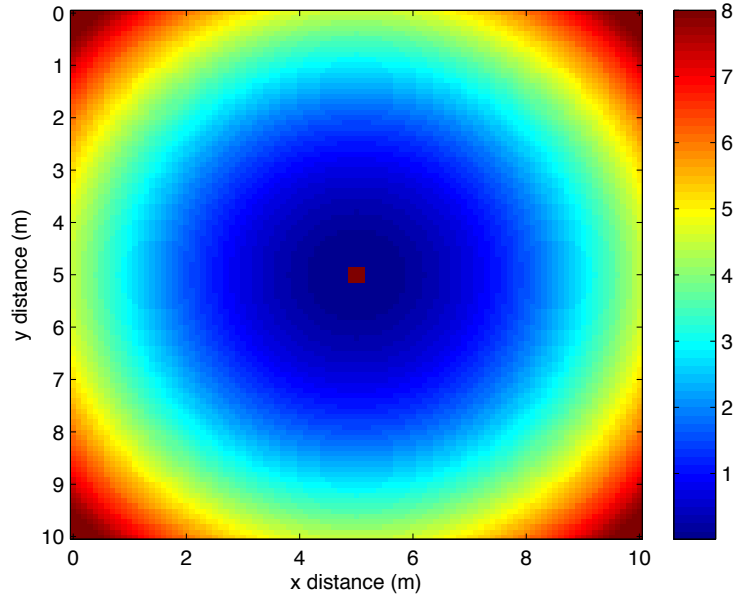
Figure 5.2: The coverage of battery recharging time (hour) for 10×10 m area. The red square at $(5,5)$ shows an RF source.
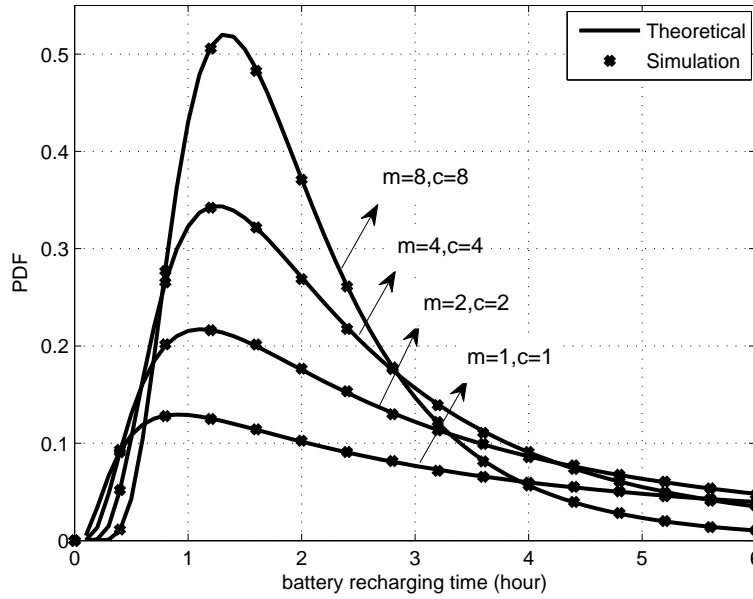
Figure 5.3: The analytical expression and simulation plots of the PDF of battery recharging time for fading parameters $m = c$ values $1, 2, 4, 8$.

condition deteriorates. The total effect can be evaluated according to the product of m and c paremeters, $(m \times c)$.

We also investigate the effects in the presence of small scale fading alone, considering the Nakagami-m channels. As, $c \to \infty$, we repeated calculations and simulations. In Figure 5.4, the red line shows the plot of $m = 1$, $c = 1$ for comparison purpose with

the shadowing case. The PDFs for $m = 1, 2, 4, 8$ are given and it can be seen that the battery recharging time becomes more predictable and smaller as the value of m increases. Furthermore, we need to emphasize that the shadowing effects have to be taken into consideration when setting up an RF energy harvesting system, as it dramatically affects the battery recharging time. Similarly, it can be proposed that the effect of small scale should not be ignored such as shadowing and path loss.
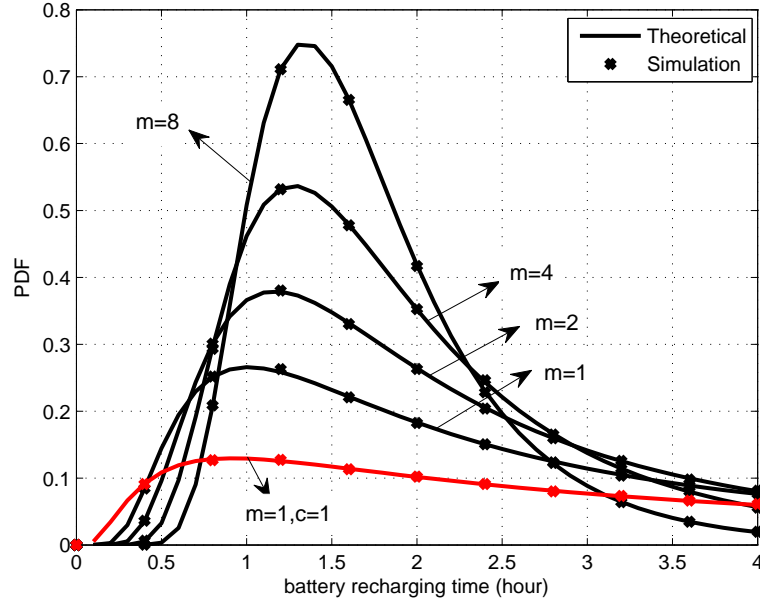
Figure 5.4: The comparison of shadowing and no-shadowing cases. The red line shows the channel with shadowing effect and the black lines are variations at no-shadowing case, namely, the Nakagami-m channel for $m = 1, 2, 4, 8$.

In the last figure, given in Figure 5.5, the tree dimensional plot of battery recharging time and distance and conversion efficiency is shown. The mean of battery recharging time are plotted at logarithmic scale. It can be seen that battery recharging time takes low values at the lowest value of distance and the highest value of conversion efficiency. It means that the improvement of conversion efficiency will have a very positive effect on the future energy harvesting systems.

5.5 Conclusions

In this chapter, energy harvesting from single RF signal source is considered. Using a continuously radiating RF source, the received power distributions for small scale and large scale channel models have been expressed. We investigated battery recharging
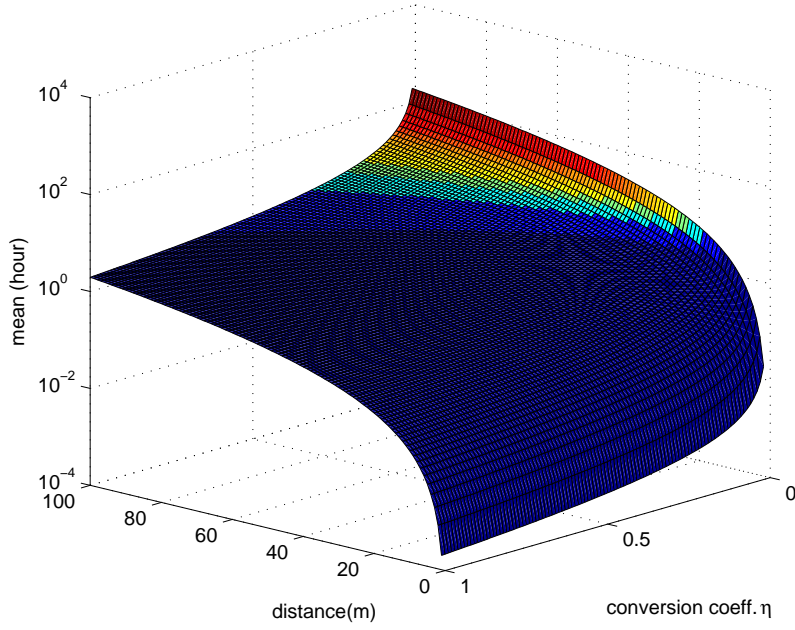
Figure 5.5: The mean value of battery recharging time vs. the distance and the conversion coefficient η. The mean values are plotted at logarithmic scale.

time of an energy harvesting receiver node. We propose battery recharging time as a critical parameter for energy harvesting devices or networks for ensuring availability of system.

We derived PDF, mean, and variance expressions of battery recharging times for lognormal shadowing channel distribution and the Nakagami-m distribution. We extended our results to PDF, mean, variance, CDF, and MGF expressions of battery recharging time for the generalized-K channel distribution. The conducted simulation results match theoretical analysis, showing the importance of distance and conversion efficiency and both of small scale and large scale fading effects.

The derived parametric expressions can be used for energy harvesting systems. In practical applications, the energy harvesting systems for wireless sensor networks can calculate the battery recharging time by distributions given in Section 5.3. Following this process, each sensor node can decide whether it will be in active or sleep mode. In the next chapter, this study will be extended to investigate the battery recharging time in the presence of multiple RF sources.

6. BATTERY RECHARGING TIME FOR MULTIPLE SOURCES

6.1 Purpose

The energy can be obtained from more than one source in the energy harvesting systems. As a continuation of the previous chapter, this chapter investigates the usage of RF signals emitted from multiple source nodes in energy harvesting systems. The system we consider consists of multiple RF source nodes, one destination node, and one energy harvesting receiver node. The total received power changes with the number of RF source nodes and the channel conditions. At the same time, the variation of instantaneous received power due to the number of source nodes affects the battery recharging time. We will investigate statistical models for battery recharging time in the presence of multiple RF source nodes for the generalized-K channel conditions. And then, we propose the Gamma distribution to obtain analitically tractable equatons. We derive the associated closed form probability density function, cumulative distribution function, moment generation function, mean, and variance expressions for battery recharging time. The simulations are used to verify the theoretical results.

6.2 System Description and Channel Models

6.2.1 System model

The energy harvesting system can use multiple RF signal sources. In this chapter, we will deal to express the distributions of battery recharging time in the event of multiple RF source nodes. Initially, we would like to find expressions for two RF source nodes, and then move from two source nodes to multi source nodes. In this context, the energy harvesting system model for two source nodes is shown in Figure 6.1. The source nodes (S_1 and S_2), the intended destination node (D), and the harvesting node (H) are
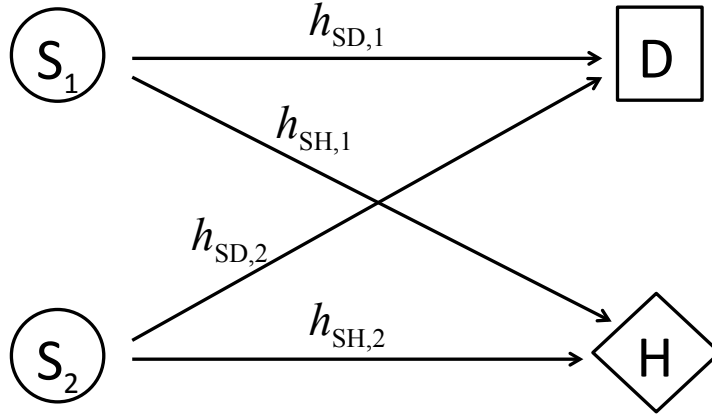
Figure 6.1: RF energy harvesting system model. S_1 and S_2 are the RF transmitters, D is the intended receiver, and H is the harvesting node. All nodes are physically separated.

the main components of system. S_1 and S_2 nodes transmit RF signals, which convey information to the destination node. At the same time, the energy of incoming signals from S_1 and S_2 nodes is harvested by the harvesting node. The harvested energy can be used to power a device directly, if the amount of harvested energy is sufficient. Now, we assume that the harvesting node uses this energy to recharge a micro-battery with finite capacity. The impacts of channel between sources and destination ($h_{SD,1}$ and $h_{SD,2}$) define the behaviours of communication channels. Since the informations are sent from the source nodes to the destination node, $h_{SD,1}$ and $h_{SD,2}$ have an important role on the accuracy of transmission and other critical issues. On the other hand, the channels between the source nodes and the harvesting node ($h_{SH,1}$ and $h_{SH,2}$) affects the amount of received energy at the front end of the harvesting node.

6.2.2 Channel models

We have already explained an overview of wireless fading channels in Chapter 4 and a summary of used channel models in Chapter 5. In this chapter, we will use the generalized-K composite fading channel model to find the statistical expressions of battery recharging time for more than one source. Further, we will use the Gamma distribution, which will be explained in the related section. Additionally, we will simulate the Friis transmission equation as deterministic expression of path loss for the instantaneous received power.

6.2.3 Transformation of multiple random variables

Probability theory allows to calculate the probability of an event that is defined as the joint behaviour of multiple random variables. In the next section, we will utilize the the relationship between random variables and their functions. Now, we would like to remind the transformation of multiple random variables.

Let $\vec{u}$ and $\vec{w}$ represent the vectors of random variables, the relationship between them and their distributions can be expressed as

$$\vec{u} \rightarrow \vec{w} \quad \Rightarrow \quad f(\vec{u}) \rightarrow f(\vec{w}) \tag{6.1}$$

where $f(\cdot)$ is the PDF of random variables. $\vec{u}$ and $\vec{w}$ are vector random variables. Assume that each of them has two random variables are shown as

$$\vec{u} = (u_1, u_2), \quad \vec{w} = (w_1, w_2). \tag{6.2}$$

Consider that the random variables u_1 and u_2 are expressed in terms of w_1 and w_2, or vice versa, as below

$$u_1 = h_1(w_1, w_2), \quad u_2 = h_2(w_1, w_2) \tag{6.3}$$

$$w_1 = h_3(u_1, u_2), \quad w_2 = h_4(u_1, u_2) \tag{6.4}$$

where $h_1(\cdot)$, $h_2(\cdot)$, $h_3(\cdot)$, and $h_4(\cdot)$ represent mathematical functions. In such a case, we can use the Jacobian matrix that is the matrix of first order partial derivatives of each function of random variables in vector

$$J_{\vec{w}}(u_1, u_2) = \begin{bmatrix} \frac{dw_1}{du_1} & \frac{dw_1}{du_2} \\ \frac{dw_2}{du_1} & \frac{dw_2}{du_2} \end{bmatrix}. \tag{6.5}$$

In this event, the matrix is a square matrix, and its determinant can be calculated as the absolute value of the Jacobian determinant of $\vec{w}$

$$J = |det(J_{\vec{w}}(u_1, u_2))|. \tag{6.6}$$

The distribution of $\vec{u}$ and the Jacobian matrix are used to obtain the PDF of $\vec{w}$, as

$$f_{\vec{w}}(w_1, w_2) = \frac{f_{\vec{u}}(u_1, u_2)}{|det(J_{\vec{w}}(u_1, u_2))|}. \tag{6.7}$$

63

And subtitude h_1, h_2, and J in (**6.7**), the expression becomes

$$f_{\vec{w}}(w_1, w_2) = \frac{f_{\vec{u}}(h_1(w_1, w_2), h_2(w_1, w_2))}{J}. \tag{6.8}$$

It is well known that the equation can be integrated to obtain the marginal distribution of only one random variable.

$$f_{w_1}(w_1) = \int_0^\infty f_{\vec{w}}(w_1, w_2) dw_2, \quad w_1, w_2 > 0 \tag{6.9}$$

Finally, the joint PDF of $\vec{w}$ is replaced with expression in terms of the joint PDF of $\vec{u}$ in (**6.8**)

$$f_{w_1}(w_1) = \int_0^\infty \frac{f_{\vec{u}}(h_1(w_1, w_2), h_2(w_1, w_2))}{J} dw_2, \quad w_1, w_2 > 0 \tag{6.10}$$

6.3 Statistical Models for Battery Recharging Time

In order to express the statistical model of battery recharging time, we need to model the distribution for the instantaneous received power, P_r, at the harvesting node. It is assumed that the channel effects are the combination of path loss, shadowing, and fading. In our system model, both of RF sources are transmitting continuously, and the received signals are non-overlapping narrowband signals, which do not reduce the total power by affecting other signal. Under these conditions, the total received power in two RF source nodes case is expressed as

$$P_r = P_{r,1} + P_{r,2} \tag{6.11}$$

where $P_{r,1}$ and $P_{r,2}$ represent the instantaneous received power when RF signal of first and second source is received at the antenna alone, respectively. It is obvious that the battery recharging time (T_r) is not equal to the total of battery recharging times for each RF source, namely, $T_r \neq T_{r,1} + T_{r,2}$. According to the definition in [5], it becomes

$$T_r = \frac{\alpha}{P_r} = \frac{\alpha}{P_{r,1} + P_{r,2}}. \tag{6.12}$$

The distribution of T_r can be obtained according to the relationship between T_r and the received powers (**6.12**) by using the distributions of received powers. We can utilize the vectoral representations of variables to achive transforming of distributions.

Now, we can use the informations mentioned in the previous section to obtain the PDF of battery recharging time. $\vec{u}$ and $\vec{w}$ can be defined as

$$\vec{u} = (P_{r,1}, P_{r,2}), \quad \vec{w} = \left(\frac{\alpha}{P_{r,1} + P_{r,2}}, P_{r,2} \right), \tag{6.13}$$

where α was defined in (**5.8**) as a positive constant parameter.

We need to find an expression for the Jacobian determinant. The absolute value of the Jacobian determinant is calculated from (**6.6**) as

$$J = \frac{\alpha}{(P_{r,1} + P_{r,2})^2}. \tag{6.14}$$

According to (**6.3**), $P_{r,1}$ and $P_{r,2}$ are expressed as

$$P_{r,1} = h_1(w_1, w_2) = \frac{\alpha}{w_1} - w_2, \quad P_{r,2} = h_2(w_1, w_2) = w_2. \tag{6.15}$$

For independent random variables, the marginal distributions of RF signals are producted to obtain the joint distribution.

$$f_{\vec{u}}(P_{r,1}, P_{r,2}) = f_{P_{r,1}}(P_{r,1}) \times f_{P_{r,2}}(P_{r,2}). \tag{6.16}$$

It is obvious that $w_1 = \tau$ (**6.12**) where τ is the outcomes of battery recharging time for two source nodes. From (**6.10**), the equation of battery recharging time for the generalized-K distributed channel becomes

$$f_{T_G}(\tau) = \int\limits_{0}^{\infty} \frac{f_{P_{r,1}}(h_1(\tau, P_{r,2})) . f_{P_{r,2}}(h_2(\tau, P_{r,2}))}{J} dP_{r,2}, \tag{6.17}$$

where J can be replaced with $J = \frac{\tau^2}{\alpha}$ by using (**6.14**) and (**6.15**).

The distributions of $P_{r,1}$ and $P_{r,2}$ are chosen as the generalized-K distribution. Then, the integration in (**6.18**) is obtained.

$$
\begin{aligned}
f_{T_G}(\tau) = \int\limits_{0}^{\infty} & \frac{\alpha}{\tau^2} \frac{2b_1^{m_1+c_1}}{\Gamma(m_1)\Gamma(c_1)} \left(\frac{\alpha}{\tau} - P_{r,2} \right)^{\frac{m_1+c_1}{2}-1} K_{c_1-m_1}\left(2b_1 \sqrt{\frac{\alpha}{\tau} - P_{r,2}} \right) \\
& \frac{2b_2^{m_2+c_2}}{\Gamma(m_2)\Gamma(c_2)} P_{r,2}^{\frac{m_2+c_2}{2}-1} K_{c_2-m_2}(2b_2 \sqrt{P_{r,2}}) dP_{r,2}
\end{aligned} \tag{6.18}
$$

This expression gives the PDF of battery recharging time for two independent RF sources, which is not a closed form expression. In this instance, we prefer to propose

a method to obtain battery recharging time by using convolution integral. Remember that the definition of convolution for two independent functions f and g is given as

$$conv(f,g)(\tau) = (f * g)(\tau) = \int_{-\infty}^{\infty} f(t).g(\tau - t)dt, \tag{6.19}$$

where $*$ denotes the convolution sign. If functions f and g are non-negative, the integration limits becomes between 0 and ∞, $[0,\infty)$, instead of $(-\infty,\infty)$.

After this reminder, it can be recognized that the equation in (**6.18**) is a form of convolution on $P_{r,1}$ and $P_{r,2}$, which was transformed by using (**5.10**). Depending on convolution, we can express battery recharging time for independent two RF source nodes as

$$f_{T_G}(\tau) = \frac{\alpha}{\tau^2}.(P_{r,1} * P_{r,2})(\frac{\alpha}{\tau}). \tag{6.20}$$

If three source nodes are available instead of two source nodes, the total received power becomes $P_r = P_{r,1} + P_{r,2} + P_{r,3}$. It is possible to write an equation for the battery recharging time as

$$f_{T_G}(\tau) = \frac{\alpha}{\tau^2}.(P_{r,3} * (P_{r,1} * P_{r,2}))(\frac{\alpha}{\tau}). \tag{6.21}$$

In order to obtain a more general expression, the number of independent source nodes can be denoted as $i = 1, 2, \ldots, N$. In that case, the total received power is expressed as

$$P_r = P_{r,1} + P_{r,2} + \cdots + P_{r,N}. \tag{6.22}$$

We can extend equations (**6.20**) and (**6.21**) to find the PDF of battery recharging time for N independent source nodes as

$$f_{T_G}(\tau) = \frac{\alpha}{\tau^2}.(P_{r,N} * (P_{r,N-1} * \cdots * (P_{r,3} * (P_{r,1} * P_{r,2})) \cdots)(\frac{\alpha}{\tau}). \tag{6.23}$$

Eventually, the PDF of battery recharging time for independent multiple RF source nodes has been calculated by using (**6.23**). This is a method, but not a closed form expression. In order to find a closed form expression, the Gamma distribution can be used, which is explained in the next section.

6.4 Gamma Distribution for Channel Approximation

The closed form expressions provide us analytical tractability. Hence, it can be tried to find alternative solutions that provide well-approximation for the generalized-K distribution. In this context, the use of the Gamma distribution approximated by the moment matching with adjustment has proposed in [59]. The Gamma PDF is also known as the distribution of the instantaneous received power on the Nakagami-m fading channel. The Gamma PDF of the instantaneous received power is given as

$$f_{P_\Gamma}(x) = \frac{x^{k-1}}{\Gamma(k)\theta^k} \exp(-\frac{x}{\theta}), \quad x > 0, \tag{6.24}$$

where k is shape parameter, and θ is scale parameter of the Gamma PDF. Depending on these two parameters, the Gamma distribution is also indicated as $Gamma(k,\theta)$.

As another definition, the amount of fading (AF) is defined as a parameter that is a scale for fading in the wireless channels [58]

$$AF = \frac{\sigma^2 - \mu^2}{\mu^2}, \tag{6.25}$$

where σ^2 represents the variance, and μ is the mean.

By using the moment matching method for the first and the second moments, k and θ become [59]

$$\theta = \left(\frac{1}{m} + \frac{1}{c} + \frac{1}{mc}\right)\mu_0 = AF\mu_0, \quad k = \frac{1}{AF}, \tag{6.26}$$

where μ_0 is the received local power. Then, the adjustment factor (ε) is used to address poor approximation in the related regions [59]. The adjusted expressions of θ and k are obtained as

$$\theta_a = (AF - \varepsilon)\mu_0, \quad k_a = \frac{1}{AF - \varepsilon}, \tag{6.27}$$

where ε is limited, $-AF \leqslant \varepsilon \leqslant AF$. Equaitions in (**6.27**) is valid for a single random variable. Considering RF energy harvesting, the Gamma distribution with the parameters in (**6.27**) describe the PDF of received power in the presence of a single RF source node.

It is possible to find expressions in the presence of more than one RF source nodes. For the sum of two independent the Gamma distributed random variables, θ_a and k_a

are given in [59] as

$$\theta_{a,12} = \frac{(AF_1 - \varepsilon_1)\mu^2_{0,1} + (AF_2 - \varepsilon_2)\mu^2_{0,2}}{\mu_{0,1} + \mu_{0,2}}, \tag{6.28}$$

$$k_{a,12} = \frac{(\mu_{0,1} + \mu_{0,2})^2}{(AF_1 - \varepsilon_1)\mu^2_{0,1} + (AF_2 - \varepsilon_2)\mu^2_{0,2}}, \tag{6.29}$$

where the indices, 1 and 2, represent the correponding random variables. Additionally, the definition of $\theta_{a,12}$ and $k_{a,12}$ can be obtained for the independent identically distribution (i.i.d.) case. The indices in (6.28) and (6.29) are removed for the i.i.d case, namely, $AF = AF_1 = AF_2$, $\varepsilon = \varepsilon_1 = \varepsilon_2$ and $\mu_0 = \mu_{0,1} = \mu_{0,2}$. As a result of this process, the parameters are simplified as

$$\theta_{a,12} = (AF - \varepsilon)\mu_0, \quad k_{a,12} = \frac{2}{AF - \varepsilon}. \tag{6.30}$$

Hence, we obtained $\theta_{a,12}$ and $k_{a,12}$ for two source nodes that have the i.i.d. RF signals. Recognize that $\theta_{a,12} = \theta_a$ and $k_{a,12} = 2 \times k_a$. It is possible to extend the Gamma distribution from the sum of two random variables to the sum of N random variables for the i.i.d. case. The PDF of the sum of N i.i.d. Gamma random variables is shown to be as [61]

$$\sum_{i=1}^{N} P_{r,i} \sim Gamma(Nk_a, \theta_a). \tag{6.31}$$

Considering the expressions for a single random variable, θ_a remains unchanged, k_a is multipled by N. The equations of shape and scale parameters for total received power from N sources are defined as

$$\theta_{a,1N} = (AF - \varepsilon)\mu_0, \quad k_{a,1N} = \frac{N}{AF - \varepsilon}. \tag{6.32}$$

Now, we can derive expressions for battery recharging time in the presence of single RF source node and also multiple RF source nodes. We know that the PDF of received power can be transformed to obtain the distribution of battery recharging time by following equation (5.10)

$$f_{T_r}(\tau) = \frac{\alpha}{\tau^2} f_{P_r}\left(\frac{\alpha}{\tau}\right). $$

By performing the transformation of the Gamma PDF (6.24) according to (5.10) together with θ_a and k_a, the PDF of battery recharging time is obtained as

$$f_{T_r}(\tau) = \frac{\alpha^k}{\tau^{k_a+1}\Gamma(k_a)\theta^{k_a}_a} \exp(-\frac{\alpha}{\tau\theta_a}), \quad \tau > 0. \tag{6.33}$$

The mean value of battery recharging time can be calculated by using the first order statistical expectation as

$$\mu_{T_r} = \int_0^\infty \tau f_{T_r}(\tau) d\tau = \frac{\alpha \Gamma(k_a - 1)}{\theta_a \Gamma(k_a)}, \quad \theta_a > 0, k_a > 1 \tag{6.34}$$

and the variance is obtained by using the first and the second moments, which is shown to be

$$\sigma_{T_r}^2 = \frac{\alpha^2}{\theta^2_a \Gamma(k_a)} \left[\Gamma(k_a - 2) - \frac{\Gamma(k_a - 1)^2}{\Gamma(k_a)} \right], \quad \theta_a > 0, k_a > 2. \tag{6.35}$$

The CDF of the Gamma distribution is given by

$$F_{P_\Gamma}(x) = \frac{Gamma(k_a, \frac{x}{\theta_a})}{\Gamma(k_a)}. \tag{6.36}$$

As the battery recharging time is inversely proportional to the received power, the CDF of battery recharging time for the Gamma distribution channel can be calculated by

$$F_{T_r}(\tau) = 1 - F_{P_\Gamma}\left(\frac{\alpha}{\tau}\right). \tag{6.37}$$

The transformation of distribution is performed by puting (**6.36**) into (**6.37**), the CDF of battery recharging time, $F_{T_r}(\tau)$, can be shown to be as

$$F_{T_r}(\tau) = 1 - \frac{Gamma(k_a, \frac{\alpha}{\tau \theta_a})}{\Gamma(k_a)}, \tag{6.38}$$

The MGF of instantaneous received power for the Gamma distribution, $\Phi_{P_r}(s)$, has been given as in (**6.39**). From the following definition of MGF as the expectation function, $\Phi_{T_r}(s) = \int_0^\infty \exp(-s\tau) f_{T_r}(\tau) d\tau$, the MGF of battery recharging time for the Gamma distribution channel, $\Phi_{T_r}(s)$, is derived as in (**6.40**).

$$\Phi_{P_r}(s) = (1 - \theta_a s)^{-k_a}, \tag{6.39}$$

$$\Phi_{T_r}(s) = \frac{2\alpha^{1+\frac{k_a}{2}}(\theta_a s)^{-1+\frac{k_a}{2}} K_{k_a-2}\left(2\sqrt{\frac{\alpha s}{\theta_a}}\right)}{\Gamma(k_a)} \tag{6.40}$$

where α, θ_a, and s are greater than zero.

As a convinience, the expressions are derived by using θ_a and k_a. All equations from (**6.33**) to (**6.40**) can be used for multiple RF source nodes by using $N \times k_a$ instead of k_a.

6.5 Numerical and Simulation Results

The numerical analyses and simulations are performed to verify the derived expressions for battery recharging time. In simulations, RF source nodes transmit signals continuously. We assume that the received RF signals are non-overlapping narrowband signals.
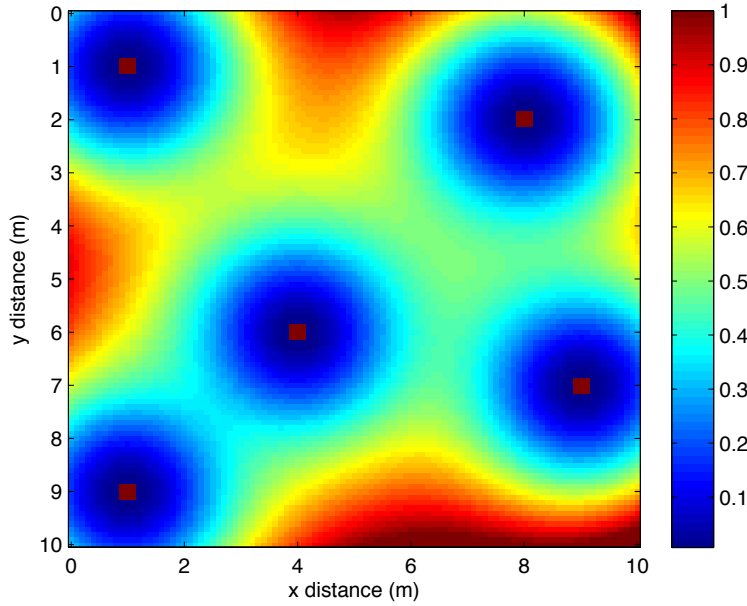
Figure 6.2: The coverage of battery recharging time (hour) for 10×10 m area. The red squares at $(1,1),(2,8),(6,4),(7,9),$ and $(9,1)$ show RF sources.

Firstly, we want to demonstrate the deterministic change of battery recharging time according to distance between RF source nodes and the harvesting node. We define a coverage area whose dimensions are 10×10 meters. Similar to the situation in single source, each point in the defined area is a potential harvesting node, which has an omnidirectional antenna. The number of RF source nodes are increased from one to five to show multi sources case. Five RF source nodes marked with red squares are placed at seperate coordinates as $(1,1),(2,8),(6,4),(7,9),$ and, $(9,1)$. RF source nodes send signals with omnidirectional antennas. Figure 6.2 illustrates the value of battery recharging time due to the path loss effect at each point of coverage area. Simulation parameters for this figure are same as the simulation parameters of single source case, as given in Table 5.1. If we pay attention to the color scale in Figure 6.2, it can be seen that the maximum value of the color scale decreases to from 10 (Figure 5.2) to 1 for the defined area. Moreover, the areas with red color are smaller

than the red colored areas in single source case. It means that the battery recharging time decrease with the increase of the number of RF source nodes. This is an expected result owing to the summation of received powers.

Secondly, the difference between the generalized-K distribution and the Gamma distribution can be indicated on a figure. The parameters are same as the single source simulation. Figure 6.3 shows battery recharging time in the presence of both channel conditions for single source. The black line is the generalized-K distribution, and the red line is the Gamma distribution for the same conditions. The Gamma distribution provides a significant approximation as shown in the figure. In the numerical calculation, the adjustment factor is equal to zero for the Gamma distribution. It means that the difference between two distributions can be decreased by searching appropriate adjustment factor.

Thirdly, we would like to investigate the use of adjustment factor in the Gamma distribution. Two RF source nodes and one harvesting node are used in the simulation. There are 2.8 meters between the source nodes and the harvesting node, which are spatially seperated. The distributions of battery recharging time for two source nodes are illustrated in Figure 6.4. The black squares show the simulation results for the parameters of $m = c = 4$. The blue line is the Gamma distribution with $\varepsilon = 0$.

We run an iterative code to minimize the absolute value of difference between the simulation results and the Gamma distribution with adjustment factor. We use 'fminsearch' command in Matlab. ε is changed step by step to find minimum difference value. After a sufficient number of trials, the resulting value of ε does not change much. Thus, the minimization code gives us the most appropriate value of ε to provide well-approximation. The value of ε is calculated as 0.095. The red dash line is drawn for the Gamma distribution with $\varepsilon = 0.095$. It can be seen that the adjustment factor should be used for fine-tuning of approximation in the calculation of battery recharging time.

Fourthly, we aim to understand the effect of second source node on the battery recharging time. Firstly, we consider that there is an energy harvesting node capturing signal from single RF source node. And then, we put another RF source node to

71
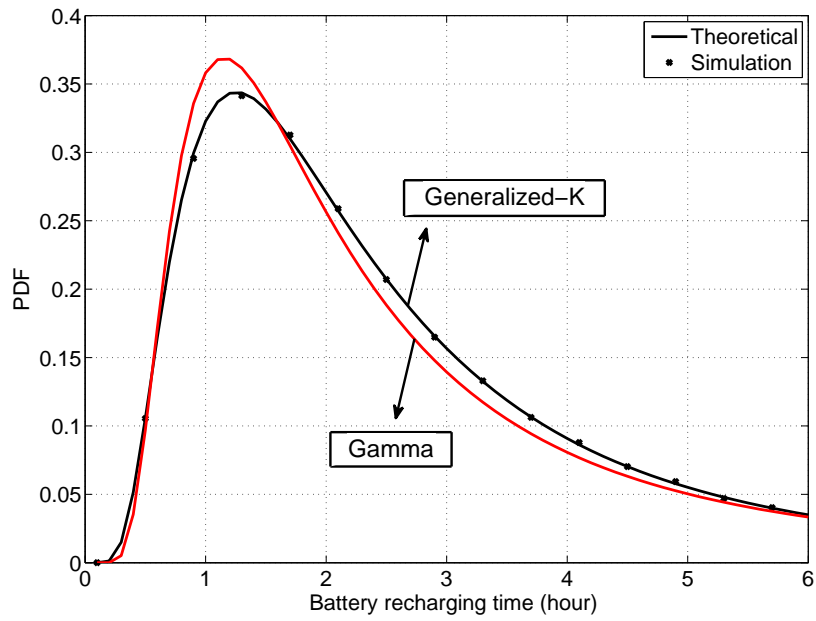
Figure 6.3: The generalized-K distribution and the Gamma distribution for the same parameters.
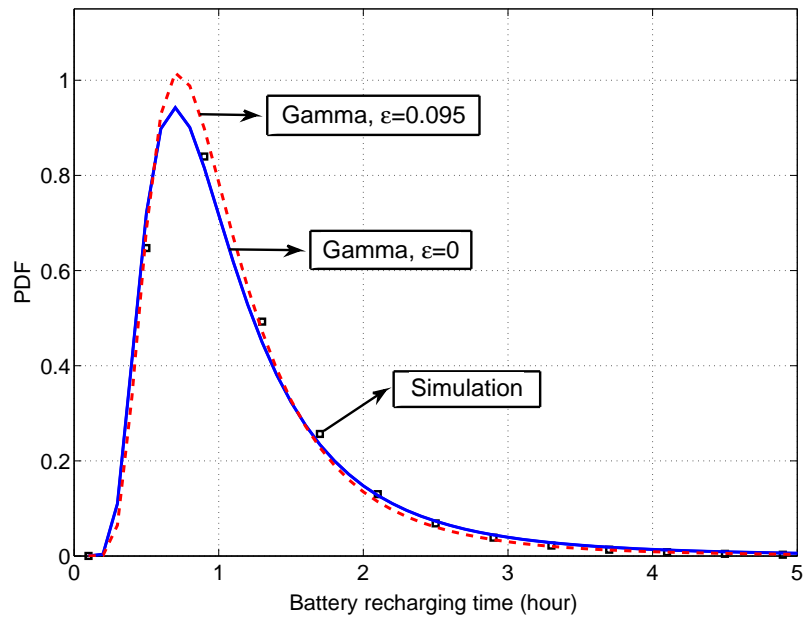
Figure 6.4: The distributions of battery recharging time with different adjustment factors, $\varepsilon = 0$ and $\varepsilon = 0.095$.

observe the change of battery recharging time. Figure 6.5 represents the results with the same parameters as in the previous simulation. The red line is for single source case, and the black line shows the battery recharging time when we add the second source. The most probable value of battery recharging time drops from 1.2 to 0.7 with the second source.
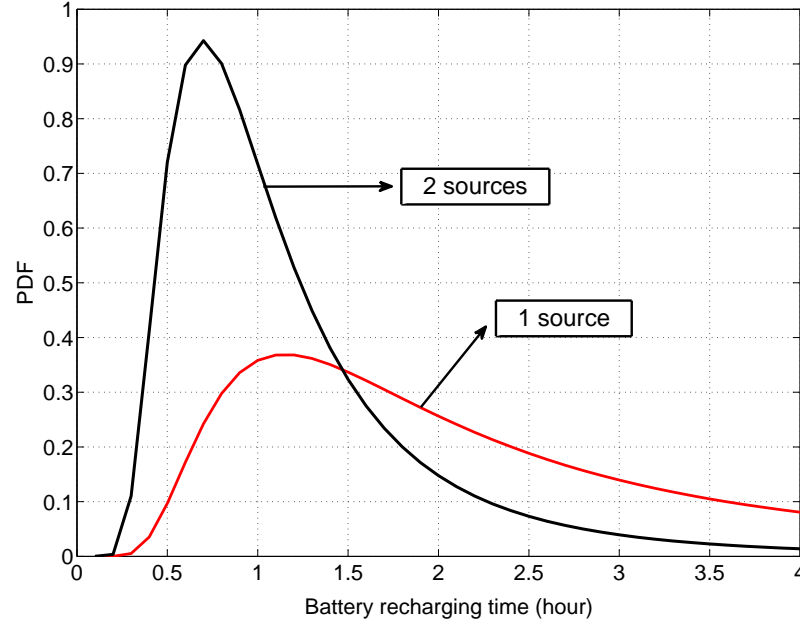
Figure 6.5: The distributions of battery recharging time for single source and two sources. Battery has 1.2V operating voltage and 10mAh capacity.

In the last simulation, we would like to include some results about the number of sources (N>2). Figure 6.6 illustrates the PDFs of battery recharging time for N sources, where N is the number of RF sources. The mean value of battery recharging time for 5 sources is calculated about 2.2 hours, while the mean value of battery recharging time for 2 sources is about 6.7 hours. It means that the increase of RF source number will cause to decrease in the battery recharging time for energy harvesting systems. At the same time, we show the effect of operating voltage and capacity of battery on the battery recharging time. The operating voltage of battery is increased from 1.2V to 3.3V and the capacity of battery is increased from 10mAh to 20mAh. This process causes an increase in the battery recharging time. It can be seen when we compare the results with the previous simulation.
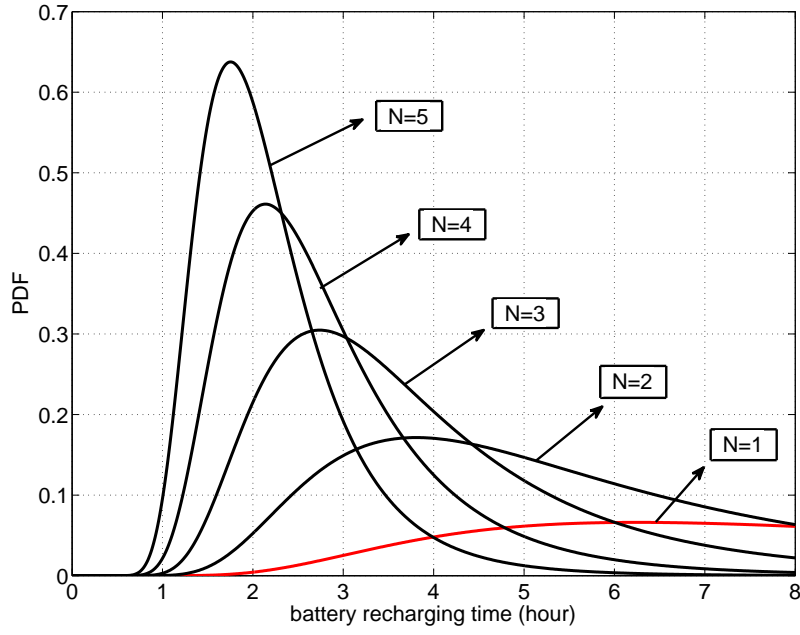
Figure 6.6: The distributions of battery recharging time for N sources, N=1,2,...,5. Battery has 3.3V operating voltage and 20mAh capacity.

6.6 Conclusions

In the previous chapter where the system model depends on single RF signal source, we proposed statistical models and derived the distribution expressions for battery recharging time. Also, it is possible for an energy harvesting system to gather signals from multi source nodes. In this chapter, we studied on a system with multi RF signal sources to obtain battery recharging time distribution equations. We tried to extend equations from single source to two sources for the generalized-K distribution. We saw that it is difficult to advance with the obtained equations. In that case, we proposed to use the Gamma distribution instead of the generalized-K distribution. We derived the PDF, the CDF, the MGF, the mean, and the variance expressions of battery recharging times for the Gamma distribution. The conducted simulation results shows that the Gamma distribution ensure well-approxiimation to the generalized-K distribution. Moreover, we propose the use of adjustment factor, which bring closer both of them. Additionally, we demonstrated the effect of second RF source node, which allow of the decrease of battery recharging time. Hence, the number of RF source is important for energy harvesting systems.

7. TEST STUDY

7.1 Purpose

So far, we have explained theoretical aspect of RF energy harvesting and statistical models of battery recharging time. Now, we would like to investigate real-life RF energy harvesting applications. Thus, we will carry out a testbed implementation.

7.2 Equipment

Powercast is a technology company producing RF energy harvesting integrated circuits, which bring wireless power capability to micro-power devices. Powercast also produce evaluation boards and development kits. These products are useful for experimental research studies. We use P2110-EVAL-01 that is an energy harvesting development kit for wireless sensors. The components of P2110-EVAL-01 are listed below.

1. Power and Data Transmitter (TX91501-3W-ID)

2. P2110 Evaluation Board Kit (P2110-EVB)

3. Wireless Sensor Board (WSN-EVAL-01)

4. Microchip 16-bit XLP Development Board (DM240311)

5. Microchip MRF24J40 PICtail/PICtail Plus Daughter Board (AC164134-1)

The image of parts can be seen in Figure 7.1.

The Powercast TX91501 transmitter sends both power and data at the center frequency value of 915MHz. It transmits signal whose power is 3W EIRP with integrated 8dBi antenna. The antenna of transmitter is designed, which has 60° horizontal and 60° vertical beam patterns.

Figure 7.1: The contents of P2110-EVAL-01 energy harvesting development kit [4].

The P2110-EVB kit contains the following parts.

- Evaluation board for P2110 Powerharvester^{TM} receiver

- PCB omnidirectional (dipole) antenna

- PCB directional (patch) antenna

The P2110 Powerharvester receiver converts RF energy into DC energy at the frequency range of 850-950MHz. It gives regulated voltage output up to 5.25V, and output current up to 50mA. If the input power level is less then -11.5dBm, it is not possible to harvest energy with P2110. There is an supercapacitor with 50 mF capacity on the evaluation board to store energy and to give regulated output power. The antennas are designed as printed circuit board. The gain of antennas are 1dBi and 6.1dBi for dipole and patch antennas, respectively. The beam pattern of patch antenna is 122° horizontal and 68° vertical, while the beam pattern of dipole antenna is 360°.

Wireless sensor board measures the values for temperature, humidity, light, and an external input. It sends these informations to the access point by adding the received power value and transmit time. Additionally, the identity number of transmitter is decoded by the microcontroller on the wireless sensor board.

16-bit XLP development board and MRF24J40 PICtail/PICtail plus daughter board are products of Microchip company [62]. 16-bit XLP development board is a development platform that works by programming Microchip's PIC24F microcontroller for the

76
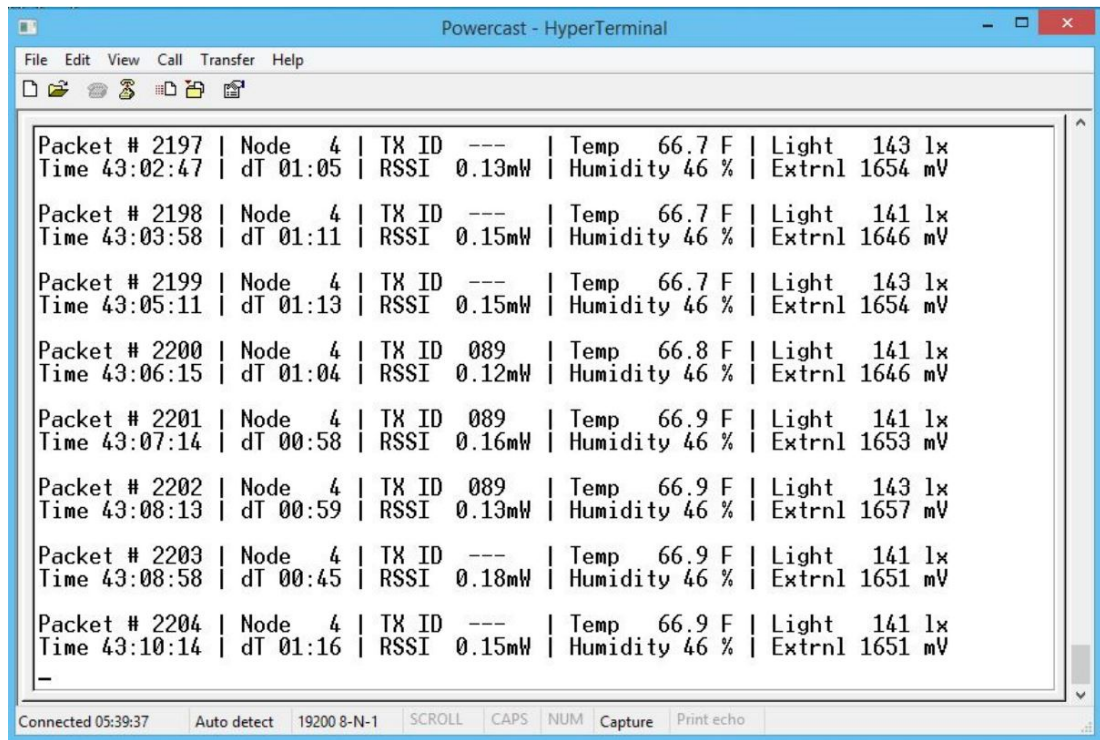
Figure 7.2: The display of HyperTerminal that shows the received data from the wireless sensor board.

desired purpose. MRF24J40 PICtail/PICtail plus daughter board is a IEEE 802.15.4 radio receiver at 2.4GHz.

7.3 Operation

The P2110-EVAL-01 is a demonstration and development platform for wireless sensor applications with RF energy harvesting. The operation of development kit is started by powering of transmitter. The TX91501 transmitter sends RF signal with the identity number of transmitter. The incident RF signal is received by the antenna of P2110 evaluation board, which the received signal is converted to DC signal by the P2110 Powerharvester component. The obtained DC energy is stored in the supercapacitor. When the charge of supercapacitor is sufficient, the regulated output of the P2110 powers the WSN-EVAL-01 wireless sensor board that sends a radio signal including ambient information to the access point. The acces point consists of 16-bit XLP development board and MRF24J40 PICtail/PICtail plus daughter board that is plugged into development board. It is programmed to receive data coming from the wireless sensor board.

The access point is connected to a laptop via an USB cable, which transfer the data to a terminal emulator program. HyperTerminal can be used as a terminal emulator program, which displays and logs the incoming data. Figure 7.2 shows the received data by HyperTerminal during our tests.

7.4 Test Models

We use P2110-EVAL-01 energy harvesting development kit as a testbed equipment. Firstly, we would like to demonstrate the variation of mean value of battery recharging time with distance. The test model depends on the energy harvesting application between a transmitter as RF source, and an evaluation board with plugin wireless sensor board as energy harvesting node. The signal energy coming from a transmitter is harvested and stored to 50mF supercapacitor by the evaluation board, and used for sending data by the wireless sensor board. The values of received power and the times between each incoming data are logged by means of HyperTerminal. The energy harvesting node is shifted to other distance at the end of each measurement. The mentioned process is repeated for various distances. In our test, we measured the received power and the incoming data time for four different distances from 3m to 6m. This test is named as Testbed-1 whose model can be seen in Figure 7.3.

The time between each incoming data gives the recharging time of supercapacitor similar to the battery as a storage unit. Hence, it can be taken as the battery recharging time.
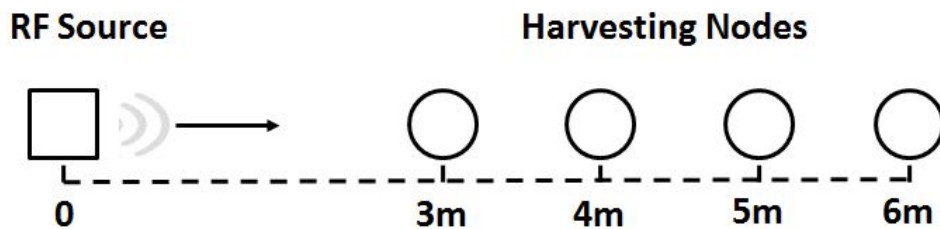
Figure 7.3: The test model for Testbed-1.

Another test model is established by using two transmitters as two RF sources, and an evaluation board with plugin wireless sensor board as energy harvesting node. Our aim is to show the energy harvesting in the presence of multi RF source. Similar to

the first test, the incident RF signal energies from two sources are captured, stored, and used to power the wireless sensor board. In our testbed named as Testbed-2, two transmitters are placed 7m distance to the energy harvesting node with same angle and 1m seperation distance. Figure 7.4 illustrates the test model for Testbed-1.

Figure 7.4: The test model for Testbed-2.

7.5 Test Results

Tests were performed on an empty area of the communication laboratory at the university. There was LOS between the transmitter node and the energy harvesting node. The nodes were placed on the taborets, which ensures same height level from ground. The acces point that was connected to a laptop with an USB cable was placed on a near table. A photo taken during the test can be seen in Figure 7.5.

The parameters for tests are listed in Table 7.1. The directional patch antenna was used at the harvesting node side for the presented test results.

Table 7.1: Test parameters for single source and two sources testbeds.

Parameters	Values
Frequency (f)	915 MHz
EIRP ($P_t \times G_t$)	3 W
Gain of Receiving Antenna (G_r)	6.1 dBi
Battery Charging Voltage (V_b)	3.3 V
Supercapacitor Capacity (C_s)	50 mF

Figure 7.5: A photo taken during the test.

First, we implemented Testbed-1 to obtain the received power and the battery recharging time. Figure 7.6 shows the mean values of received power versus the distance between the transmitter and the harvesting node. Additionally, the computed standard deviation of received power is given to see the variations due to the effect of wireless channel. It is computed about 0.19 for 5 meters distance. The mean value of received power was measured as 2.7mW for 3m, which is the maximum value among the test results of 3-6m distances. The received power decreases with the increasing distance as expected.

The mean values and variations of battery recharging time versus the distance are illustrated in Figure 7.7. We measured the mean value of battery recharging time for 3m as 1.8 seconds. It increased up to 8.5s for 6m distance. As a result, the battery recharging time increases severely with the increasing values of distance. Moreover, it can be seen that the battery recharging time is reversely proportional to the received power. The values of standard deviation are computed between 0.42 to 0.81 for battery recharging time.
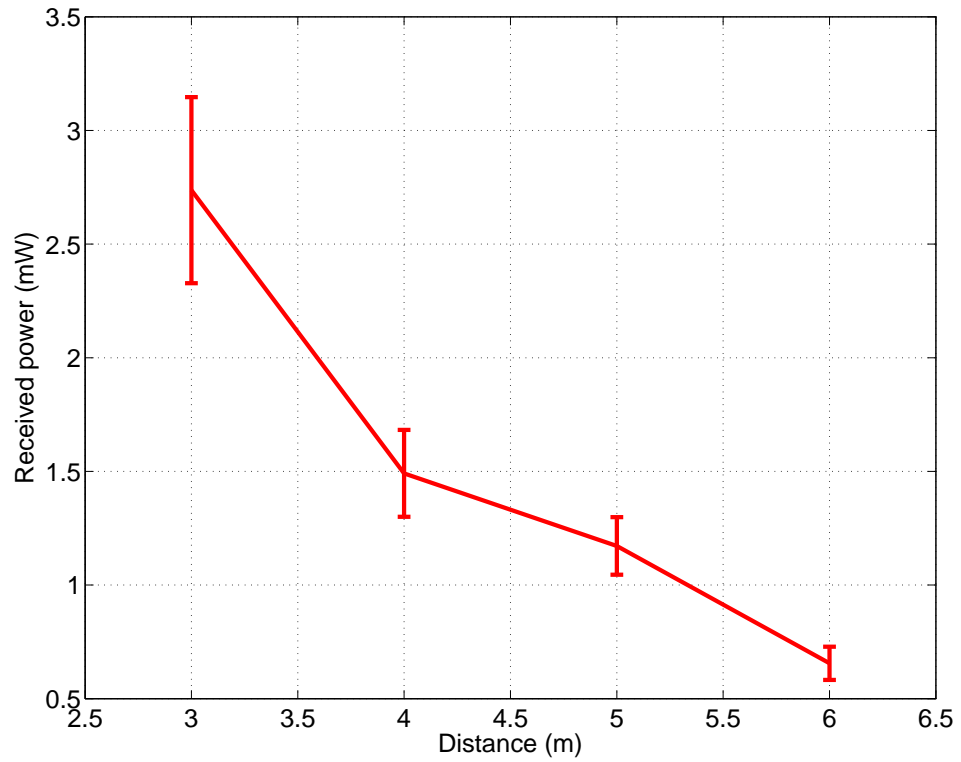
Figure 7.6: The received power versus the distance for energy harvesting with single RF source node. Bars show the standard deviation of received power.
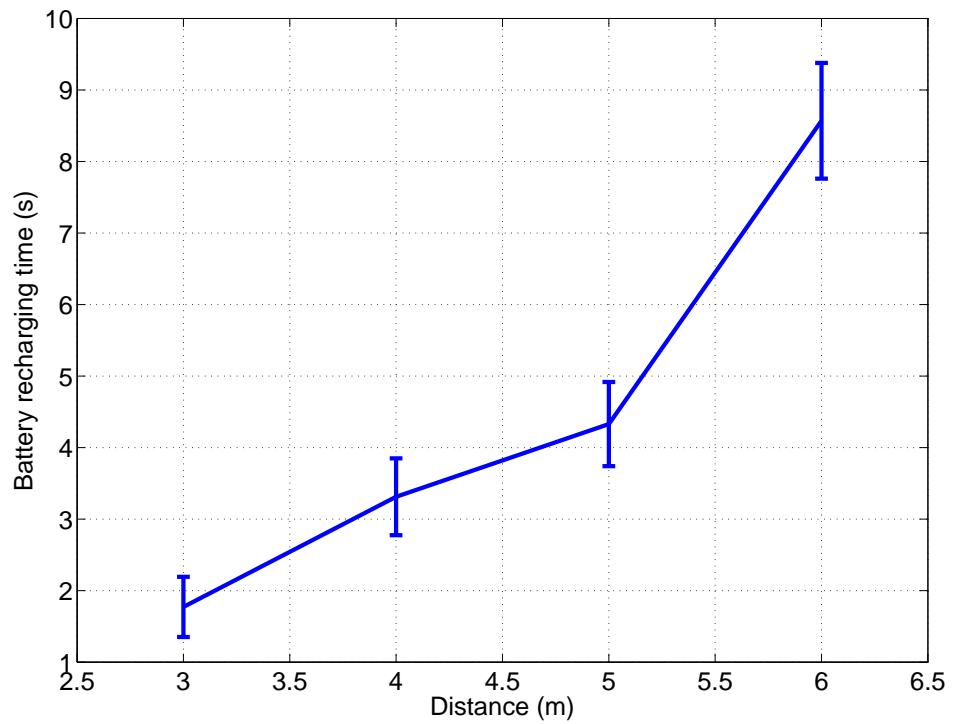
Figure 7.7: The battery recharging time versus the distance for energy harvesting with single RF source node. Bars show the standard deviation along a curve.
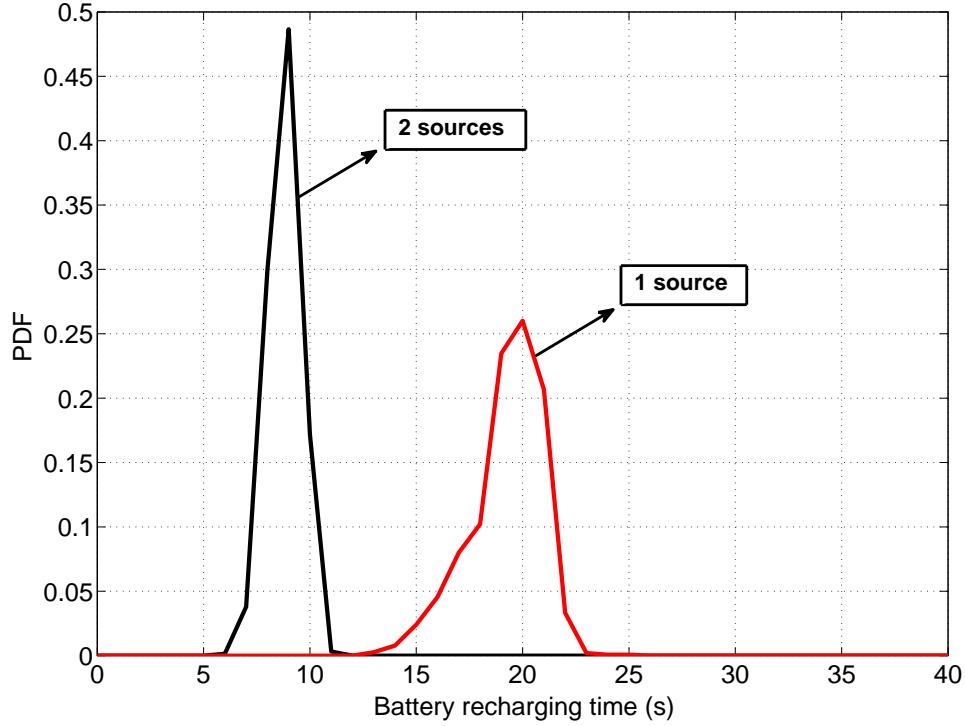
Figure 7.8: The battery recharging time for one RF source and two RF sources.

Secondly, we set-up Testbed-2 to investigate multi RF source nodes case. We measured battery recharging time for the first transmitter and the second transmitter alone, and then both of them together. In two transmitters case, RF signals are sent by two transmitters and received together by the energy harvesting wireless sensor. Figure 7.8 illustrates the distributions of battery recharging time for both one transmitter and two transmitters. As shown in the figure, the mean value of battery recharging time was reduced from 19.2s to 8.8s with the activation of the second source. It is inferred that the battery recharging time decreases with the increasing number of RF source nodes.

We also would like to compare the distribution of battery recharging time obtained by test study with the distribution of battery recharging time obtained by simulation. Figure 7.9 illustrates the simulation and the test distribution. The red points show simulation results and the black points show test results. It is possible to extract the parameters of wireless channel from the comparison of them. As a comparision criterion, we calculate the summation of difference between them. The values of α,
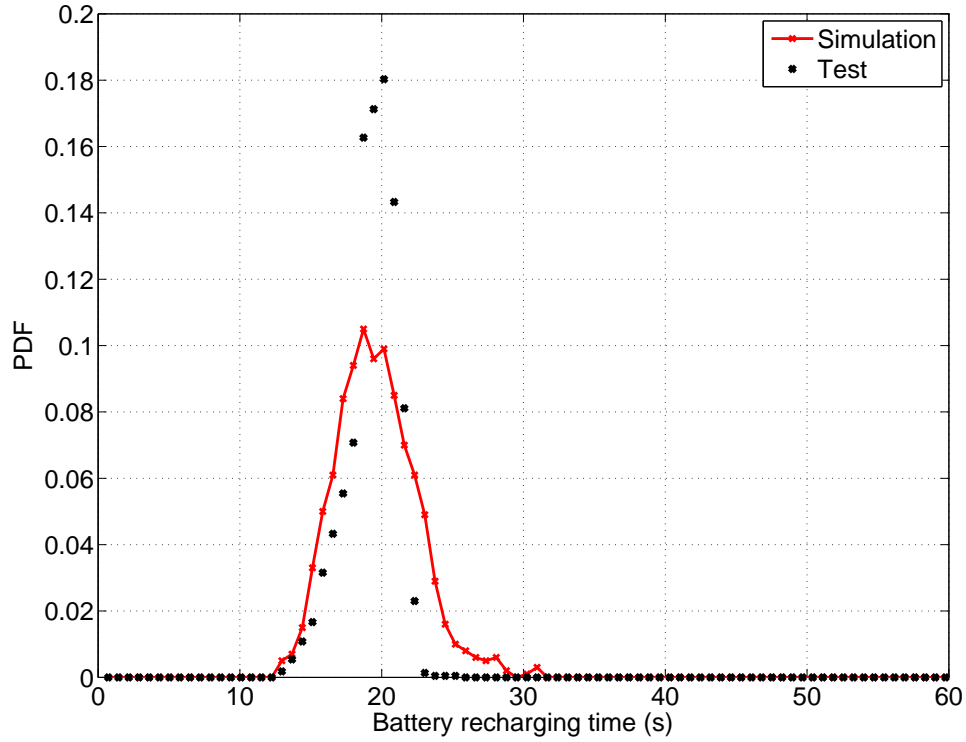
Figure 7.9: The distributions of battery recharging time obtained by simulation and test results.

m, and c that provide the minimization of calculated difference can be found as the parameters of wirelss channel.

We use 'fminsearch' command in Matlab and run an iterative code to minimize the absolute value of difference between the simulation results and the test results. The values of m and c parameters are changed iteratively to obtain minimum difference value. After a sufficient number of trials, the values of parameters approach stable values. According to our simulation and test results, we found the channel parameters about $m = 90.2$ and $c = 100.8$ for the first transmission line in Testbed-2. The values of m and c are very high due to stationary medium. It can be stated that, our tests was performed in good channel conditions.

7.6 Conclusions

Two testbeds are implemented to show practical applications of RF energy harvesting. According to test results, the distance between the source node and the harvesting node is very important, which the battery recharging time increase with distance. The

number of source is also influential factor. When the number of source increases, the battery recharging time decreases significantly. Actually, we performed other tests that include one source, two sources, directional antenna and omnidirectional antenna. The battery recharging time of wireless sensor node increases when we use omnidirectional antenna as expected. The test results are generally similar and consistent.

8. CONCLUSIONS AND RECOMMENDATIONS

RF energy harvesting is proposed as an energy source to capture RF signal energy from ambient sources in our thesis. It is easy to access to RF signals, because RF signal is ubiquitous due to the wide use of wireless communication systems. The received power of RF signal is not high to power wireless communication devices directly. However, thin film solid-state rechargeable micro-batteries and supercapacitors are used to store energy, and then to power wireless communication devices when needed. The time required for charging the battery is defined as battery recharging time. In the literature, there are no research depending on the nature of the medium between the source and the harvesting node in RF energy harvesting system. This medium is called as wireless channel in communication systems, which is described by a statistical wireless channel model. We state that wireless channel models have an important impact on the battery recharging time.

In this thesis, a study on the statistical characterization of battery recharging time is carried out for RF energy harvesting systems. The battery recharging time of an energy harvesting node is defined and modeled depending on the statistical models of wireless channels between the source node and the harvesting node. Additionally, testbeds are set, and measurements are performed to show real-life applications of RF energy harvesting. The battery recharging time is proposed an important parameter for the wireless devices and networks with RF energy harvesting circuit, and modeled as a random variable.

It is shown in our thesis that the battery recharging time is reversely proportional to the received power. Based on this information and given distribution of the received power, the statistical equations of the battery recharging time are obtained for RF energy harvesting systems. The closed form expressions for the battery recharging time are derived in the presence of single RF source. The PDF, the mean, and the variance expressions of battery recharging time are derived for the lognormal

shadowing distribution and the Nakagami-m distribution. Additionally, the PDF, the CDF, the MGF, the mean, and the variance expressions are derived for the generalized-K distribution. The battery recharging time in the presence of multiple RF sources is also investigated to generelize expressions. The PDF of the battery recharging time is derived by cascading convolution process for the generalized-K distribution in the presence of multiple sources. Moreover, the PDF, the CDF, the MGF, the mean, and the variance expressions are derived in the presence of both single source and multiple sources for the Gamma distribution as an approximation of the generalized-K distribution.

The derived distributions are verified by the numerical and simulation studies. In figures, it can be seen that the distribution of battery recharging time changes with channel conditions. The high values of m and c parameters, which mean good channel conditions, cause to approach a certain value as an impulse function. The conversion coefficient and distance have an important impact on the value of battery recharging time. The high values for conversion coefficient and the low values of distance ensure fast recharging, namely, decrease the battery recharging time. The number of RF source is also very important. When the number of source is increased, the value of battery recharging time is decreased proportional to the number of source. In addition to the simulations, testbeds are implemented to show real applications of the RF energy harvesting. The tests on the energy harvesting of an wireless sensor node from both single RF source and two RF sources are performed. Test results show that the mean value of received power decrease with distance, and the mean value of battery recharging time increase with distance. The addition of a second source accelerates the charging of battery, which ensures low battery recharging time.

As a conclusion, we would like to emphasize that the effects of channel conditions should be taken into account while designing an RF energy harvesting system. The derived parametric expressions can be used for RF energy harvesting systems. We propose the battery recharging time as a critical parameter for RF energy harvesting devices, especially for the wireless sensor networks to ensure the sustainability of

system. As a recommendation, the effect of energy profile of source on RF energy harvesting can be investigated for future work.

REFERENCES

[1] **Global Mobile Suppliers Association**, Interim Evolution to LTE, `http://www.gsacom.com/`, the date of receipt: 28.02.2014.

[2] **Open Mobile Alliance**, Management and Provisioning of M2M Devices and Applications, `http://openmobilealliance.org/`, the date of receipt: 30.06.2012.

[3] **Arveni S.A.S.**, `http://www.arveni.com`, the date of receipt: 25.04.2014.

[4] **Powercast Corporation**, `http://www.powercastco.com`, the date of receipt: 25.04.2014.

[5] **Altinel, D. and Kurt, G.K.**, 2014. Statistical models for battery recharging time in RF energy harvesting systems, Wireless Communications and Networking Conference (WCNC), IEEE International Conference on.

[6] **Zungerul, A.M.**, **Ang, L.M.**, **Prabaharan, S. and Seng, K.P.**, 2012. Green Mobile Devices and Networks: Energy Optimization and Scavenging Techniques, chapterRadio Frequency Energy Harvesting and Management for Wireless Sensor Networks, CRC Press, pp.342–364.

[7] **Visser, H. and Vullers, R.**, 2013. RF Energy Harvesting and Transport for Wireless Sensor Network Applications: Principles and Requirements, *Proceedings of the IEEE*, **101(6)**, 1410–1423.

[8] **Lumpkins, W.**, 2014. Nikola Tesla's Dream Realized: Wireless power energy harvesting., *Consumer Electronics Magazine, IEEE*, **3(1)**, 39–42.

[9] **Sarkar, S.**, **Bhavani.V**, **Shanavas, I. and Nallusamy, V.**, 2013. Energy Harvesting Method in Wireless Sensor Network., *International Journal of Education (IJE)*, **1(1)**.

[10] **Gunathilaka, W.**, **Gunasekara, G.**, **Dinesh, H.**, **Narampanawe, K. and Wijayakulasooriya, J.**, 2012. Ambient Radio Frequency energy harvesting, Industrial and Information Systems (ICIIS), 2012 7th IEEE International Conference on, pp.1 –5.

[11] **Balanis, C.A.**, 2005. Antenna Theory Analysis and Design, John Wiley and Sons.

[12] **Zainuddin, N.**, **Zakaria, Z.**, **Husain, M.**, **Derus, B.**, **Aziz, M.**, **Mutalib, M. and Othman, M.**, 2013. Design of wideband antenna for RF energy harvesting system, Instrumentation, Communications, Information Technology, and

Biomedical Engineering (ICICI-BME), 2013 3rd International Conference on, pp.162–166.

[13] **Sabaawi, A. and Tsimenidis, C.**, 2013. Circular truncated patch antennas for energy harvesting applications, Antennas and Propagation Conference (LAPC), 2013 Loughborough, pp.369–373.

[14] **Pinuela, M.**, **Mitcheson, P. and Lucyszyn, S.**, 2013. Ambient RF Energy Harvesting in Urban and Semi-Urban Environments, *Microwave Theory and Techniques, IEEE Transactions on*, **61(7)**, 2715–2726.

[15] **Noguchi, A. and Arai, H.**, 2013. Small loop rectenna for RF energy harvesting, Microwave Conference Proceedings (APMC), 2013 Asia-Pacific, pp.86–88.

[16] **Rahim, R.**, **Hassan, S.**, **Malek, F.**, **Junita, M. and Jamlos, M.**, 2012. An investigation of ambient radio frequency as a candidate for energy harvesting source, Industrial Electronics and Applications (ISIEA), 2012 IEEE Symposium on, pp.95–99.

[17] **Ding, Y. and Arslan, T.**, 2013. Broadband differential antenna for full-wave RF energy scavenging system, Antennas and Propagation Conference (LAPC), 2013 Loughborough, pp.325–328.

[18] **Shigeta, R.**, **Sasaki, T.**, **Quan, D.M.**, **Kawahara, Y.**, **Vyas, R.**, **Tentzeris, M. and Asami, T.**, 2013. Ambient RF Energy Harvesting Sensor Device With Capacitor-Leakage-Aware Duty Cycle Control, *Sensors Journal, IEEE*, **13(8)**, 2973–2983.

[19] **Sudevalayam, S. and Kulkarni, P.**, 2011. Energy Harvesting Sensor Nodes: Survey and Implications, *Communications Surveys Tutorials, IEEE*, **13(3)**, 443–461.

[20] **Prasad, R.**, **Devasenapathy, S.**, **Rao, V. and Vazifehdan, J.**, 2014. Reincarnation in the Ambiance: Devices and Networks with Energy Harvesting, *Communications Surveys Tutorials, IEEE*, **16(1)**, 195–213.

[21] **Infinite Power Solutions Inc.**, `http://www.infinitepowersolutions.com`, the date of receipt: 25.04.2014.

[22] **Cymbet Corporation**, `http://www.cymbet.com`, the date of receipt: 25.04.2014.

[23] **Yang, J. and Ulukus, S.**, 2012. Optimal Packet Scheduling in an Energy Harvesting Communication System, *Communications, IEEE Transactions on*, **60(1)**, 220 –230.

[24] **Tutuncuoglu, K. and Yener, A.**, 2012. Optimum Transmission Policies for Battery Limited Energy Harvesting Nodes, *Wireless Communications, IEEE Transactions on*, **11(3)**, 1180 –1189.

[25] **Yang, J.**, **Ozel, O. and Ulukus, S.**, 2012. Broadcasting with an Energy Harvesting Rechargeable Transmitter, *Wireless Communications, IEEE Transactions on*, **11(2)**, 571 –583.

[26] **Ozel, O.**, **Yang, J. and Ulukus, S.**, 2012. Optimal Broadcast Scheduling for an Energy Harvesting Rechargeable Transmitter with a Finite Capacity Battery, *Wireless Communications, IEEE Transactions on*, **11(6)**, 2193 –2203.

[27] **Berbakov, L.**, **Matamoros, J. and Anton-Haro, C.**, 2012. Optimal transmission policy for distributed beamforming with energy harvesting and battery operated sensor nodes, Wireless Communication Systems (ISWCS), 2012 International Symposium on, pp.441 –445.

[28] **Medepally, B. and Mehta, N.**, 2010. Voluntary Energy Harvesting Relays and Selection in Cooperative Wireless Networks, *Wireless Communications, IEEE Transactions on*, **9(11)**, 3543 –3553.

[29] **Gurakan, B.**, **Ozel, O.**, **Yang, J. and Ulukus, S.**, 2013. Energy Cooperation in Energy Harvesting Communications, *Communications, IEEE Transactions on*, **61(12)**, 4884–4898.

[30] **Gunduz, D. and Devillers, B.**, 2011. Two-hop communication with energy harvesting, Computational Advances in Multi-Sensor Adaptive Processing (CAMSAP), 2011 4th IEEE International Workshop on, pp.201–204.

[31] **Orhan, O.**, **Gunduz, D. and Erkip, E.**, 2013. Optimal packet scheduling for an energy harvesting transmitter with processing cost, Communications (ICC), 2013 IEEE International Conference on, pp.3110–3114.

[32] **Reddy, S. and Murthy, C.**, 2012. Dual-Stage Power Management Algorithms for Energy Harvesting Sensors, *Wireless Communications, IEEE Transactions on*, **11(4)**, 1434 –1445.

[33] **Bouchouicha, D.**, **Latrach, M.**, **Dupont, F. and Ventura, L.**, 2010. An experimental evaluation of surrounding RF energy harvesting devices, Microwave Conference (EuMC), European, pp.1381 –1384.

[34] **Baroudi, U.**, **Qureshi, A.**, **Mekid, S. and Bouhraoua, A.**, 2012. Radio Frequency Energy Harvesting Characterization: An Experimental Study, Trust, Security and Privacy in Computing and Communications (TrustCom), 2012 IEEE 11th International Conference on, pp.1976 –1981.

[35] **Mi, M.**, **Mickle, M.**, **Capelli, C. and Swift, H.**, 2005. RF energy harvesting with multiple antennas in the same space, *Antennas and Propagation Magazine, IEEE*, **47(5)**, 100 – 106.

[36] **Visser, H.J.**, **Keyrouz, S.**, **Kihshen, A. and Paraschiv, I.**, 2012. Optimizing RF energy transport: Channel modelling and transmit antenna and rectenna design, Antennas and Propagation Conference (LAPC), 2012 Loughborough, pp.1 –8.

[37] **Keyrouz, S.**, **Visser, H.J. and Tijhuis, A.G.**, 2012. Ambient RF energy harvesting from DTV stations, Antennas and Propagation Conference (LAPC), 2012 Loughborough, pp.1 –4.

[38] **Arrawatia, M.**, **Baghini, M. and Kumar, G.**, 2011. RF energy harvesting system from cell towers in 900MHz band, Communications (NCC), 2011 National Conference on, pp.1 –5.

[39] **Jabbar, H.**, **Song, Y. and Jeong, T.**, 2010. RF energy harvesting system and circuits for charging of mobile devices, *Consumer Electronics, IEEE Transactions on*, **56(1)**, 247 –253.

[40] **Nintanavongsa, P.**, **Muncuk, U.**, **Lewis, D. and Chowdhury, K.**, 2012. Design Optimization and Implementation for RF Energy Harvesting Circuits, *Emerging and Selected Topics in Circuits and Systems, IEEE Journal on*, **2(1)**, 24 –33.

[41] **Elanzeery, H. and Guindi, R.**, 2012. Frequency Survey Simulation for Developing Novel Radio Frequency Energy Harvesting Model, Computer Modelling and Simulation (UKSim), 2012 UKSim 14th International Conference on, pp.476 –479.

[42] **El-Anzeery, H.D.**, **El-Bagouri, M.A. and Guindi, R.**, 2012. Novel Radio Frequency Energy Harvesting model, Power Engineering and Optimization Conference (PEDCO) Melaka, Malaysia, 2012 Ieee International, pp.209 –213.

[43] **Dolgov, A.**, **Zane, R. and Popovic, Z.**, 2010. Power Management System for Online Low Power RF Energy Harvesting Optimization, *Circuits and Systems I: Regular Papers, IEEE Transactions on*, **57(7)**, 1802 –1811.

[44] **Mishra, T.**, **Panda, S.**, **Karim, M.**, **Ong, L. and Chiam, T.**, 2012. 2.4GHz square slot antenna and power management circuit for wireless energy harvesting applications, Antennas and Propagation (APCAP), 2012 IEEE Asia-Pacific Conference on, pp.223 –224.

[45] **Zhao, W.**, **Choi, K.**, **Bauman, S.**, **Dilli, Z.**, **Salter, T. and Peckerar, M.**, 2012. A Radio-Frequency Energy Harvesting Scheme for Use in Low-Power Ad Hoc Distributed Networks, *Circuits and Systems II: Express Briefs, IEEE Transactions on*, **59(9)**, 573 –577.

[46] **Lee, S.**, **Huang, K. and Zhang, R.**, 2012. Cognitive energy harvesting and transmission from a network perspective, Communication Systems (ICCS), IEEE International Conference on, pp.225 –229.

[47] **Park, S.**, **Heo, J.**, **Kim, B.**, **Chung, W.**, **Wang, H. and Hong, D.**, 2012. Optimal mode selection for cognitive radio sensor networks with RF energy harvesting, Personal Indoor and Mobile Radio Communications (PIMRC), 2012 IEEE 23rd International Symposium on, pp.2155–2159.

[48] **Grover, P. and Sahai, A.**, 2010. Shannon meets Tesla: Wireless information and power transfer, Information Theory Proceedings (ISIT), 2010 IEEE International Symposium on, pp.2363–2367.

[49] **Zhou, X.**, **Zhang, R. and Ho, C.K.**, 2013. Wireless Information and Power Transfer: Architecture Design and Rate-Energy Tradeoff, *Communications, IEEE Transactions on*, **61(11)**, 4754–4767.

[50] **Zhang, R. and Ho, C.K.**, 2013. MIMO Broadcasting for Simultaneous Wireless Information and Power Transfer, *Wireless Communications, IEEE Transactions on*, **12(5)**, 1989–2001.

[51] **Sample, A. and Smith, J.**, 2009. Experimental results with two wireless power transfer systems, Radio and Wireless Symposium, 2009. RWS '09. IEEE, pp.16 –18.

[52] **Cheng, J.**, **Xia, L.**, **Ma, C.**, **Lian, Y.**, **Xu, X.**, **Yue, C.**, **Hong, Z. and Chiang, P.**, 2012. A near-threshold, multi-node, wireless body area sensor network powered by RF energy harvesting, Custom Integrated Circuits Conference (CICC), 2012 IEEE, pp.1 –4.

[53] **Boquete, L.**, **Barea, R.**, **Rodriguez-Ascariz, J.**, **Cantos, J. and Miguel, J.**, 2012. A radio frequency energy harvesting laboratory practice, Technologies Applied to Electronics Teaching (TAEE), 2012, pp.204 –209.

[54] **Bilgi Teknolojileri ve İletişim Kurumu**, Milli Frekans Planı, `http://www.btk.gov.tr/`, the date of receipt: 15.03.2014.

[55] **Garg, V.K.**, 2007. Wireless Communications and Networking, Elsevier Inc.

[56] **Rappaport, T.S.**, 2002. Wireless Communications: Principles and Practice, Prentice Hall.

[57] **Goldsmith, A.**, 2005. Wireless Communications, Cambridge University Press.

[58] **Shankar, P.M.**, 2011. Statistical Models for Fading and Shadowed Fading Channels in Wireless Systems: A Pedagogical Perspective, *Wireless Pers Commun*.

[59] **Al Ahmadi, S. and Yanikomeroglu, H.**, 2010. On the Approximation of the Generalized K Distribution by a Gamma Distribution for Modeling Composite Fading Channels, *Wireless Communications, IEEE Transactions on*, **9(2)**, 706–713.

[60] **Bithas, P.**, **Sagias, N.**, **Mathiopoulos, P.**, **Karagiannidis, G. and Rontogiannis, A.**, 2006. On the performance analysis of digital communications over generalized-K fading channels, *Communications Letters, IEEE*, **10(5)**, 353–355.

[61] **Al-Ahmadi, S. and Yanikomeroglu, H.**, 2009. On the Approximation of the Generalized-K PDF by a Gamma PDF Using the Moment Matching Method, Wireless Communications and Networking Conference, 2009. WCNC 2009. IEEE, pp.1–6.

[62] **Microchip Tecnology Inc.**, `http://www.microchip.com/`, the date of receipt: 25.04.2014.

CURRICULUM VITAE

Name Surname: Doğay Altınel

Place and Date of Birth: Diyarbakır, 1971

Adress: Istanbul Medeniyet University Usküdar/Istanbul

E-Mail: dogayaltinel@gmail.com

B.Sc.: Electronics Engineering at Hacettepe University

M.Sc.: Telecommunication Engineering at Istanbul Technical University

Professional Experience and Rewards:

- **Expert**, (2012 – ...) at Istanbul Medeniyet University.

- **Executive**, (2010 – 2012) at Alben.

- **Regional Operations Responsible**, (2007 – 2009) at Turkkule.

- **Network Planning and RF Optimization Expert** , (1999 – 2007) at Turkcell.

- **Service and Maintenance Engineer**, (1995 – 1999) at Toshiba (Incekaralar+TMST).

- **Electronics Engineer**, (1992 – 1993) at Seka.

PUBLICATIONS/PRESENTATIONS ON THE THESIS

- **Altinel D.**, Karabulut Kurt G., "Statistical Models for Battery Recharging Time in RF Energy Harvesting Systems", in Wireless Communications and Networking Conference (WCNC), IEEE International Conference on, Apr. 2014.